STABILITY OF BLOCK COPOLYMER SURFACTANT-BASED EMULSIONS IN THE PRESENCE OF A SALT

By

Mwamb Alain Kabong

Dissertation submitted in partial fulfilment of the requirements for the degree of

Master of Science

In

Applied Sciences Chemical Technology

In the Faculty of Engineering, Built Environment and Information Technology

University of Pretoria

Pretoria

January 2020

Declaration of Plagiarism

Full names	Mwamb Alain Kabong
Student number	14333733
Topic of work	Master's Thesis – Stability of block copolymer surfactant-based emulsions in the presence of a salt

Declaration

1. I understand what plagiarism is and am aware of the University's policy in this regard.
2. I declare that this dissertation is my own original work. Where other people's work has been used (either from printed source, internet or any other source), this has been adequately acknowledged and referenced by the requirements as stated in the University's plagiarism prevention policy.
3. I have not used another student's past written work to hand in as my own.
4. I have not allowed, and will not allow, anyone, to copy my work with the intention of passing it off as his or her own work.

Signature: 

Publication

The work presented in this thesis has given rise to the following paper:

Kabong, Mwamb A, Walter W Focke, Elizabeth L Du Toit, Heidi Rolfes, and Shatish Ramjee. 2020. 'Breakdown mechanisms of oil-in-water emulsions stabilised with Pluronic F127 and co-surfactants', *Colloids and Surfaces A: Physicochemical and Engineering Aspects*, 585: 124101.

STABILITY OF BLOCK COPOLYMER SURFACTANT-BASED EMULSIONS IN THE PRESENCE OF A SALT

Author: Mwamb Alain Kabong

Supervisor: Prof. Walter W. Focke

Department: Chemical Engineering

Degree: Masters (Chemical Technology)

Abstract

This project deals with the mixed micellar and interfacial properties of mixtures of three surfactants [sodium dodecyl sulphate (SDS), cetyltrimethylammonium bromide (CTAB), and tetraethylene glycol monododecyl ether ($C_{12}E_4$)] with ABA symmetrical triblock copolymer (Pluronic F127), which has many industrial applications. Evidence of F127 micellisation and interaction with surfactants in the aqueous phase is inferred through interfacial tension measurements. The solution containing diluted monomeric F127 showed complex formation with surfactants before the latter self-aggregate as pure micelles.

The simultaneous presence of ionic surfactants and micellar F127 in solutions displayed a decrease of interfacial activity and led to the conclusion of F127 micelles disruption. $C_{12}E_4$ was found to interact differently with micellar F127 in forming mixed micelles, and no loss of interfacial activity was recorded. This “association-dissociation” behaviour of F127 and surfactants was leveraged to understand the stability of mineral oil in water emulsions formulated with them in the presence of sodium phosphate (Na_3PO_4).

The mechanisms of emulsions breakdown were found to rely on aggregation behaviour and complex structure of F127 and surfactants mixtures in solution. Laser diffraction showed that unlike SDS and CTAB, mixed-emulsifier systems containing $C_{12}E_4$ are stable to both flocculation, Ostwald ripening and coalescence. Due to electrostatic repulsion between its head group and F127 hydrophilic block, and also because of the combined effect of Ostwald ripening and coalescence, CTAB emulsifier containing systems displayed quicker instability than SDS.

SDS containing systems showed a progressive shifting of droplets size distributions to bimodality as SDS concentration was increased and heat exposure pursued, revealing the activity of two distinct population of droplets in the emulsions. More insight on the mechanisms underlying the stability of the three mixed emulsifier systems was gained in performing optical microscopy and rheology measurements; the results were found to be consistent with particle size distribution.

Keywords: Micelles, interfacial tension, emulsions, particle size distribution, Ostwald ripening, coalescence

Dedication

Aux soleils de mon enfance,

A ma mère,

Et à la mémoire de mon père.

Acknowledgements

I would like to give thanks to my God Almighty for the strength, bravery and abilities through the accomplishment of the project.

My sincere gratitude goes to Professor Walter W. Focke for his guidance, support and valuable criticism throughout the project.

My gratitude goes to Dr Heidi Rolfes for having initiated the project.

I am grateful to CSIR-Pretoria for their technical support and equipment at the Department of Polymers and Composite Materials.

I acknowledge with gratitude the support of BASF South Africa with the provision of Pluronic samples.

My joy knows no bounds in expressing my cordial gratitude to my special friend and partner Nathalie Kala Konga. Her keen interest and encouragement were a great help throughout the course of this research work.

My deepest gratitude, thankfulness and appreciation go to my parents, brothers and sisters, for their unconditional love, understanding, encouragements and never-ending support. Without you, it would have not been possible for me to finish this project.

To my father, whose untimely death shocked us all – thank you for everything.

I humble extend my thanks to all concerned persons who cooperated with me during the completion of this research project.

Table of Content

List of Figures

List of Tables

List of acronyms

SDS	Sodium Dodecyl Sulphate
CTAB	Cethyltrimethylammonium bromide
$C_{12}E_4$	Tetraethylene glycol monododecyl ether
CMC	Critical Micelle Concentration [mol]
CAC	Critical Aggregation Concentration [mol]
PEO	Poly(ethylene oxide)
PPO	Poly(propylene oxide)
DSD	Droplet Size Distribution
HLB	Hydrophilic Lipophilic Balance
DLS	Dynamic Light Scattering
EMF	Electromotive force
CMT	Critical Micelle Temperature [° C]
GS	Gemini Surfactant
PVP	Polyvinylpyrrolidone
PHS	Polyhydroxystyrene
CP	Cloud Point [° C]
DMSO	Dimethyl Sulfoxide
LCST	Low Concentration Solution Temperature [° C]
LSW	Lifshitz-Slyozov-Wagner
ACE	Associated Chemical Enterprises
DSA	Drop Shape Analysis
DIC	Differential Interference Contrast
OM	Optical Microscopy
DLVO	Derjaguin-Landau-Vervey-Overbeek

List of symbols

Γ	Excess interfacial concentration [mol m^{-2}]
R	Gas constant [8.314 J mol^{-1} K^{-1}]
T	Absolute temperature [K]
C	Surfactant concentration [mol]
γ	Interfacial tension [mN m^{-1}]
χ	Flory-Huggins polymer-solvent interaction parameter
V	Molar volume [m^3 mol^{-1}]
δ	Solubility parameter
M	Molecular mass [g mol^{-1}]
E	Energy of attachment to fluid-fluid interface [J m^{-2}]
r	Particle radius [nm]
θ	Contact angle [º]
ϵ	Counter-ion dissociation constant
m	Carbon number of surfactant tail
β	Surfactant interaction parameter
X_t	Total surfactant concentration [mol]
X_1	Single dispersed surfactant
X_f	Surfactant free micelle [mol]
X_b	Surfactant bound as aggregates [mol]
g_f	Average aggregation number of the free micelles
K_f	Intrinsic-equilibrium constant of free micelles formation
g_b	Micelles average size
K_b	Intrinsic-equilibrium constant for the binding of the surfactant on the polymer
X_p	Total concentration of polymer molecules in solution [mol]
a_{pol}	Area per surfactant molecule of the micellar core shielded by the polymer
υ	Creaming rate [S^{-1}]
ρ	Density [g cm^{-3}]

η	Viscosity [Pa]
k	Boltzmann constant [J K^{-1}]
D	Diffusion coefficient [m^2 s^{-1}]
$\Delta_{Vap}H$	Enthalpy of vaporisation [J g^{-1}]
ΔG	Free energy [J K^{-1} mol^{-1}]
α_p	Isobaric expansibility
k_T	Isothermal compressibility
p	Vapor pressure [mm Hg]
$\Delta_{Vap}S$	Molar entropy of vaporisation [J g^{-1} K^{-1}]
T_b	Normal boiling point at atmospheric pressure [℃]
ΔS_{struct}	Structural entropy [J g^{-1} K^{-1}]
ΔS_{hydr}	Entropy of hydration [J g^{-1} K^{-1}]
S_{rot}	Rotational entropy [J g^{-1} K^{-1}]
ε_r	Relative permittivity [F m^{-1}]
ε_0	Permittivity of free space [F m^{-1}]
φ	Surface potential [m^2 s^{-2}]
κ	Debye-Huckel parameter
Z_i	Valence of ion
μ	Chemical potential [J mol^{-1}]
N_{av}	Avogadro's constant [mol^{-1}]
Ω	Number of configuration
K_C	Apparent coalescence rate [S^{-1}]
C_W^{aq}	Aqueous oil solubility [g L^{-1}]
ω_C	Coalescence rate [S^{-1}]
E_C	Cohesive energy of flocculated structure [Jm^{-3}]

Chapter 1 Introduction

1.1 Background

The primary objective of this project is to explore the interactions between water-soluble polymer and surfactants in the aqueous media. This was achieved through surface tension measurements and was further pursued through emulsion stability. The aforementioned interacting solutes can be described as macromolecular and low molecular entities, respectively. The distinguishing property of surfactants with other solutes is their surface activity, responsible for their adsorption at the interface of two immiscible substances, and which is conferred to them by the presence of the two opposing polar (hydrophilic) and non-polar (hydrophobic) moieties in the same molecule. This determining characteristic of surfactants gives rise to a unique behaviour in aqueous solutions, as a direct consequence of their surface active property. This behaviour is the aggregation of surfactant molecules in bulk solution, in a manner to minimise the contact of non-polar moiety with water.

In this study, uncharged triblock copolymer figuring as a macromolecule, is consecutively associated with ionic (anionic and cationic) and neutral surfactants. The interaction between them is substantiated by the binding of surfactants to the macromolecular chain. The governing property of both aggregation in bulk solution and binding to water-soluble polymer is hydrophobicity, i.e., the extent to which surfactant molecules are expelled from water. This repellence from water is the fundamental process defining the hydrophobic effect, and is subjected to many quantitative factors such as (Southall et al., 2002):

- Surfactant concentration
- Surfactant aliphatic chain length
- Solvent ionic strength
- Temperature increase and decrease.

In addition to hydrophobicity, another factor which influences surfactants aggregation and binding behaviour in aqueous solutions is electrostatic effect, due to the surfactant polar heads. Aggregation in solution starts at each surfactant characteristic concentration termed critical micelle concentration (cmc) and this phenomenon is termed micellisation or self-micellisation. It is the concentration at which water-air interface becomes saturated with surfactant molecules, giving rise to the first micelle formation in the bulk solution. In the presence of water-soluble

polymer, the concentration at which first surfactant binds to the polymer backbone is termed critical aggregation concentration (cac), and it is the concentration at which surfactant molecules start adsorbing on the polymer chain after being adsorbed at the water-air interface, to form a polymer-surfactant aggregate complex. Therefore, in this case, there are two thermodynamic adsorbing sites, which are the solution-air interface and the polymer chain.

Interactions between surfactants and uncharged water-soluble synthetic macromolecules have been investigated for many decades, because of their importance in many industrial applications (Goddard, 2018). Depending on their combination, the interactions they give rise to can result in substantial improvement in the adsorption behaviour at the interface, in the solubilisation capabilities of aqueous solutions, and in the stability of colloidal dispersion, etc. It is generally agreed that the presence of non-ionic polymer in an aqueous solution of surfactants provides a thermodynamic alternative to surface adsorption and self micellisation (Rulison, 2004). For strongly interacting systems, i.e., interaction with anionic surfactants, polymer behaves as a nucleation site (Li et al., 2011), and surfactants aggregates on the polymer backbone at a concentration well below its critical micelle concentration (cmc). The majority of studies on polymer-surfactant interactions relate those alterations of surfactant aqueous solution properties to cooperative binding of surfactant molecules to the polymer chain, leading to competition between formation of polymer-free surfactant micelles and polymer-surfactant association complexes (Nagarajan, 1985, Shirahama et al., 1974).

The expertise in the field of water-soluble homopolymer interactions with surfactants is quite advanced since many reliable thermodynamic model attempts explanning their aggregation behaviour are available (Ruckenstein, 1999, Ruckenstein et al., 1987, Nikas and Blankschtein, 1994, Nagarajan, 1980, Nagarajan, 1985, Shirahama, 1974). These early investigations on homopolymers and surfactants interaction were followed in the recent years by increasing interest in the interaction of low molecular surfactants with surface-active macromolecules, yet, no comparable advance has been reported for surfactant and surface active block copolymer mixed solutions, indicating that this field is still emerging. Although interest in micellisation of block copolymers is quite old (Tuzar, 1996), their association with surfactants did not so far attracted an attention comparable to the interest raised by association of the latter with water-soluble homopolymers (Sastry and Hoffmann, 2004).

Block copolymers are polymers in which the repeat units exist only in blocks of the same type that are covalently bonded. Depending on the monomers' repeating units arrangement, the

blocks could be alternately placed, randomly, in star, or graft manner. In an alternate [AB] or symmetrical [ABA] triblock copolymer, the two polymer blocks are usually incompatible with one another. As a consequence, they prefer to exist in a demixed rather than in a mixed state, giving rise to self-assembled microstructures in solution, resembling in essential aspects to the micellar aggregates formed by low molecular surfactants (Nagarajan and Ganesh, 1989a, Nagarajan and Ganesh, 1989b).

Many block copolymers have been found to self-aggregate in water and their properties are widely exploited in detergency, lubrication, foaming, formulation of cosmetics, pharmaceutics, bioprocessing, separation processes, dispersion stabilisation and emulsification (Alexandridis et al., 1994b). When used in emulsion technology, this block copolymers aggregating property enables them to facilitate emulsification and to promote emulsion stability. Indeed, during the emulsification process, the dispersed phase oil molecules are entrapped into the copolymer micelles, and by forming an adsorbed film around the dispersed droplets in the medium, the amphiphilic block copolymers prevent coalescence. This stability is due to steric repulsion of the non-ionic block copolymer hydrophilic chains wrapped around the droplets (Nagarajan and Ganesh, 1989b). It can be significantly enhanced when mixing such non-ionic amphiphiles with ionic surfactants. Indeed, when present in a solution of non-ionic copolymer at concentrations far below their critical micelle concentration, ionic surfactants incorporate into the copolymer micelle and create electric charges on the micellar surface, causing repulsion between the copolymer micelles (Manohar and Kelkar, 1990, Mata et al., 2004). Thus, to the steric repulsion of the droplet induced by copolymer chains is added the electrostatic repulsion arising from charged droplets electrical double-layer overlapping.

In many industrial applications, this ability of ionic surfactants to enhance pluronics emulsion stability through a substantial increase in cloud point (CP) (Sharma and Bahadur, 2002) is widely exploited. CP of non-ionic surfactants and neutral copolymers is defined as the temperature at which the surfactant precipitates out of the solvent medium (Johnson et al., 1990b). At this point, and due to the decrease of hydrogen bonding between the surfactant hydrophilic moiety and water, no affinity exists any more between the solvent and the surfactant, and the system results in separation of aqueous and surfactant phases.

In this project, a complementary action is to quantify the kinetic stability of oil in water (O/W) emulsion stabilised by a mixture of poly(ethylene oxide)$_{100}$-poly(propylene oxide)$_{65}$-poly(ethylene oxide)$_{100}$ (Pluronic F127) with ionic sodium dodecyl sulphate (SDS) and cetyl

trimethylammonium bromide (CTAB), and neutral tetraethylene glycol monododecyl ether ($C_{12}E_4$) surfactants is studied. The latter surfactant increases emulsion stability by addition of its steric hindrance to block copolymer chains overlapping layers. As has been stated above, the former ones add to the copolymer layers steric repulsion their electrostatic interaction, which is also repulsive. Since breakdown of dispersions through coalescence and/or Ostwald ripening is a clouding related phenomenon (Johnson et al., 1990b, Johnson et al., 1990a), increasing temperature in a single Pluronic F127 (or in emulsion stabilised by mixture of Pluronic and non-ionic surfactant) stabilised emulsion would be enough to force merging of dispersed droplets and speed up coalescence or the Ostwald ripening rate. However, since temperature changes do not affect appreciably charged surfactant solutions CP (Shinoda and Lindman, 1987), this single factor becomes insufficient when ionic surfactants enhance the stability of emulsion by adding electrostatic repulsion to copolymer chains' steric hindrance.

Therefore, an additional way to reach CP of such a suspension or solution would be by including the effect of additives which induce clouding behaviour of ionic surfactants. Indeed, when adding a charged surfactant to a neutral emulsifier stabilised emulsion, the CP of the system becomes sensitive to the presence of electrolytes, and can decrease drastically at an extent depending on the valence of a salt (Nagarajan and Ganesh, 1989a, Manohar and Kelkar, 1990). The addition of an electrolyte to an ionic/non-ionic micellar solution or dispersion causes the original charge distribution to swamp, and the corresponding intermicellar electrostatic repulsion is screened (Mukherjee et al., 2011, Marszall, 1988). This results in micelle-micelle aggregation leading to lowering of the CP.

The possibility of CP to be advantageously used under diverse conditions in industrial applications relies on its property to be conveniently decreased or increased by the presence of different additives (Sharma and Bahadur, 2002). Clouding behaviour of micellar solutions and emulsions is widely exploited for extraction and preconcentration of various metal ions, organic compounds, biomolecules like amino acid and proteins, industrial pollutants, removal of oily soil from the substrate, etc. In all these applications, the property of micellar solution to phase separate upon heating above CP is leveraged. Indeed, the cloud point is used to entrap the wide variety of analytes due to their higher solubility in surfactant rich phase (Mukherjee et al., 2011). In many cases, the CP method is becoming a credible alternative to liquid-liquid separation which usually involves toxic solvent to extract a solute phase from a complex mixture.

In practice, the CP separation technique proceeds by chelating ions or molecules of interest in an aqueous solution with a suitable ligand, followed by addition of a surfactant, and separation through clouding. However, in many cases, the high temperature required to reach CP is the principal factor accountable for the denaturation of bioorganic compounds such as proteins (Mukherjee et al., 2011). In this situation, salt becomes the crucial factor to avoid denaturation during clouding extraction, since it is known to lower the cloud temperature, and can thus provide a way to extract protein without denaturation. In addition to improving the extraction efficiency, the use of salt in extraction processes also provides a more economical way of feasibility, by reducing the energy expenditure required for clouding.

With regards to this study, kinetic stability of emulsions has been preceded by study on emulsifiers' interactions and association behaviour in aqueous medium, as these are prerequisites for a deep understanding of emulsion breakdown processes. Systematic theoretical study of the interaction between aggregating block copolymers and low molecular surfactants are still stammering, and instead, an extended experimental activity in this field has been ongoing on for many years. Although many excellent reviews are available (Sastry and Hoffmann, 2004), they have always dealt in fractionated manner with the huge extent of the field concerned by the interactions between surfactant and copolymer.

Following qualitative assessments of association and dissociation behaviours between amphiphilic block copolymers and low molecular surfactants (Bahadur et al., 1988, Hecht and Hoffmann, 1994, Zheng and Davis, 2000), numerous attempts of their quantitative aggregation characterisation have been successfully conducted (Li et al., 2001a, Couderc-Azouani et al., 2005, Ortona et al., 2006, Li et al., 2011). Very few of these studies have, in a very concise manner, approached the question in a unified experimental treatment in all the extent of its facets, i.e., in associated and nonassociated states of the block copolymer, and with the three major classes of surfactants, namely anionic, cationic and neutral. Such a study is performed in this project, as a preliminary to the kinetic study of emulsions stability.

The experimental pursuit of these interactions' study was preceded by a presentation on the advances accomplished in the field of colloids. Chapter Two provides a background to the issue addressed in this project. Theoretical aspects of surfactants and polymers behaviours in aqueous phases are exposed. Surfactants aggregation and their interactions with polymers are emphasized. The role of amphiphiles on the kinetic stability of emulsions and the intervention of salt in the emulsion breaking down processes are also highlighted.

Chapter Three is dedicated to the presentation of experimental methods used for characterisation of F127/surfactant interactions.

In Chapter Four, block copolymer-surfactant mixtures in aqueous solutions and stability of emulsions formulated with mixed emulsifiers in the presence of salt are examined. The aggregation behaviour of surfactant in the presence of associated and diluted non-associated Pluronic F127 is studied by surface tension. Quantification of emulsions destabilisation through measurements of dispersed phase droplets size distribution (DSD) over time is attempted, and emulsions structures are studied through rheology and optical microscopy (OM).

1.2 Aim

The aim of this study is to build up knowledge and produce a comprehensive explanation of the behaviour of mixed emulsifiers' (Pluronic F127 and surfactants) stabilised emulsions that could be used as a basis for understanding and treatment of oil in water (O/W) emulsions.

1.3 Objectives

1. Assess interaction of Pluronic F127 and surfactants in aqueous media.
2. Compare the mixed emulsifiers (Pluronic F127 and Surfactants) systems' hydrophobic behaviors at water/air and water/mineral oil interfaces.
3. Express stability and destabilisation mechanisms of emulsions formulated with mixed emulsifiers and salt in terms of emulsifiers' molecular interaction and adsorption behavior in the aqueous phase.

Chapter 2 Literature Survey

2.1 Introduction

The aim of this chapter is to provide an overview of the achievements in the field of amphiphiles' behavior in aqueous solutions and their emulsion stabilising property. It prepares the understanding and interpretation of the results of our tests by widening horizons of interaction between surfactants and polymers in an aqueous solution. However, this review is limited to the strict framework of our work and only covers essential of what in the abundant literature on surfactants and polymers in aqueous solution, relates to our project.

An overview of the general aspects of amphiphiles and their behavior in solution is carried out. Their ability to aggregate is stressed, as well as external physical factors that can influence it. The ability to agglomerate in a solution is possible for many materials, as listed below. For those not related to the scope of our project, a very brief description is given. A thermodynamic model of surfactant micellisation is also approached. Mixture and synergism of binary surfactant systems are reviewed, followed by interactional aspects of the simultaneous presence of polymers and surfactants in the aqueous solutions.

Finally, the question of stability and instability of emulsions is addressed. Emulsions breakdown processes are described and the importance of emulsifiers in the emulsion stability is emphasised. Further, salts' effects on micellar solutions and emulsions clouding behaviour is stressed, and the effect of ions on water structure is highlighted. Thermodynamic and kinetic models of emulsion stability are then presented.

2.2 General considerations on surfactants and amphiphiles' self-assembly

Amphiphiles are common materials that are used in emulsion stabilisation and in solubilisation of nonpolar compounds in aqueous media. They derive their properties from their molecular constitution, i.e., from the fact that they consist of two distinct regions, one polar and one nonpolar. With respect to an aqueous medium, this dissimilarity results in hydrophilic (water-soluble) and hydrophobic (water-insoluble) portions on the molecule.

The partition of the molecule in the function of polar and nonpolar regions is responsible for the tendency of amphiphiles to accumulate and orient accordingly at the interface between phases of different polarities. For this reason, amphiphiles are termed surface-active agents or "surfactants". The polarity of the two parts of surfactant molecules determines their affinity

toward a solvent. In an aqueous solution, a surfactant will normally orients with its polar region in water and its nonpolar one in a less polar phase as shown in Figure 1a. The accumulation of surfactants at the interface tends to saturate it, giving rise to a limit concentration at which surfactants start to aggregate in water as shown in Figures 1b and 1c (Tadros, 2006a). This surfactant adsorption at the interface gives rise to a decrease in the interfacial tension between the two phases, described by the Gibbs' isotherm equation:

$$\Gamma = -\frac{1}{RT}\frac{\partial \gamma}{\partial lnC}, \tag{2.1}$$

in which Γ is the excess interfacial concentration of surfactant, R the gas constant, T the absolute temperature, C the bulk surfactant concentration, and γ the interfacial tension.

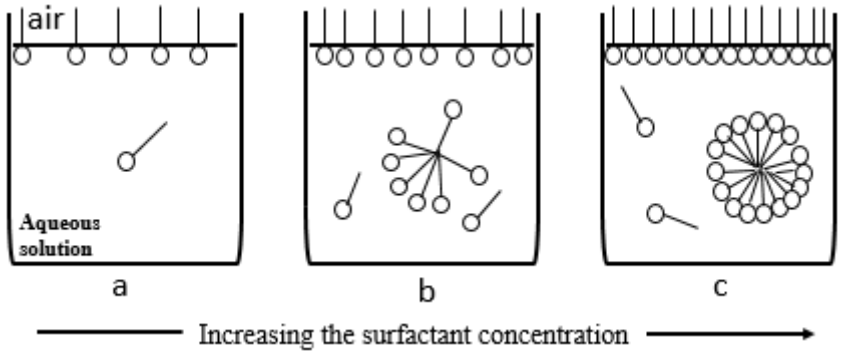

Figure 1. Surfactant aggregation in aqueous solution.

Surfactants molecular constitutions give rise to their classification according to the nature of hydrophilic moiety, mostly designated as a head group (Figure 2). Three surfactant classes can then be distinguished, namely ionic (anionic and cationic), neutral, and zwitterionic surfactants. Ionic surfactants dissociate in water into two oppositely charged species (the surfactant ion and its counterion). A surfactant is said to be anionic when its ion has a negative charge and cationic in the opposite case (Eastoe). Non-ionic surfactants do not have electrical charges in solution. Instead, they entail highly polar groups such as hydroxyl, polyoxyethylene or ether (Yalkowsky, 1999). Zwitterionic surfactants, also known as amphoteric surfactants, combine both positive and negative charges in their polar head. Table 1 lists some common hydrophilic groups found in commercial applications.

Table 1. Common hydrophilic groups found in commercial applications (Eastoe).

Class	General Structure
Sulfonate	$R-SO_3^-M^+$
Sulfate	$R-OSO_3^-M^+$
Carboxylate	$R-COO^-M^+$
Phosphate	$R-OPO_3^-M^+$
Ammonium	$R_xH_yN^+X^-(x=1-3, y=4-x)$
Quaternary ammonium	$R_4N^+X^-$
Betaines	$RN^+(CH_3)_2CH_2COO^-$
Sulfobetaines	$RN^+(CH_3)_2CH_2CH_2SO_3^-$
Polyoxyethylene (PEO)	$R-OCH_2CH_2(OCH_2CH_2)_nOH$
Polyols	Sucrose, sorbidan, glycerol, ethylene glycol, etc
Polypeptide	$R-NH-CHR-CO-NH-CHR'-CO-\cdots-CO_2H$
Polyglycidyl	$R-(OCH_2CH[CH_2OH]CH_2)_n-\cdots$ $-OCH_2CH[CH_2OH]CH_2OH$

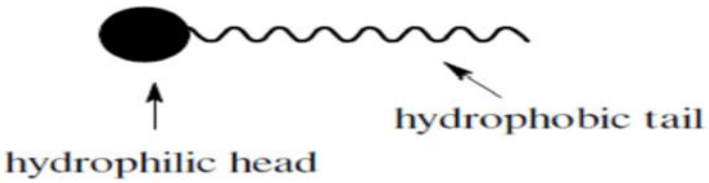

Figure 2. Schematic of a surfactant molecule.

The polar and nonpolar properties characterising surfactants are also found in some amphiphilic block copolymers. Block copolymers are polymers in which the repeat units exist only in blocks of the same type (Young and Lovell, 2011). Surface-active block copolymers are characterised by large molecular weight blocks (Figure 3) of different compatibility with selective solvents. In some block copolymers, the A and B blocks are so different in their nature that they exhibit a substantial degree of mutual incompatibility among them, thus interacting differently with water or any other solvent (Nagarajan and Ganesh, 1989b). As a result, such copolymers are molecules in which one of the blocks is hydrophobic while the other is hydrophilic. The analogy between an AB diblock or ABA symmetrical triblock surface-active copolymer (in which A and B stand for different blocks, and a low molecular surfactant) is that the solvent-incompatible block plays the role of hydrophobic tails while the solvent-compatible block plays the role of hydrophilic heads. Generally, instead of hydrophobicity or hydrophilicity, one can mention solvophobicity or solvophilicity, indicating the broad possibility of solvent to which the concept could be applied.

AAAAAABBBBBB a **AAAAAABBBBBBAAAAAA** b

Figure 3. Types of copolymers synthesised from two kinds of monomers: a) AB diblock copolymer, b) ABA symmetrical triblock copolymer.

Diblock or symmetrical triblock copolymers for which the blocks are sufficiently dissimilar in their solvation properties often self-assemble in micelle structures (Gao and Eisenberg, 1993). Such block copolymers are said to be surface-active block copolymers. In solution, the two incompatible blocks end up segregating from one another, forming aggregates whose incompatible solvent block constitute the inner core (Nagarajan, 2001) (figured as the darker lines in Figure 4). For example, for an AB diblock or ABA triblock copolymer in solvent S which is selective for block B, i.e., compatible with block B, the copolymer organises itself in such a way that the resulting aggregate consists of a core region made up of A block and a surrounding shell region consisting of B block, as shown ideally in Figure 4 (Nagarajan and Ganesh, 1989b).

However, it should be pointed out that surface tension decrease borne by copolymer surfactants is much smaller compared to that produced by low molecular-weight surfactants; their cmc in comparison is reached at relatively low concentration. This can be accounted for in considering the high molecular weight of hydrophobic moiety of copolymers which induces fast saturation of interface, reducing the concentration at which the first micelle forms (Bahadur et al., 1988).

Figure 4. The geometrical structure of a diblock copolymer in a selective solvent (Nagarajan and Ganesh, 1989b).

The solvent selectivity for copolymeric blocks reflects the solubility of each block in the solvent, and can be described using the *Flory-Huggins polymer-solvent interaction parameter*, χ. This parameter characterizes polymer-solvent interactions by measuring the solvation of copolymer chains by the molecules of the medium (Milner et al., 2009). It is a temperature-

dependent dimensionless quantity which can be estimated from the knowledge of the Hildebrand solubility parameter of both solvent and polymer (Young and Lovell, 2011):

$$\chi_{SP} = \frac{V_S(\delta_S - \delta_P)^2}{RT}, \tag{2.2}$$

where V_S is the molar volume of the solvent, δ_S and δ_P are the solubility parameter of solvent and polymer, respectively. For a copolymer molecule in aqueous solution, χ_{SP} has a different numerical value for each block, describing different solvation in water. The solvent is selective for a block in the copolymer when the interaction with that block is favourable to solvency, i.e., when χ_{SP} is less than 0.5 for that block. For example, the block B in AB diblock or ABA triblock copolymer will be solvophilic in a given solvent if χ_{SB} is at most 0.5 while it exceeds this limit for the A block, i.e., χ_{SA}>0.5.

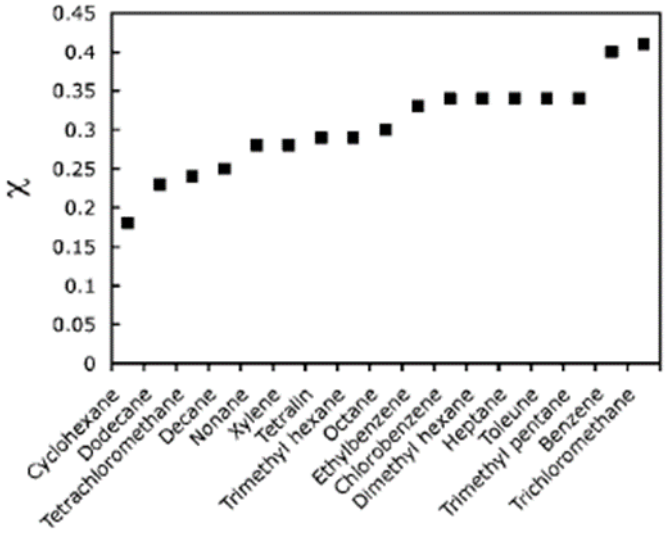

Figure 5. A rank-ordered list of χ values for F127 common good solvent for polyethylene. Most of the values are at or above 0.3 (Milner et al., 2009).

This limit is termed *theta condition* and expresses the point at which a polymer solution behaves ideally. Figure 5 displays a rank-ordered list of χ values for common solvents for polyethylene. These solvents become less good as their interaction parameters increase and approach the limiting value of 0.5. Thus, a factor promoting aggregation of surface-active block copolymer should increase dissimilarity between the two blocks by increasing the gap between their *Flory-Huggins polymer-solvent interaction parameters.* Copolymer with blocks displaying close values of χ parameters in a common solvent will exhibit poor dissimilarity between its blocks and will tend to behave like a homopolymer. In other words, the gap between

the χ parameters of blocks constituting a copolymer in a common solvent is a measure of its surface activity in that solvent.

The concentration at which surfactants or amphiphilic block copolymers start assembling in solution is termed cmc. It is a characteristic quantity for each surfactant, indicating the onset of its aggregation into discrete structures. This phenomenon is termed micellisation, and has "hydrophobicity" as the main driving force. The extent to which surfactant or amphiphile block copolymer can be hydrophobic is quantified in terms of hydrophilic lipophilic balance (HLB) number, which is a ratio of the size and strength of hydrophilic and hydrophobic moieties of a surfactant molecule (Young and Lovell, 2011). It corresponds to the degree of water or oil solubility of a given surfactant.

At its origin, the HLB concept has been introduced for practical application purpose, which is selection of suitable surface active agent (surfactant) for targeted industrial applications (wetting agent, detergent, emulsifier, etc,.) (Griffin, 1949) and its theoretical relevance is rather limited. Table 2 provides a basic framework of surfactants application suitability in diverse formulations according to their HLB. Numerous methods have been proposed to estimate surfactants HLB. Griffin's method for non-ionic (Kwaśniewska et al.) surfactants represented by Equation 2.3 in which M_h and M stand for molecular mass of the hydrophilic portion and molecular mass of the whole molecule, respectively, indicates that HLB should have a lower value for a surfactant with a massive head group, in which case it is very oil soluble, whereas it would be water-soluble for higher HLB. In this regard, high water-soluble surfactants are used for applications such as solubilisation and detergency, whereas hydrophobic surfactants are used to couple water-soluble materials in non-aqueous oil-based systems (Johansson and Somnasiliidarall, 2007).

$$HLB = 20 \times (M_h/M) \tag{2.3}$$

Table 2. HLB scale showing the classification of surfactant application (Binks and Clint, 2002).

HLB Numbers	Applications
2-3	Antifoaming agents
3-6	Water-in-oil Emulsifiers
7-9	Wetting and spreading agents
8-16	Oil-in -water emulsifiers
13-15	Detergents
15-18	Solubilizing agents

In both low molecular surfactants and amphiphilic block copolymers solutions, the formed micelles are aggregations of a determined number of monomeric surfactants or copolymer molecules into discrete structures in an aqueous medium. Micellar aggregations can adopt several shapes and sizes depending on the molecular structure of the surfactant, as well as solution conditions such as surfactant concentration, temperature, ionic strength, etc. However, they all retain a common characteristic, consisting of the orientation of the surfactant's nonpolar region in such a way that they maximise contact with one another. In the same way, surfactant polar regions in the micelle will orient so that they are in maximum contact with water.

For block copolymers, it is the difference in solvation of the distinct copolymer blocks in solution which is responsible for their orientation in the phases of similar compatibility, and their aggregation in microstructures which resemble (in essential aspects) the well-known micellar aggregate formed from low molecular surfactants (Nagarajan and Ganesh, 1989b). As for low molecular surfactants, the onset of block copolymer micellisation in bulk solution only occurs after completion of adsorption at the water/air interface, at the maximum surface tension decrease described by the Gibbs isotherm (Equation 2.1).

Surfactants and block copolymers are not, however, the only materials susceptible to display assembling properties in aqueous media. Coated spherical colloidal particles such as Barium Sulfate ($BaSO_4$), Carbon Black, Silica, metal oxides, etc., can act in surfactant molecules like manner, regarding the adsorption at fluid-fluid interfaces, the partition between immiscible liquids, and even the stabilisation of emulsions (Dickinson, 2009). If the hydrophobicity of surfactants and block copolymers is quantified in terms of the HLB, that of spherical colloidal particles is described in terms of their contact angle with the interface (Figure 6) and their wettability. Analysis of energy of attachment to a fluid-fluid interface is given by:

$$E = \pi r^2 \gamma_{\alpha\beta}(1 \pm cos\theta)^2, \quad (2.4)$$

where r is the particle radius, $\gamma_{\alpha\beta}$ is the fluid-fluid interfacial tension in which the sign inside the bracket is negative for removal from the water phase, and positive for removal from the non-polar phase. This equation shows that the particle is most strongly attached to the interface for $\theta = 90°$ at the maximum anchoring energy. Indeed, for truly hydrophilic particles, e.g. metal oxides, the measured θ angle is generally < 90° and the particle surface largely resides in water than in non-polar phase; on the other side, for truly hydrophobic particles, e.g. silica, θ is more generally > 90° and the particle largely resides in non-polar phase than in water (Binks and Clint, 2002).

It follows from these two cases that homogeneous coating of particles, e.g. with alkylsilane and fluorocarbon, impedes them from acting as amphiphilic materials. In order to achieve partial wetting of their solid surface by either fluids at interface responsible of their strong anchoring at the interface, the homogeneous coating has to be altered so that the particle is portioned in water-liking and non-polar fluid-liking specific areas (Chevalier and Bolzinger, 2013). This heterogeneous coating can be achieved in the gaseous phase and makes colloidal particles act as amphiphilic. At their critical aggregation concentration, their hydrophobically and hydrophilically coated parts will orient accordingly into the bulk, minimising or maximising their contact with water phase.

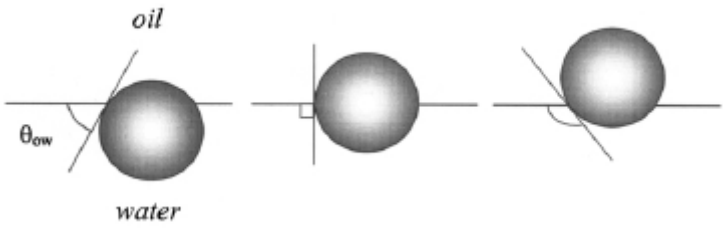

Figure 6. Position of a small spherical particle at a planar oil-in-water interface for a contact angle less than 90□ (left) equal to 90□ (centre) and greater than 90□ (right) (Binks, 2002).

All these above-described amphiphilic materials can display the same activity and related phenomena in all solvents discriminating its affinity between the distinct solvophobic and solvophilic regions of amphiphiles. In many cases, they display similar behaviours as in water, the only difference being the magnitude of interfacial tension or the solvent macroscopic properties correlated to hydrophobicity. Such similarities have been demonstrated in ethylene glycol (Nagarajan and Wang, 1996) and water-ethylene glycol mixed solvents (Nagarajan and

Wang, 2000) for surfactants, and in binary and ternary solvent mixtures for amphiphilic block copolymers (Sarkar et al., 2013).

When studying the surfactants or amphiphile block copolymers surface properties, the most important quantity to track is the cmc, which is the concentration at which surfactants start aggregating in the bulk solution. Many indirect and few direct experimental techniques are available to measure surfactant cmc in aqueous solution. Among indirect methods, fluorescence probing and dynamic light scattering (DLS) are some of the most encountered.

Figure 7 summarises some techniques characterised by different dependence of surfactant concentration on physical properties of micelle-forming amphiphile solutions. In most of the used methods, cmc is estimated as the point of intersection of two lines that interpolate the experimental data for low and high surfactant concentrations (Hadgiivanova and איבנובה'חדג, 2009). It should be pointed out that surface tensiometry, which is used in this project, is the only technique in which surfactant concentration is directly related to the micellisation driving force, i.e., hydrophobicity. In all other techniques, the variation of a given solution macroscopic property is monitored as surfactant concentration is increased. This variation is then related to hydrophobicity by some correlations.

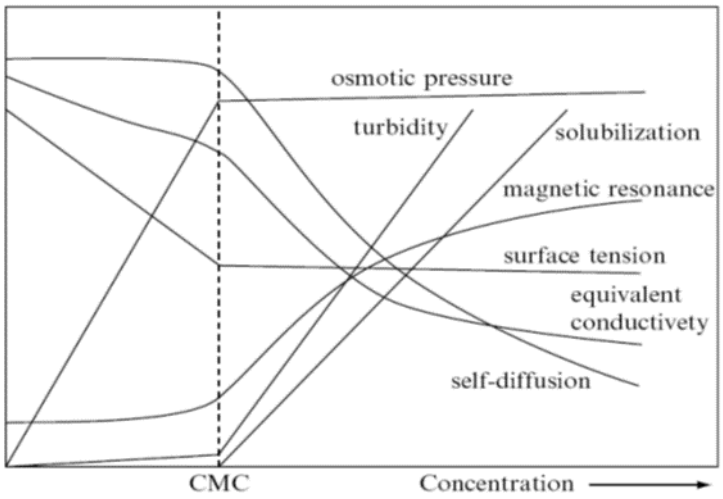

Figure 7. Schematic representation of concentration dependence of some physical properties of micelle-forming surfactant solution.

In fluorescence technique, a hydrophobic fluorescence dye is involved which displays different fluorescence characteristics depending upon the polarity of the solubilising medium (Goddard et al., 1985). A fluorescence probe, typically pyrene, which is sensitive to the polarity of solubilising medium, will display different fluorescence behaviour in micellar and nonmicellar

media. The change in polarity of medium surrounding pyrene, like its incorporation in micelle, results in the variation of fluorescence intensity, which increases with increasing surfactant concentration in solution (Figure 8).

The fluorescence spectra of pyrene as shown in Figure 8, exhibits five typical peaks but only the intensity of the first (I_1 at 373 nm) and the third peaks (I_3 at 384 nm) are related to the polarity of pyrene microenvironment, and variation of their ratio (I_1/I_3) with an increase in surfactant concentration is a sensitive parameter to estimate the onset of micellisation. Occurrence of a fairly sharp break in I_1/I_3 values versus concentration is then taken as the indication of solubilisation of the probe in a more hydrophobic environment than water (surfactant micelles in this case), indicating the onset of micellisation (Topel et al., 2013, Goddard et al., 1985).

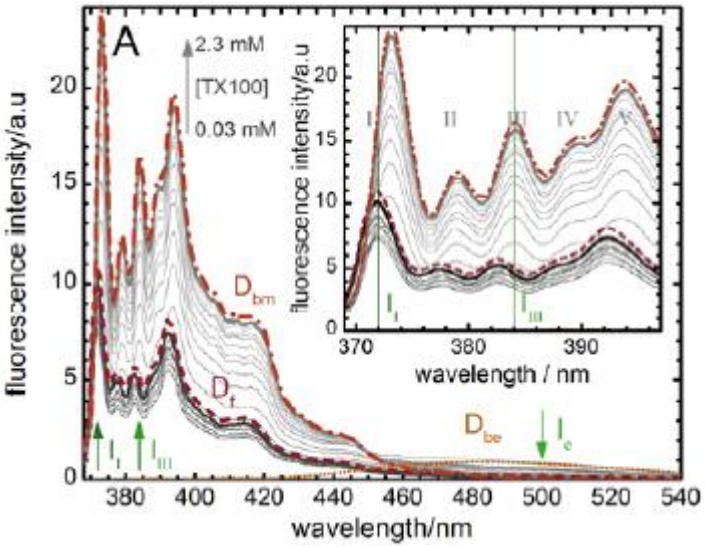

Figure 8. Fluorescence spectra of an aqueous solution of pyrene in Triton X-100 (Mohajeri and Noudeh, 2012).

To estimate the cmc from DLS technique, the intensity values of scattered light are monitored as a function of the surfactant concentration. Results provided via this method show trends similar to that displayed for turbidity in Figure 7. The scattering intensities detected below cmc have relatively constant values corresponding to that of deionised water (Topel et al., 2013). As surfactant concentration increases, scattering intensity starts rising suddenly due to an increase in the number of micelles formed in the solution. This break point is taken as the indication of aggregation beginning in the solution.

As can be seen from the two preceding paragraphs, these two techniques and others, go through indirect macroscopic properties of a micellar solution, namely fluorescence and scattered

intensities, to estimate aggregating property of surfactant in solution. When surface tensiometry is used to estimate the onset of micellisation, the interfacial tension decrease is simply recorded as surfactant concentration is increased, up to the point where a sharp break in the surface tension versus surfactant concentration appears, indicating the occurrence of the first surfactant aggregate (Figure 7).

This technique, contrary to the indirect methods, relates surfactant concentration to the micellisation driving force which is hydrophobicity directly. This direct relation between the aggregating species and the aggregation driving force in the surface tensiometry method has the advantage of being exclusively sensitive to factors affecting hydrophobicity. This is not the case with indirect methods. For example, fluorescence spectra of some amphiphiles in electrolytic solutions show existence of excimer formation upon excitation, whose quantity is monitored by salt concentration. In this case, steady state fluorescence not only correlates hydrophobicity to fluorescence intensity, but also captures the parasite relation between the salt effect on micelle formation and pyrene in the same micellar hydrophobic medium.

Indeed, when salt is added to the micellar solution, more micelles are formed and the total volume of hydrodynamic domain increases, diluting the pyrene and decreasing excimer formation (Pandit et al., 2000). Such a fact can be valuable for the method in the studies in which the purpose includes its understanding, but in all other cases, it can become a parasite phenomenon hindering comprehension of hydrophobicity.

Generally, impurities which can be sensitive in indirect detection methods such as steady-state fluorescence in causing alteration of results, are often insensitive to surface tensiometry, since they are generally not surface-active. This aspect makes surface tensiometry a more reliable method to study the surface activity of amphiphiles solutions. Moreover, surface tensiometry is not subjected to any restriction due to the nature of amphiphile, such as conductivity and electromotive force (emf) measurements, which are limited to ionic surfactants. All these aspects have made the surface tension method a reference technique in determining the cmc of self-aggregating species.

When applied to some block copolymers, surface tensiometry displays two breaks on the observed Gibbs isotherm. The first is ascribed to the wide molecular weight distribution of copolymer and the presence of hydrophobic impurities (Alexandridis et al., 1994b, Linse, 1994). The second is recognised, including by means of other investigation techniques, as the block copolymer cmc.

2.2.1 Factors affecting surfactants and block copolymers micellization

Factors not depending on the molecular structure of surfactants, but rather on the conditions of the solution such as temperature, presence of an electrolyte or a cosolvent, have a profound influence on the aggregation behaviour of surfactants. Change in temperature produces a profound effect on surfactant critical behaviour and thus on its self-assembly. This is due to the fact that subtle changes affect surfactant monomer polarity toward the water and hence its solubility in water.

Increasing temperature decreases hydration of the head hydrophilic part of surfactant. That is, it breaks hydrogen bonds between the water and surfactant polar region. As a consequence, surfactant becomes more hydrophobic and aggregates easily. Thus, the cmc initially decreases with increasing temperature, passing through a minimum beyond which it starts increasing again. This ambivalent aspect of temperature change effect on the onset of micellisation can be explained by the modification of surfactant nonpolar region solubilisation it gives rise to. The tail nonpolar region of a surfactant becomes less hydrophobic and more soluble in water as a further increase in temperature causes breakdown of the structured water surrounding it, disfavouring micellisation (Mohajeri and Noudeh, 2012). As a consequence, the onset of micellisation tends to occurs at higher surfactant concentration. Therefore, as temperature increases, the cmc (after passing through a minimum) starts rising. Beyond this minimum, the effect of hydrophobic group solubilisation in unstructured water begins to predominate in the dehydration of the head hydrophilic part of the surfactant and cmc increases again. Thus, the cmc versus temperature profile slop exhibits a “U” shape (Figure 9).

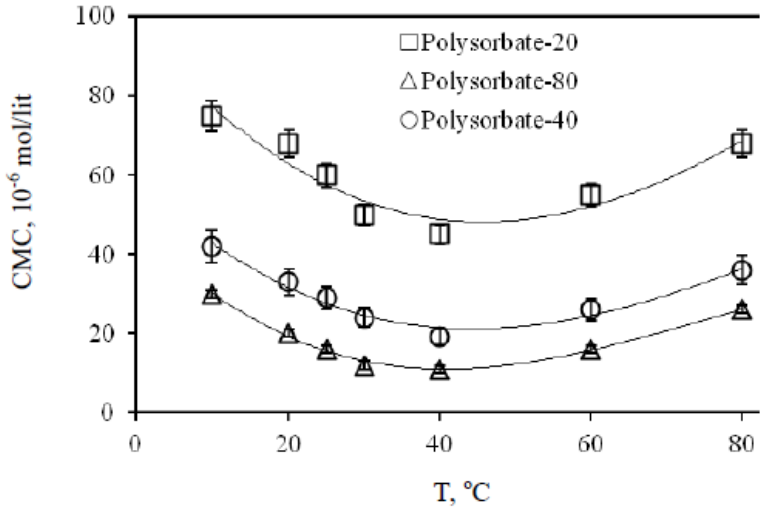

Figure 9. Cmc behaviour as a function of temperature for different surfactants (Banipal and Sood, 2013).

Inorganic electrolytes, typically inorganic salts (NaCl, KBr, LiF, Na_2SO_4, etc.), can increase the polarity of pure water while increasing solubility of polar solutes and decreasing solubility of nonpolar ones (Yalkowsky, 1999). These effects are respectively termed "salting in" and "salting out"(Saito, 1969). Since surfactant has two regions of different polarities, electrolytes will act accordingly on each of them. The solubility of nonpolar hydrocarbon region of the surfactant is decreased because its surrounding water is made more polar and therefore less like the nonpolar solute, increasing its squeezing out effect.

The effect on the polar region is the total opposite of that on its nonpolar counterpart. The solubility of the former is increased because the high polarity of water enhanced by electrolytes makes it more like the polar solute, therefore promoting hydrogen bonding between the water and surfactant head group region. Ultimately, the addition of electrolytes makes the hydrophobic region more hydrophobic and hydrophilic one more hydrophilic. This results in an even stronger dissimilarity of the two surfactant regions, enhancing amphiphilic effect in water, thus decreasing cmc.

In single ionic surfactant aqueous solutions, electrolytes decrease electrostatic interaction between like-charged head groups. This electrolyte effect arises by buffering repulsive interaction between the ionic head group with the same charges. Consequently, increasing inorganic salt concentration suppresses antagonistic effect due to like-charged head groups by leading to the screening of repulsive electrostatic interactions, thus bringing the mixture closer

to ideality (Sarmoria et al., 1992). Addition of electrolytes thus has an effect of lowering cmc for all types of surfactants in an aqueous solution.

This is not the case for cosolvents which are another class of additive compounds susceptible to induce modification of a surfactant behaviour in solution. Cosolvents are defined as organic compounds that are substantially miscible with water (Yalkowsky, 1999). They derive this property from their molecular structure. Having hydrogen bond donor groups (OH, SH, NH, NH_2, etc.) and sometimes in the same time hydrogen bond acceptor groups (≡N, =N—, =O, =S, —NH—, —O—, etc.), they interact strongly with water by bridging hydrogen bonds, ensuring mutual miscibility and aqueous solubility.

However, the distinguishing effect of cosolvents from electrolytes is that cosolvents are always less polar than pure water, thus decreasing water polarity. This is because the presence of hydrogen bond groups (donors and/or acceptors) is offset by that of hydrocarbon groups which reduce cosolvent polarity. This aspect provides cosolvents with a unique property, that of being miscible with both water and water-immiscible solutes.

Ultimately, cosolvents decrease polarity of water whilst electrolytes increase it. As a consequence, cosolvents increase water-solubility of the nonpolar hydrocarbon region by making its surrounding water less effective in squeezing it out. They also decrease hydrogen bonds density between water and the surfactant polar head group. These two effects reduce the driving force of surfactant self-association and increase cmc. Thus, electrolytes are more likely to increase water polarity while cosolvents decrease it. This is why the latter increase solubility of nonpolar solutes whereas the former increase solubility of polar ones. Their influences on amphiphiles self-assembly depend on their combined effects on the two surfactant dissimilar regions.

For amphiphilic block copolymers, one should always remember that the interaction parameter of each block increases with increasing temperature so that the dissimilarity in their interaction with the solvent decreases, favouring aggregation. More than for low molecular surfactants, the critical behaviours of copolymeric surfactants display strong dependence on temperature variation due to a difference in the hydration of the different blocks (Banipal and Sood, 2013, Sarmoria et al., 1992). The high molecular weight of their incompatible blocks makes their solvation extremely dependent on temperature variation. This temperature-dependence difference in solvation of incompatible parts of block copolymers is particularly pronounced in *ethylene oxide-propylene oxide*-based (PEO-PPO) copolymers, giving rise to a highly

thermally reversible micellisation process (Table 3) (Hecht and Hoffmann, 1994, Linse, 1993, Linse and Malmsten, 1992). More than for low molecular surfactants, this reversible micellisation has led to the widespread use of the critical micellar temperature (cmt) as a micellar parameter (Li et al., 2001b).

Adding salt and increasing the temperature have no selective effects on the blocks constituting a copolymer. The only difference between the consequences they generate on the blocks is a difference of degree and not of nature. By distorting water structure, the increase in temperature further increases the hydrophobicity of PPO and progressively causes that of PEO. By promoting water polarity through strengthening hydrogen bonds, most electrolytes make water more structured, inducing squeezing out of both PEO which becomes much less ordered compare to an aqueous electrolyte structure and PPO which is naturally more hydrophobic than PEO.

Table 3. Cmc of some Pluronics copolymer aqueous solutions as a function of solution temperature (Alexandridis et al., 1994b).

	L64 (40 % EO)		**P65 (50 % EO)**		**F68 (80 % EO)**		**F127 (70 % EO)**	
temp °C	**% w/v**	**mM**	**% w/v**	**mM**	**% w/v**	**mM**	**% w/v**	**mM**
20							4	3.174
25							0.7	0.555
30	1.5	5.172	4	11.78			0.1	0.079
35	0.4	1.379	1	2.941			0.025	0.019
40	0.1	0.344	0.35	1.029	7	8.333	0.008	0.006
45	0.02	0.069	0.1	0.294	3	3.571		
50			0.04	0.117	0.9	1.071		
55					0.3	0.357		

Cosolvents, unlike salts and temperature, have very selective effects on specific blocks constituting copolymers. Generally, all factors distorting water structure in a way to reduce the gap between the respective interaction parameters of different blocks, will make copolymer less able to aggregate. Due to the dissimilarity between the blocks being reduced, the copolymer will tend to behave like a polymer made of one species of monomer. For example, adding ethanol to a PEO-PPO based copolymer distorts the water structure in a way to provide better solvent conditions for the hydrophobic PPO block compared to pure water and disfavours micellisation. On the other hand, the addition of glucose and glycerol to water alters the water

structure in a way to dehydrate the hydrophilic PEO interface, thus reducing block copolymer critical micelle concentration (Table 4) (Sarkar et al., 2013).

A cosolvent modifies the respective *Flory-Huggins polymer-solvent interaction parameters* of the two blocks in a manner which results in dehydration or swelling of one of them by changing water polarity, favouring or disfavouring micellisation. Thus, by cleverly managing the variations in composition of the mixed solvent, the selectivity for a particular block can be managed and the micelle composition could ultimately be adjusted at will (Hamley, 2005). The most important copolymer structural parameter influencing cmc is the hydrophobic block length. In all surface active copolymers, the cmc is found to decrease with increase in hydrophobic block length. Generally speaking, the lower the relative hydrophilic block content, the larger the influence of the hydrophobic block on micellisation (Hamley, 2005).

Table 4. Cmc contribution due to the cosolvent for Pluronic F105 and F127 at 25 ℃ (Sarkar et al., 2013).

Solvent used (%v/v)	**P105**	**F127**
	cmc (%w/v)	**cmc (%w/v)**
Water	0.31	0.71
10% Glycerol	0.1	0.29
20% Glycerol	0.05	0.11
40% Glycerol	0.01	0.02
10% Glucose monohydrate	0.1	0.18
15% Glucose monohydrate	0.05	0.08
10% Ethanol	0.41	1
20% Ethanol	0.59	1.5
40% Ethanol	0.62	1.71

Another distinguishing feature making block copolymer critical behaviour in solution more complex to study is their inherent polydispersity (Alexandridis et al., 1994b, Zheng and Davis, 2000, Gao and Eisenberg, 1993) and the presence of impurities (Linse, 1994) which introduce third surface-active agents in the molecule, inducing parasitic critical behaviours.

2.2.2 Surfactant Micellization Models

Simple amphiphile solutions consist of singly dispersed surfactant molecules, water molecules and surfactant aggregates of various sizes and shapes. Many empirical relations have been developed relating structural surfactant features to their respective cmc. Among them, some of the most famous show that ionic surfactants' cmc are linearly dependent on the solution ionic

strength (Corrin and Harkins, 1947) (which can vary with the addition of electrolytes). For non-ionic surfactants, it has been found that their cmc(s) obey the following equation (Klevens, 1953):

$$\log(cmc) = A - Bn, \tag{2.5}$$

in which n is the number of carbon atoms in the alkyl chain, A and B are empirical coefficients whose values are tabulated for homologous series in Table 5.

Table 5. Constants for the relation log(cmc)=A-Bn (Rosen and Kunjappu, 2004).

Surfactant Series	**Temp** ℃	**A**	**B**
Na carboxylates (soaps)	20	1.8	0.3
K carboxylate (soaps)	25	1.9	0.29
Na alkane-1-sulfonates	40	1.5	0.29
Na alkane-1-sulfonates	55	1.1	0.26
Na alkyl-1-sulfates	45	1.4	0.3
Na alkyl-1-sulfates	60	1.3	0.28
Na alkyl-2-sulfates	55	1.2	0.27
Na p-alkylbenzenesulfonates	55	1.6	0.29
Na p-alkylbenzenesulfonates	70	1.3	0.27
Alkyltrimethylammonium bromides	25	2.0	0.32
Alkyltrimethylammonium bromides	60	1.7	0.29

The main modelling approaches of surfactant solutions consider micellisation either as equilibrium between aggregates and surfactant monomers with respect to the exchange of each component in a multi-component surfactant mixture, or a chemical reaction resulting in aggregate made up of N surfactant ions and p counterions (in case of ionic surfactants) (Danov et al., 2014). These *phase separation* and *mass action models*, respectively, can be applied to both single and multi-component surfactant mixtures.

From the measured cmc of a single component surfactant solution, various thermodynamic parameters may be deducted. Among these, the free energy of surfactant micellisation ΔG_M° has been determined using the following relationships for non-ionic and ionic univalent surfactants, respectively:

$$\Delta G_M^\circ = RT \ln X_{cmc} \tag{2.6}$$

$$\Delta G_M^\circ = RT(1+\epsilon) \ln X_{cmc}, \tag{2.7}$$

in which X_{cmc} is the *cmc* value expressed in mole fraction, R and T have their usual meaning and ϵ is the counter-ion dissociation constant. In the phase separation model, these free energies of single surfactant solution micellisation are viewed as the free energy of transfer of one surfactant from the aqueous phase to the micellar pseudo-phase. In many studies dealing with classical ionic surfactants, i.e., those made up of monovalent ionic group bonded to one alkyl chain, Equation 2.6 is used rather than 2.7, irrespective of counter-ion dissociation constant (Rosen and Kunjappu, 2004, Zana, 1996).

For such surfactants, with only one ionic head group, the plot of ΔG_M° vs m (carbon number of surfactant tail) is quite similar to that of a non-ionic surfactant, so that in this specific case, Equations 2.6 and 2.7 are equivalent. Strictly speaking, the relationship between cmc and free energy of micellisation for ionic surfactants is critically dependent on the valance, number of head groups and alkyl chains of the surfactant (Bhattacharya and Haldar, 2004). From a surfactant ion, $A_j^{iz_s}$ made up of i charged groups of valency z_s (total charge iz_s) and j alkyl chains, the mass action model allows the reaction of micellisation to be written as:

$$NA_j^{iz_s} + pX^{z_c} \rightarrow A_{j,N}^{NiZ_s - pz_c}, \tag{2.8}$$

in which $A_{j,N}^{NiZ_s - pz_c}$ stands for micelle of aggregation number N, counterions p, containing N_j alkyl chains and of electrical charges $Niz_s - pz_c$. One must remember that the electroneutrality condition leads to the number of counterions per surfactant molecule to be given by $n_c = i|z_s|/|z_c|$, in which z_c is the valance of the counterion X^{z_c}. It can then be derived through the equilibrium constant K obtained by applying mass action law, the condition of electroneutrality of the system at cmc, and the fraction ϵ of micellised surfactant ions neutralised by micelle-bound counterions, the general free energy of ionic surfactant micellisation which, in taking into account the fact that $\left[A_j^{iz_s}\right] \sim cmc$, can be written as (Zana, 1996, Bhattacharya and Haldar, 2004):

$$\Delta G_M^\circ = RT\left(\frac{1}{j} + \epsilon\frac{i}{j}\left|\frac{z_s}{z_c}\right|\right)\ln X_{cmc} + RT\left(\frac{i}{j}\left|\frac{z_s}{z_c}\right| \varepsilon\, ln\, \frac{i}{j}\left|\frac{z_s}{z_c}\right| - \frac{\ln j}{j}\right) \tag{2.9}$$

Sometimes, the second term on the right-hand side of this equation is very small compared to the first one and can be neglected (Shukla and Tyagi, 2006, Moroi et al., 1985). Depending on the structural features of the ionic surfactant in solution, Equation 2.9 can take various forms,

dictated by the number i of charged groups, j of alkyl chains, and the numerical values of z_s and z_c valances.

Classical Surfactants with Monovalent Counterions

Example of such a surfactant is sodium dodecyl sulfate (SDS), and in this case, $i = j = |z_c| = |z_c| = 1$. Equation 2.9 can then simply be reduced to Equation 2.7 and even to 2.6 for very low dissociation rates.

Classical Surfactants with Divalent Counterions

Examples of such surfactants are calcium and magnesium dodecyl sulfate. In this case, $i = j = |z_c| = 1, |z_c| = 2$, and the two terms in the right-hand side of Equation 2.9 reduce to:

$$\Delta G_M^{\circ} = RT(1 + \epsilon/2) \ln X_{cmc} - (RT\epsilon \ln 2)/2, \qquad (2.10)$$

in this instance, the second term on the right-hand side is very small (smaller than $0.5\ RT$ (Moroi et al., 1985, Zana, 1996)]) and can be neglected with respect to the first term.

Bolaform Surfactants with Monovalent Counterions

Bolaform surfactants, also known in contracted form as Bolaamphiphiles, refer to surfactant molecules that have polar hydrophilic head groups at both end sides of hydrophobic tails (Dzulkefly et al., 2010) (Figure 10). Examples of Bolaform surfactants are dodecane 1,12 bis (trimethylammonium bromide) and dodecane 1,12 bis (triethylammonium bromide) for which $i = 2,\ j = |z_c| = |z_s| = 1$. Equation 2.9 becomes for them:

$$\Delta G_M^{\circ} = RT(1 + 2\epsilon) \ln X_{cmc} + 2RT \ln 2 \qquad (2.11)$$

One can notice how far the contribution of the counterions is important in this equation because of factor 2 multiplying ϵ and the whole second right-hand side term, which actually increases the free energy of micellisation greatly. This contribution cannot be neglected in the estimation of Gibbs energy associated with micellisation of these kinds of surfactants if correct quantities are targeted.

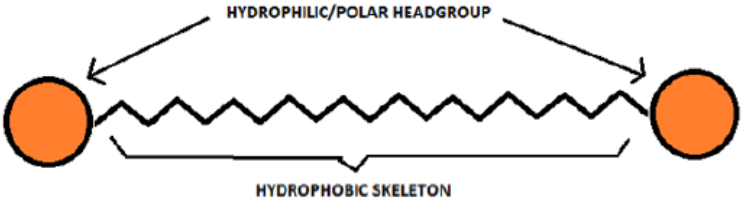

Figure 10. Schematic representation of bolaform surfactant (Sharma et al., 2017).

Gemini (Dimeric) Surfactants with Monovalent Counterions

A Gemini or dimeric surfactant (GS) is an amphiphile consisting of two conventional surfactant molecules covalently linked together by a spacer (Shukla and Tyagi, 2006). It is made of at least two hydrophobic tail and two polar hydrophobic heads (Figure 11). The spacer could be polar or nonpolar, and its effect on aggregation behaviour can be determinant (Zana, 2002). For instance, in the case the spacer is non-polar and hydrophobic, it has been found to increase micellisation tendencies of cationic GS when sufficiently long, and to increase adsorption propensity at interface when short (Zana and Xia, 2003). Other characteristics of spacers such as their flexibility and their polarity could also have a determinant influence on GS bulk and adsorption behaviours

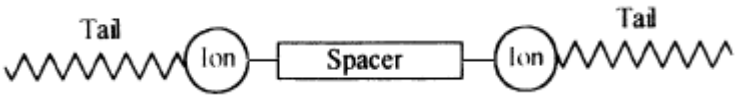

Figure 11. Schematic representation of an ionic GS (Gilanyi and Wolfram, 1981).

Examples of GS include hexanediyl-α,ω-bis-N-(2-hydrox-yethyl)-N-methylhexadecyl ammonium dibromide (G_{16}) (Sharma et al., 2017) for which $i = j = 2$ and $|z_c| = |z_s| = 1$. Equation 2.9 then becomes:

$$\Delta G_M^{\circ} = RT\left(\frac{1}{2} + \epsilon\right)\ln X_{cmc} - (RT/2)\ln 2 \qquad (2.12)$$

One can notice that free energy associated with micellisation of GS should be much lower than what expected for bolaamphiphiles, not least because of the disappearance of the ϵ multiplying factor. Actually, this relative promptness of GS to micellisation when compared to bolaamphiphiles, can further be increased by choice of gemini with an appropriate spacer.

2.3 Mixture and synergism in binary surfactants systems

The solubility of organic hydrophobic molecules in aqueous media is enhanced by the addition of surfactants to the solution (Nagarajan et al., 1984). Added surfactants molecules aggregate

to form micelles which provide a more compatible environment for the sparingly organic soluble molecules. The micelles' tendency to entrap hydrophobic molecules and thus to solubilise them is the basis of surfactant applications in numerous biological, pharmaceutical and separation processes. Surfactants are however rarely singly used in industrial applications and ordinarily, mixed surfactants systems form aggregates with enhanced physicochemical properties resulting in improvement of their performance in terms of solubilisation efficiency, surface activity, synergistic mixing and other properties (Banipal and Sood, 2013). For practical and economic reasons, a low value of critical micelle concentration is always sought.

According to the phase separation model, binary mixed micellar aggregates formation is described by the equation below (Hierrezuelo et al., 2005):

$$\frac{1}{CMC_{mix}} = \frac{\propto_1}{f_1 CMC_1} + \frac{(1-\propto_1)}{f_2 CMC_2}, \tag{2.13}$$

in which CMC_{mix} , CMC_1, and CMC_2 are critical micelle concentrations of the mixture of pure surfactant 1 and pure surfactant 2, respectively; $\propto_1$ is the mole fraction of surfactant 1 in the total surfactant mixture, and the variables f_1 and f_2 are the micellar activity coefficients of surfactants 1 and 2, respectively. The micellar activity coefficients f_1 and f_2 can be calculated from:

$$f_1 = \exp[\beta_{12}(1-X_1)^2] \tag{2.14}$$

$$f_2 = \exp[\beta_{12}X_1^2], \tag{2.15}$$

where β_{12} is a parameter that reflects specific interactions between surfactants 1 and 2, and X_1 is the mole fraction of surfactant 1 in the mixed micelle.

In many practical applications, one often mixes different types of surfactants in order to enhance the desired properties of the resulting system (Shiloach and Blankschtein, 1997, Shiloach and Blankschtein, 1998). If this occurs, then the system is said to exhibit synergism. When it is desired to use less surfactant to achieve a given effect in surfactant solution, one can use a surfactant mixture that shows greater efficiency than that attainable by either surfactant by itself. For example, a mixed system that exhibits synergism in surfactant aggregation can have a cmc which is considerably lower than that of each pure surfactant.

Synergism is a result of negative deviation from ideality. When this deviation is positive, the resulting effect is termed antagonism, which is the opposite of synergism. A negative deviation reveals an attractive interaction between two surfactants and is characterised by a negative

value of the interaction parameter (β_{12}). To maximise the lowering of cmc, the combined surfactants should show strong attractive interaction in the mixed micelle, i.e., they should display a large negative value of interaction parameter (Rosen, 1989). The same criteria is applied for maximising efficiency in surface tension reduction. In this case, combined surfactants should show strong interaction in the mixed monolayer at the interface between aqueous solution and air.

The mixture of given surfactants can exhibit either departure from ideality. Thus, it is convenient to select suitable pairs or sets of surfactant species that optimise the desired properties of the formed system. Surfactants' chemical structure has a decisive influence on such a selection. In this respect, the highest negative values of β_{12} for maximum synergism are achieved when surfactants of opposite charges are mixed. In this case, to the combined hydrophobicity of the mixed surfactants is added their attractive interaction which further favours the reduction of the surface tension in the interface monolayer and onset of micellisation in the bulk.

Ionic-nonionic surfactants mixtures also exhibit a negative value of β_{12}, yet not as high as for opposite surfactant mixtures. Non-ionic surfactants have no electrical charges. Instead, they contain groups such as hydroxyl and ether, as polar components (Yalkowsky, 1999). These oxygenated groups are however less polar than ionic groups contained in ionic surfactants. This is why a combination of ionic and non-ionic surfactants while showing attractive interaction and negative β_{12} value, is less synergistic than that of opposite surfactant mixture. Combination of non-ionic surfactants tends to mix ideally ($\beta_{12}=0$) (Sarmoria et al., 1992).

2.4 Polymer-surfactant interaction in aqueous solution

Polymers can exhibit interactions with surfactants. The aggregation behaviour of any surfactant can be greatly influenced by the presence of polymers. Interactions between polymers and surfactants are however substantially different depending on polymer skeletal structure. Linear, cyclic, branched and network polymers alter the amphiphilic character of surfactants in solution differently. The following presentation is limited to interactions with linear polymers. They will further be classified into homopolymers which are polymers derived from one species of monomer, and block copolymers which are polymers in which the repeat units exist only in blocks of the same type (Young and Lovell, 2011).

2.4.1 Homopolymer-surfactant interaction mechanisms

Mixed systems of macromolecules and surfactants are used in numerous industrial applications. Controlling interactions between macromolecules and low molecular weight amphiphiles is of crucial importance for the technical performance of these applications. Combination of water-soluble polymers and surfactants in aqueous media gives rise to the formation of association structures instead of unique micelles only. The occurrence of these complex structures and their properties depend on polymer and surfactant molecular characteristics.

It is generally understood that the simultaneous presence of water-soluble polymers and surfactants in aqueous solution provides a third thermodynamic alternative to surface adsorption and self-micellisation of the surfactant (Rulison, 2004). If the polymer contains hydrophobic segments, either pendant to or incorporated in the backbone, then in virtue of the hydrophobic effect, it can become thermodynamically favourable for the surfactant to adsorb on the polymer and to form aggregates with a hydrophobic portion of the polymer. It follows that interaction between polymer and surfactant in aqueous media represents a competition between the formation of polymer-free surfactant aggregates and polymer-surfactant association complexes. Factors controlling this competition are molecular features of polymer and surfactant.

Polymer-surfactant isotherm in aqueous solution, unlike surfactant isotherm, displays two critical points instead of one as surfactant is added to the solution. In the presence of a polymer in solution, surfactant adsorbs at the water/air interface and decreases surface tension as shown between positions 1 and 2 in Figure 12. As water/air interface saturation by surfactant molecules approaches, it can appear more thermodynamically favourable for the surfactant to adsorb on the polymer, instead of being continually expelled to the water/air interface or aggregating as free micelles in the bulk solution. This occurs at point 2 on the graph, which is termed “critical aggregation concentration” (cac) for the polymer-surfactant pair. Beyond cac and throughout a certain interval (up to point 4), solution surface tension is relatively independent of increases in surfactant concentration while added surfactant is adsorbed onto polymer.

As surfactant concentration increases further, the polymer becomes saturated with surfactant (point 4) and beyond this point, increases in the surfactant concentration resulting in increasing concentration of surfactant at the water/air interface, which is termed “surface excess

concentration". Consequently, water/air interfacial tension begins to decreases as surfactant concentration is increased. Finally, point 5 is the critical micelle concentration of surfactants in the presence of the polymer. At this point, both the polymer and the water/air interface are saturated with surfactant molecules and surfactant pure micelles formation becomes thermodynamically favourable, while the water/air interfacial tension remains constant.

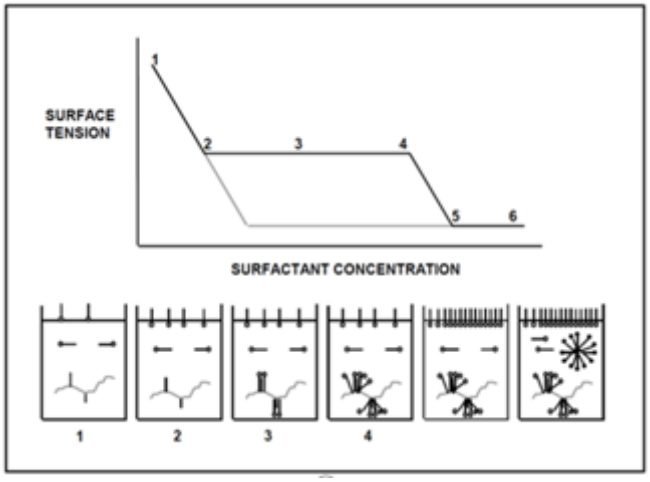

Figure 12. Polymer-surfactant isotherm in aqueous solution (Rulison, 2004).

The distinct regions in the Figure 12, however, do not appear so sharply in reality, even for the most carefully performed measurements. The lack of a distinct cac for example when the shape of the isotherm is affected by the polymer cosolute characteristics can be attributed to the fact that hydrophobic parts grafted on portions of the modified homopolymer always displays a distribution of the extent of hydrophobic modification instead of unique quantity characterising this property. Therefore, there is not simultaneous adsorption of all hydrophobic parts grafted on the polymer. The most hydrophobic portions of the polymer chains, or generally the most hydrophobic chains, are the first to begin to compete with the water/air interface for surfactant adsorption and the cac becomes a distribution of points pertaining to the distribution of polymer molecules (Rulison, 2004).

A similar effect is displayed for polymer polydispersity. In this case, there is preferential adsoption of larger molecules on smaller ones, giving rise to a cac distribution of points pertaining to the distribution of polymer molecular chains, instead of unique cac. Impurities in the surfactant or polymer can have similar effects. Generally, it can be stated that the distribution of polymer characteristics in its architecture causes a distribution in the points at which it becomes thermodynamically active and able to interact with surfactant molecules. Consequently, the general shape of isotherm in Figure 12 is distorted, typically exhibiting

parabolic curvature around point 2 and all critical points, instead of a sharp change in slope at these points.

Association of surfactants and polymers in aqueous media represents a balance between several forces favouring and resisting complex formation. The main force favouring complex formation is polymer hydrophobicity. The hydrophobic properties in a given polymer are promoted by grafting along its chain hydrophobic modifiers which impart some hydrophobicity to the molecule. The grafting density along the polymer determines the extent of its hydrophobicity. The interaction between polymer and surfactant then arises as an effect of biding of the surfactant by the hydrophobic segments of the macromolecule. These hydrophobic segments are termed "binding sites".

Polymer molecules usually associate with not just one surfactant but micellar aggregates of surfactant (Shirahama et al., 1974). This is indicated by the experimental fact that the binding of some surfactants to non-ionic polymer arises only beyond a critical surfactant concentration, suggesting that surfactants bind cooperatively to the polymer molecules as surfactant aggregates rather than as individual molecules (Nagarajan, 1985).

The competitive micellisation and complexation equilibrium of polymer and surfactant is described by the following mass balance equation of solution in which are supposed to be free micelles and complex structures, i.e., micelles bound to the polymer molecule:

$$X_t = X_1 + g_f(K_f X_1)^{g_f} + g_b n X_P \left[\frac{(K_b X_1)^{g_b}}{1 + (K_b X_1)^{g_b}}\right], \tag{2.16}$$

in the above equation, the total surfactant concentration X_t is partitioned into a single dispersed surfactant X_1, surfactant-free micelles X_f represented by the second-hand right term, and surfactant bound as aggregates X_b represented by the third-hand right term in the equation. In the second term, g_f is the average aggregation number of free micelles, and K_f is the intrinsic-equilibrium constant for their formation. In the third term, each polymer is assumed to have n binding sites for micelles of average size g_b. K_b is the intrinsic-equilibrium constant for the binding of the surfactant on the polymer, and can also be visualised as the intrinsic-equilibrium constant for the formation of polymer-bound micelles (Goddard, 2018). X_P is the total concentration of polymer molecules in solution, and the quantity nX_P expresses the effective mass concentration of polymer in a solution which is independent of polymer molecular weight. This implies that for polymers of different molecular weights, but at the same mass concentration in solution, one should observe essentially similar surfactant binding behaviour.

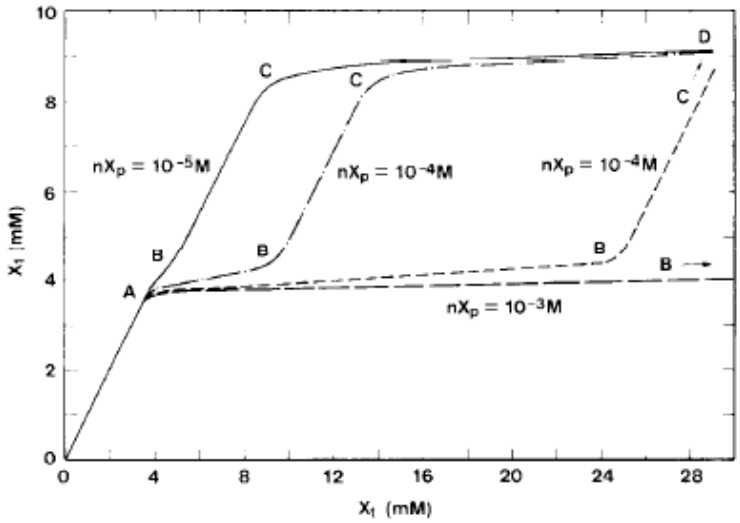

Figure 13. The equilibrium concentration of a singly dispersed surfactant (X_1) as a function of the total concentration of the surfactant (Xt) for various polymer concentrations. Case of PEO+SDS solution (Goddard, 2018).

The occurrence of surfactant complexation with polymer is determined by the relative magnitude of K_b, K_f, g_b, and g_f. If $K_f > K_b$ and $g_b \approx g_f$, the formation of micelles occurs in preference to complexation. If $K_f < K_b$ and $g_b \approx g_f$, complexation-aggregation on the polymer takes place first and upon saturation of the polymer, free micelles form. If $K_f < K_b$, but g_b is much smaller than g_f, then the formation of free micelles can occur even before saturation of the polymer. A first critical surfactant concentration is observed close to $X_1 = {K_b}^{-1}$ (cac) represented by point A in Figure13, and the second and final critical concentration will occur near $X_1 = {K_f}^{-1}$ (cmc). In Figure 13 plotted singly dispersed surfactant concentration (X_1) versus total surfactant concentration (X_t) are shown as well as the calculated relations between these two concentrations on the basis of the values for the parameters K_b, K_f, g_b, and g_f for the sodium-dodecyl-sulfate−polyethylene-oxide (SDS-PEO) system. In this system, $K_f < K_b$ and g_b is slightly smaller than g_f (Gilanyi and Wolfram, 1981).

In the region from O to A, surfactant molecules remain singly dispersed. In the region from A to B, the formation of polymer-bound micelles occurs. One can note that the monomeric surfactant concentration X_1 increases very little in this region. This results from the relatively large size g_b of the polymer-bound micelles and reflects the cooperative nature of the formation of bound micelles. In contrast, if g_b is small, then X_1 would increase more significantly in the region AB. It can also be noted that if the mass concentration of the polymer is very small (if nX_P is small), then the region AB is confined to a narrow range of surfactant concentrations

and this region may even escape detection ($nX_P = 10^{-5}M$ in Figure 13). Alternatively, if nX_P is very large, then saturation point B may not be reached. These two scenarios express the surfactant concentrations X_t at points A and C in relation to polymer concentration. The total surfactant concentration X_t at point C (surfactant cmc) depends directly on the mass concentration (nX_P) of the polymer, while the first critical concentration A (cac) is independent of the concentration of the polymer in solution.

However, while complexation of non-ionic polymer with anionic micelles has been detected by means of several techniques, no indication of complex formation or only weak complexation occurs for such polymers with a cationic and non-ionic surfactant. It follows from this observation that some solutions exhibit two critical concentrations, but not all. This is because the competition between the formation of polymer-free surfactant aggregates and polymer-surfactant association complexes is mainly governed by the nature of interactions at the micellar surface (Nagarajan, 1985).

In surfactant association with polymer molecules to form a polymer-micelle complex, the polymer segment penetrates the interfacial region of the micelle and shields a part of the micellar core from water (Figure 14). This shielding of a micellar part by a polymer segment is known as the area per surfactant molecule of the micellar core shielded by the polymer (a_{pol}). a_{pol} will generally be large for a very flexible polymer which can largely surround the micelle. Contrariwise, for a rigid polymer, a_{pol} should be expected to be small.

The consequence of this shielding is the decrease of the positive interfacial free energy of the head groups lying at the micellar surface as well as increase of their steric repulsions. For anionic surfactants, such as SDS, the first effect dominates, resulting in the lowering of X_b below X_f, thus favouring complexation. For many non-ionic surfactants, because of their bulky polar head groups, the second effect dominates, increasing X_b above X_f and consequently preventing complexation.

Figure 14. Schematic representation of polymer-micelle complexes topology in aqueous solution (Nagarajan, 1985)

For a cationic surfactant, in addition to the shielding effect, a polymeric electrostatic effect can come into account. Indeed, for some polymers, such as PEO and Polyvinylpyrrolidone (PVP) (Brackman, 1990), there is an electrostatic contribution from the electron-deficient oxygen atom of the ether linkage which can be regarded as a free ion providing the molecule with a cationic character and interacting electrostatically with the surfactant head groups. For cationic surfactants interacting with a water-soluble polymer exhibiting such an electrostatic effect, the interaction is repulsive and thus, unfavourable to polymer-micelle association. However, it is very favourable for anionic surfactant and acts as an additional driving force for complexation.

2.4.2 Interaction between amphiphilic block copolymers and surfactants

In contrast to homopolymers which only have grafted hydrophobic sites on their chains, block copolymers contain entire hydrophobic blocks which exhibit solvation incompatibility with water. Thus, Interactions of low molecular surfactants with block copolymers appear more complex to study than that with homopolymers, even when hydrophobically modified, because both cosolutes are subjected to critical behaviours in solution.

Block copolymers and surfactants are both classes of solutes likely to aggregate in aqueous solutions. For this reason, their interaction mechanisms are better understood in distinguishing between the associated and non-associated phase behaviours of one of them in solution. Depending on whether the copolymer is associated in micellar form or not, the binding with surfactant can be stated as “complex formations” or “surfactant-polymer interactions”

respectively (Li et al., 2011). The best thing to do is thus to study their interactions below and above copolymer cmc.

Block copolymers, whether associated or not, interact differently with low molecular surfactants, depending on whether they are ionic or non-ionic. This difference lies in the distinction between the involved binding mechanisms. The implications of this distinction are different for the two copolymer phase behaviours in solution, namely associated and non-associated. For a non-associated block copolymer solution in which is added non-ionic surfactant, the only binding mechanism is the polymer-induced micellisation driven by hydrophobic aggregation. It follows that only hydrophobic blocks of copolymer and surfactant are involved in the interaction in such a mixture. If the added surfactant is ionic, irrespective of whether it is positively or negatively charged, the ion-dipole interaction between surfactant heads and copolymer chain is added to the above hydrophobic driving force.

An important feature in the case of mixture with anionic surfactants is the strong interaction due to full-binding of the surfactant on the whole chain of the copolymer. Figure 15 describes the binding mechanism of SDS, or generally anionic surfactants, with PEO-PPO-based copolymer (Dai et al., 2001). One can see that SDS first starts binding with the PPO block through induced micellisation at low SDS concentration, and deeply dehydrates PPO segments from water. As SDS concentration is increased, the PEO segment is also dehydrated through the same polymer-induced micellisation. Phase C indicates the beginning of copolymer reorganisation through ion-dipole association where PEO first rehydrates followed by PPO segments. The aggregation number of SDS is thus optimised by fully binding to the copolymer backbone.

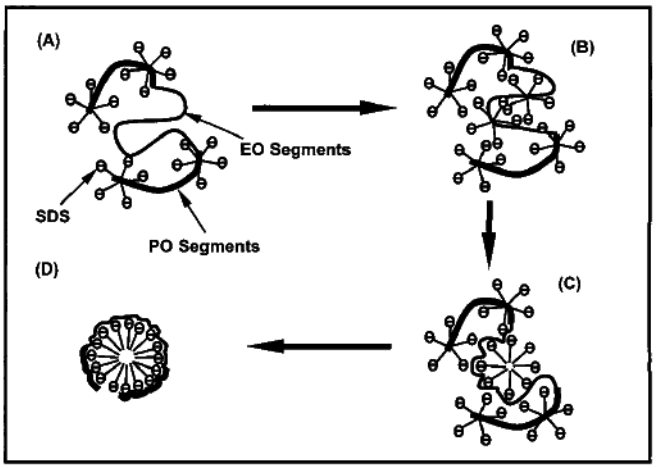

Figure 15. Schematic binding process of SDS and PEP copolymer. Regions A and B represent the polymer-induced micellisation process at low SDS concentrations where PPO segments dehydrate from water phase first followed by PEO segments. Regions C and D indicate reorganisation of SDS-PEP aggregation complex to form the ion-dipole association complex, where PEO segments first rehydrate into the water followed by PPO segments. The darker lines represent the hydrophobic PPO block while lighter ones are PEO (Dai and Tam, 2001).

One must remember that cationic surfactants in a PEO-based copolymer aqueous solution bind only to the hydrophobic counterpart of the copolymer because of the protonation of the hydrophilic PEO segment providing molecule with a cationic character. Anionic surfactants are not subjected to such a restriction. During the early binding process with PPO and PEO segments driven by hydrophobic aggregation, surfactant micelles of lower aggregation number adsorb on the polymer chain and the latter is solubilised in the hydrophobic core of surfactant micelle (regions A and B of Figure 15) (Qiu et al., 2002). This process corresponds to a dehydration mechanism of the copolymer chain.

As surfactant concentration increases in solution, the dominant interaction becomes the binding between ionic charged surfaces of anionic surfactant micelle and the copolymer backbone driven by ion-dipole mechanism. In this process, the hydrophilic block dehydrates first, followed by the hydrophobic PPO segment (regions C and D of Figure 15). The entire copolymer then rehydrates and is excluded from the micelle core to interact with surfactant head group. The balance between these two binding mechanisms determines the strength of copolymer-surfactant interaction and copolymer-surfactant complex aggregation number.

One must keep in mind that the interaction of low molecular surfactants with monomeric block copolymer is subjected to thermodynamic association with individual blocks of copolymer molecule. From the comparison of thermodynamic profiles of mixed copolymer-surfactant systems and individual copolymer blocks-surfactant systems, the binding affinity of a given surfactant with each block of amphiphilic copolymer can be inferred. Thus, while a cooperative

binding between amphiphilic PEO-based copolymer and anionic surfactants has been found on the whole chain of such copolymers, cationic surfactant only exhibits binding with their hydrophobic blocks (Sastry and Hoffmann, 2004). This is because of the cationic character conferred to PEO by electron deficiency bonds inducing repulsion with cationic surfactant head groups. Pure surfactant micelles in a mixed system with block copolymer only form after completion of the two binding mechanisms monitoring interaction with copolymer, at a point indicating saturation of copolymer chain. This is why copolymer-surfactant systems can exhibit two critical points just as homopolymer-surfactant systems do (Figure 12).

Both homopolymer-surfactant and nonassociated copolymer-surfactant systems in solution can exhibit two transition points which bear similar significances, in indicating onset and saturation of binding with copolymer. The value $cmc - cac$ can be used to estimate the amount of anionic surfactant bound to the copolymer backbone (Dai and Tam, 2001). These physical significances are the same for all surfactant/non-ionic polymer systems but can involve different binding mechanisms underlying each transition.

The salient characteristic in mixed copolymer-surfactant systems when the former is associated in micellar structure, is the enhancement of block copolymer solubility, resulting in micelles dissociation into single dispersed monomeric species (Bahadur et al., 1988). In a PEO-PPO based copolymer, this is likely to happen if a surfactant is ionic (Sastry and Hoffmann, 2004, Alexandridis and Hatton, 1995). At copolymer cmc in solution, single dispersed monomeric copolymers are in equilibrium with copolymer micelles. Little informations are available on the general trend of isotherm when copolymer micelle is subjected to disruption by ionic surfactants. However, it is generally observed that at low surfactant concentrations, due to high concentration of block copolymer monomers in equilibrium with their micelles, surface tension remains unaffected since block copolymer monomers dominate at interface and inhibit surfactant adsorption. It is generally agreed that presence of surfactant ionic charges inside copolymer micelles is accountable for micelle disruption due to their mutual electrostatic repulsion. Finally, pure surfactant micelles only form after completion of surfactant adsorption at interface and binding to copolymer backbone, which is correlative to block copolymer micelles disruption.

Mixed copolymer/non-ionic surfactant system displays a concentration range of mixed micelle of the two cosolutes before the surfactant starts forming pure micelles. In this region, surface tension remains unaffected due to weak activity of surfactant at the interface. In this case, there

is only one critical point as for pure surfactant solutions, instead of two as for ionic surfactant-copolymer systems. The portion 1-2 in Figure 12 is excluded from the surface tension graph. The 2-4 region is then the range of copolymer-surfactant mixed micelle occurrence, before surfactant pure micelle start forming at point 5.

2.5 Emulsion Stability

Emulsions are colloids in which both the dispersed phase and the dispersion medium are liquids. They are obtained by shearing together two immiscible liquids, leading to fragmentation of one phase into the other. Depending on the size of the dispersed liquid droplets, the dispersion can be said to be nanoemulsion (10-100 nm), miniemulsion (100-1000 nm) or macroemulsion (0.5-100 µm) (Tadros, 2013). Unlike microemulsions which are thermodynamically stable, nanoemulsions and macroemulsions are only kinetically stable, i.e., they break over time (McClements, 2015). This instability of emulsion can be of different types, according to their breakdown mechanisms (Figure 16), and can be categorised as reversible and irreversible processes (Abismaıl et al., 1999).

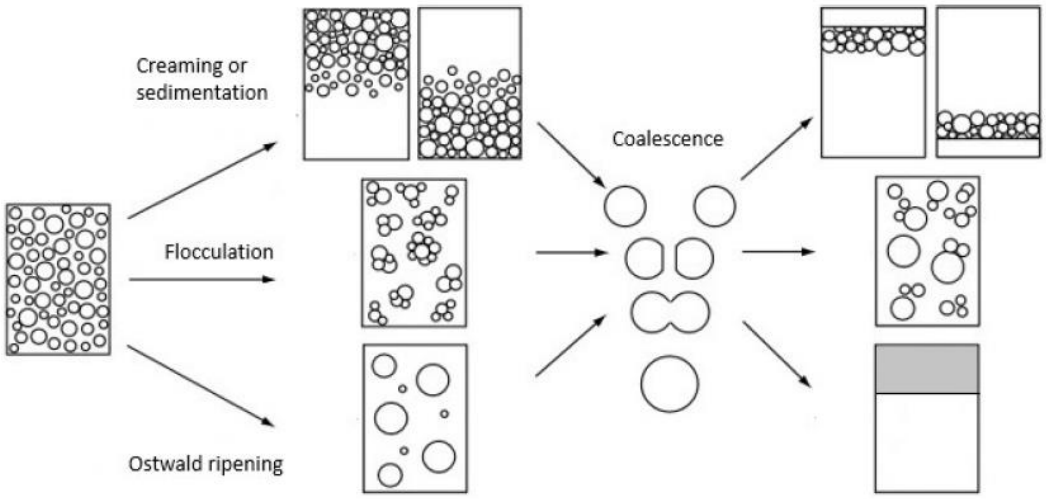

Figure 16. Schematic representation of common instability mechanism. Note that different mechanisms may occur simultaneously (Costa et al., 2019)**.**

Reversible processes are related to particle aggregation and migration and mainly, but not exclusively, include creaming and sedimentation which are the separation of the emulsion into two emulsions, one being richer in the dispersed phase (cream) and the other in the continuous phase. These two reversible breakdown mechanisms rely on gravitational separation, i.e., the difference of density between the two immiscible phases. Due to its lower density compared to the surrounding medium, the lighter phase droplets will move upward while the heavier ones

will go down. Unlike irreversible processes, these reversible breakdown mechanisms do not lead to increase in droplet size and change in particle size distribution (Piacentini, 2016).

Creaming is said to lead the emulsion reversible breakdown process when the dispersed phase is lighter than the continuous phase, and sedimentation takes place when the continuous phase is lighter than the dispersed phase. Reversible breakdown processes are quantified by Stokes law, which expresses the creaming rate (or the sedimentation rate for continuous phase being lighter than dispersed phase) in function of phases density

$$v = 2r^2(\rho - \rho_0)g/9\eta, \tag{2.17}$$

where v is the creaming (sedimentation) rate, r is the droplet radius, ρ is the density of the dispersed droplet, ρ_0 is the density of the dispersion medium, η is the viscosity of the continuous phase and g the acceleration due to gravity. One can see that the density difference $(\rho - \rho_0)$ will be negative for creaming while it will be positive for sedimentation. In addition, analysis of Equation 2.17 shows that creaming or sedimentation can be inhibited by a small droplet radius, a highly viscous continuous phase and a low-density difference between the two immiscible phases. This is why, among other reasons, nanoemulsions are so resistant to creaming and sedimentation.

Another encountered reversible breakdown process is flocculation. This is the process by which droplets associate with each other without losing their individual integrities (Figure 16). Flocculation processes can be divided into two general categories: that resulting from creaming-sedimentation aggregation and that from Brownian motion of the droplets. In many emulsion systems, the polydispersity of the droplets makes them cream or sediment at different rates, generating the tendency for the faster-moving (larger) droplets to collide with and potentially trap slower (smaller) moving droplets. Brownian aggregation results when the attractive van der Waals interaction dominates the repulsive electrostatic interaction in the random movement of the droplets. In reality, both types of flocculation occur simultaneously and an estimate of the relative rates of each type of flocculation can be attempted form the following equation (Tadros, 2004)

$$\Gamma_{max} = 2\pi(\rho - \rho_0)gr^4/3k\,T, \tag{2.18}$$

where k is the Boltzmann constant and T is absolute temperature.

The two irreversible emulsion breakdown processes which involve long-term stability and change in particle size and particle size distribution are Ostwald ripening and coalescence.

They involve the formation of larger drops through particle modification and lead progressively to an unstable emulsion, resulting ultimately in phase separation. Ostwald ripening occurs from the difference in solubility between small and large droplets in a polydispersed emulsion (Tadros, 2004). Due to larger solubility of smaller particles, the dispersed phase molecules can diffuse from them to larger droplets through the continuous phase. This is mainly because the differences in the chemical potential of oil in the two droplets, and the fact that pressure of dispersed material is greater for smaller droplets than for larger ones as shown by the following equation:

$$P = 2\gamma/r, \tag{2.19}$$

in which P is the Laplace pressure and γ is the surface tension between the two immiscible phases. The mass diffusion rate is directly related to the viscosity of the continuous phase and is given by the Stokes-Einstein equation

$$D = kT/6\pi\eta r, \tag{2.20}$$

in which D is the diffusion coefficient of the droplet and η is the continuous medium viscosity.

If the differential solubility between small and large droplets in the continuous medium constitutes the diffusion driving force, the rate of diffusion depends on the solubility of the dispersed phase in the continuous phase. The higher the concentration of the dispersed phase, the greater its relative vapour pressure (and thus the solubility) will be, as shown by the Kelvin equation

$$ln\frac{P_i}{P_0} = 2\gamma V_m/rRT, \tag{2.21}$$

in which P_i is the vapour pressure of the liquid droplets, P_0 is the vapour pressure of the continuous phase, r is the droplet radius and V_m is the molar volume of the dispersed phase.

Coalescence is the process through which two or more dispersed droplets merge together to form a single larger droplet (Mcclements, 2007) (Figure 16). The consequence of coalescence is that it causes the droplet in the emulsion to cream or sediment more rapidly because of the increase in their size. Coalescence is caused by the thinning and disruption of the liquid film between approaching droplets during Brownian motion, in the cream layer or in floc (Tadros, 2004).

These emulsion breakdown processes make the measurement of droplet size crucial for the assessment of emulsion kinetic stability. They also show that to prepare emulsion of practical

kinetic stability, a third component, an emulsifying agent (or an emulsifier), is essential. This material can be a low molecular surfactant (classical emulsion), a finely divided solid particles (Pickering emulsion) (Pickering, 1907) or a polymeric surfactant (Figure 17). The emulsifying agent has the role of facilitating emulsification and promoting emulsion stability (Shaw, 1992). It does so by forming an adsorbed film around the dispersed droplets, helping to prevent coalescence. The following factors promoted by the emulsifying agent at an extent depending on its nature favour emulsions stability:

- Low interfacial tension: Adsorption of surfactant at oil-water interfaces causes a decrease of interfacial energy, enhancing the stability of the large interfacial areas associated with emulsion formation.
- A mechanically strong and elastic interfacial film: the stability of emulsions stabilised by solid particles or surfactant arises from the mechanical barrier provided by films around the droplets.
- Electrical double layer repulsions: when ionic emulsifying agents are used, interparticle repulsion due to the overlap of similarly charged electrical double layers prevents the formation of a closed-packed film.
- Steric stabilisation: when two droplets containing adsorbed non-ionic surfactant or polymer layers (with an adsorbed layer thickness of δ) approach a distance of separation h whereby these layers begin to overlap, i.e., when $h < 2\delta$, repulsion occurs to prevent merging of the droplets.

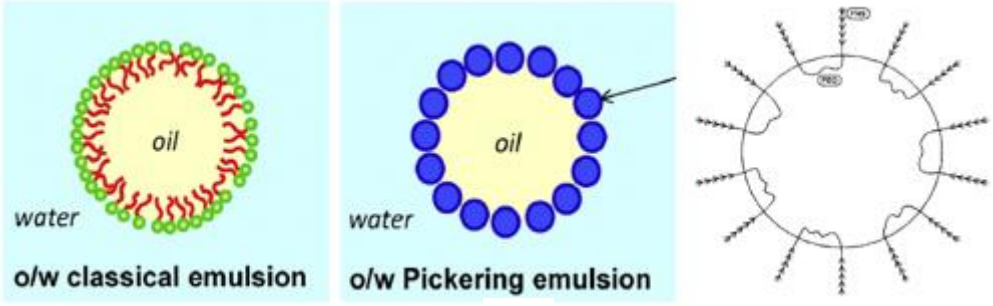

Figure 17. Conformation of amphiphiles materials at the fluid-fluid interface: a) surfactants stabilised emulsion (Chevalier and Bolzinger, 2013), b) solid particles stabilised emulsion (Chevalier and Bolzinger, 2013), c) PHS-PEO-PHS block copolymer based emulsion with the soluble PEO chain in the water droplet (Tadros, 2006a).

The type of emulsion, oil-in-water (O/W) or water-in-oil (W/O), is determined by the nature of the emulsifying agent. Although the higher phase volume liquid is more likely to become the continuous phase or dispersion medium, this intuitive rule has often been denied in many

circumstances, so that the distinction between different types of emulsion has come to lie on the nature of the emulsifier. In classical and polymer-based emulsions, emulsion type is controlled by the hydrophilic-lipophilic balance. In this regard, it is generally admitted that the phase in which the emulsifying agent is more soluble tends to be the continuous phase (Bancroft rule) (Bancroft, 2002). Thus, a water-soluble hydrophilic emulsifier, i.e., with high HLB, orients the emulsification process towards an O/W emulsion type, whereas hydrophobic emulsifier gives a W/O emulsion. Optimum HLB for stabilisation of W/O emulsions is 3-7 and 9-15 for O/W. There is a gap between these two ranges where none of these two emulsion types is stable (Chevalier and Bolzinger, 2013).

In the same way, for Pickering emulsions, emulsion type is controlled by the wettability of the solid particles (Binks and Lumsdon, 2000, Aveyard et al., 2003). Hydrophilic particles favour O/W Pickering emulsions. Indeed, O/W emulsions are favoured when the contact angle in the air θ_w is smaller than 90° and conversely, $\theta_w > 90^{\circ}$ favours W/O emulsions. This is the equivalent of the Bancroft rule in Pickering emulsions. Optimum stability of Pickering emulsions is achieved at a contact angle of 90°, i.e., for balanced particles regarding their wetting properties. Example of such particle is Janus which is used as stabilizing agent (Tu and Lee, 2014, Kim et al., 2008).

Another emulsion breakdown process not strictly classified between reversible and irreversible processes is phase inversion. Phase inversion is the process whereby an emulsion changes from O/W to W/O and vice versa. Emulsion droplets occur in only one of the phases at any composition but critical changes in oil-water ratio, in temperature, in electrolyte concentration or emulsifier concentration can induce complete transfer of aggregate from one phase to the other, inducing change in type of emulsion, i.e., from O/W to W/O or vice versa (Binks, 2002).

When increasing volume fraction of dispersed phase beyond a critical composition, the emulsion will ultimately result in “catastrophic” and irreversible phase inversion (Aveyard *et al.*, 2003). Sometimes, for practical purposes, it could be important to change the HLB of a surfactant (or mixture of surfactants) in order to reach an optimum HLB at which a large solubilisation or even complete mixing of oil and water phases with less surfactant is attained (Shinoda and Lindman, 1987). In the event this change of HLB goes up to the point where the affinity of the surfactant for water phase equilibrates with that of the oil phase, the phase inversion is said to be transitional (Sevcikova et al., 2011).

Transitional phase inversion can be achieved either by addition of a surfactant of different HLB or an electrolyte, or by alteration of temperature (Sevcikova et al., 2011). Change in HLB by surfactant is achieved by mixing low and high HLB surfactants. However, the addition of salt and increase in temperature, separately or simultaneously, shift the HLB more appreciably than addition of a surfactant of different HLB. These two factors dehydrate the surfactant's hydrophilic part, shifting its HLB towards lipophilic property.

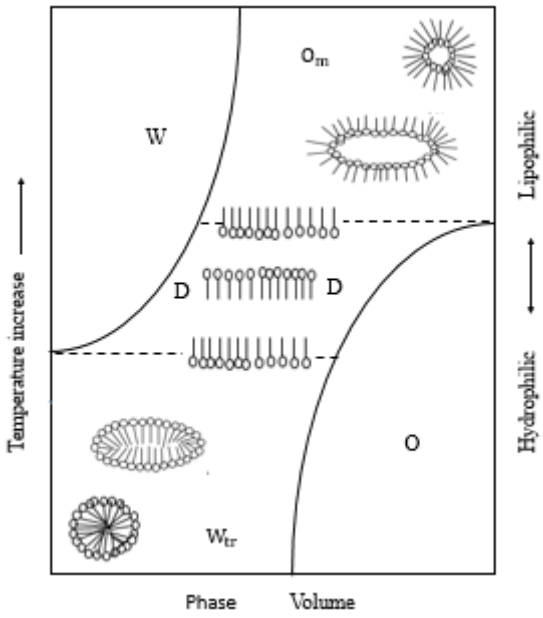

Figure 18. Schematic representation of changes in solution behaviour of surfactant organisation with the HLB of surfactant (Shinoda and Lindman, 1987).

The change in emulsion behaviour with electrolyte concentration and temperature increase is illustrated in Figure 18 (Shinoda and Lindman, 1987). This figure shows the increase in surfactant aggregation number and dispersed phase solubility with the change in HLB of the surfactant from hydrophilic to lipophilic, as well as the region in which the HLB of surfactant balances between water and oil. In this region, the surfactant aggregation number becomes infinite (D phase), i.e., surfactant phase separates. The solubility of oil in this region increases and finally becomes infinite. With further change of HLB to lipophilic character above this critical point or region, surfactants aggregate again and reverse (O_m); it is the ultimate stage of transitional phase separation marking the transition from O/W type emulsion to W/O. Conversely, the solubility of water in reversed micellar solution, O_m, increases with the decrease in temperature and salt concentration. These phase inversion processes based on composition and surfactant affinity changes have been increasingly used as a basis for low

energy emulsification methods for the preparation of narrow size distribution emulsions (Tadros et al., 2004, Solans and Solé, 2012, Forgiarini et al., 2001, Calderó and Solans, 2013).

2.5.1 Salts' effects on micellar solutions and emulsions clouding behaviour

In a surfactant solution, the occurrence of phase separation region in Figure 18 is termed CP and it is a reversible process. At this point, solvation and desolvation balances are affected and surfactant solution separates into two parallel phases, one of which being the surfactant-rich phase and the other one the aqueous phase (Parekh et al., 2013). Thus, emulsion breakdown processes via coalescence and Ostwald ripening are CP related phenomena (Johnson et al., 1990b). The clouding phenomenon is due to the interaction of uncharged surfactant and polymeric micelles via an attractive potential, whose depth is enhanced by temperature (Mukherjee et al., 2011). Temperature increase causes dehydration of hydrophilic moieties in micelles. For example, dehydration of the oxyethylene group in PEO-based copolymers or non-ionic surfactants results in contraction of the hydrophilic chains and their clustering, ultimately ending by coalescing.

CP of a block copolymer is highly dependent on the content of the hydrophilic moiety. Table 6 shows that the more PEO content is higher in a polymer chain, the higher the CP of the copolymer is. Conversely, CP decreases with decreasing polymer PEO content. In a highly PEO concentrated solution, the energy to be supplied to dehydrate sufficient hydrophilic chains and cause their coalescence to become larger because the extended hydration in solution becomes less sensitive to temperature increase. In this circumstance, the presence of additives becomes important to reach CP with minimum temperature increase.

Table 6. Influence of EO content on polymer Cloud point (Lad et al., 1995).

Polymer	**Structure**	**MW** $g\ mol^{-1}$	**% EO**	**CP (1%)** ℃
PEO	EO_{136}	6000	100	>100
F68	$EO_{78}PO_{30}EO_{78}$	8300	80	>100
P85	$EO_{25}PO_{40}EO_{25}$	4500	50	86
L64	$EO_{13}PO_{30}EO_{13}$	2900	40	62
L61	$EO_{4}PO_{30}EO_{4}$	1950	10	24

Adding inorganic salts to uncharged micellar solutions can notably shift the CP to lower temperatures. Inorganic salts affect the water structure in a manner to alter its affinity with polymer hydrophobic moiety. Hydration has a central role in the effects of ions on water structure. By increasing the polarity of water by hydrogen bonding with it, inorganic salts

increase water structure beyond the limit at which a less polar compound becomes insoluble. Consequently it dehydrates and coalesces as a consequence of "salting out" effect. An electrolyte producing salting out effect is termed a "structure making" electrolyte. If on the opposite, a salt reduces the polarity of water by a less extended hydrogen bond network, it reduces its structure below the limit at which a less polar compound becomes soluble. Consequently, it hydrates further as a consequence of the "salting in" effect. An electrolyte producing salting in effect is termed a "structure breaking" electrolyte.

In each case, hydration increase or decrease appears to be a consequence of alteration of interaction between hydrophilic moiety of an uncharged polymer or surfactant with water molecules. In the case a given salt displays salting out effect, a lower temperature increase will be required to reach polymer CP, because of their combined effect on the dehydration of hydrophilic moiety. The repulsive force between hydrophilic surfaces in water is reduced in the presence of a salting out electrolyte and temperature (Cacace et al., 1997). In the opposite case, much energy must be supplied to compensate for the hydration effect provided by the structure breaking electrolyte (Figure 19).

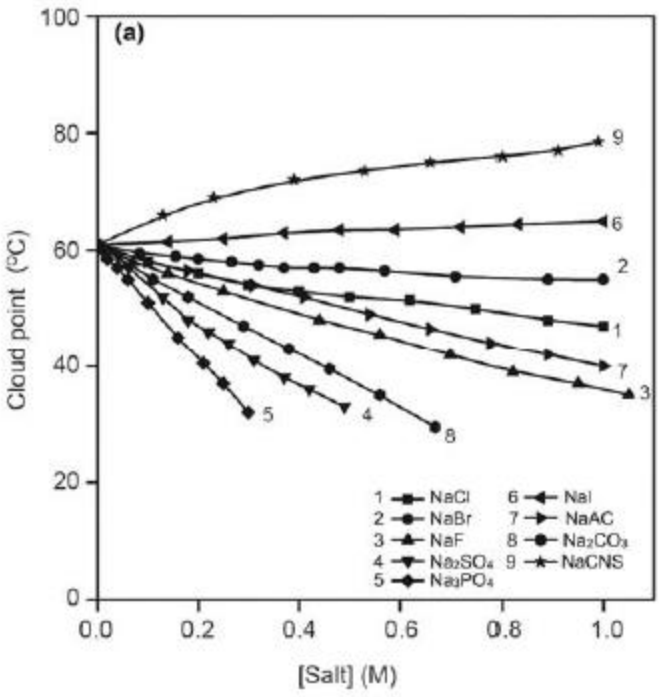

Figure 19. CP variation in the presence of salts (Parekh et al., 2013).

The effects of salts on polymer and surfactant solutions clouding behaviour depends on the particular ions involved. Classifications of ions in order of their ability to salt out or salt in organic compounds are termed Hofmeister series. Hofmeister series refer to solutes which are

susceptible to be highly hydrated, i.e., hydrogen-bonded to water when in aqueous solution. It is an experimental fact that the alteration of water structure in these series is dominated by anions. That is, for a given change in ionic radius, anionic parameters have by far more decisive effects than cationic ones (Cacace et al., 1997). It has been found that depression of CP was equivalent for monovalent electrolytes with different cations but with the same anion, leading to the conclusion that cations do not play major role in the CP depression of micellar aqueous systems.

If the influence of temperature on uncharged micellar solutions HLB decreases with an increase of surfactant hydrophilic moiety content, its effect on ionic surfactant solutions HLB is even less significant. More than temperature, salt concentration greatly influences ionic micelles HLB (Shinoda and Lindman, 1987). Ionic micelles in solution undergo electrostatic repulsion, which prevents micelle aggregation and coalescence. While repulsion between hydrophilic moieties caused by osmotic pressure is progressively overcome upon increasing temperature to bring in close proximity squeezed PEO from water, such a parameter does not have any effect on electrostatic repulsion between charged micelles. However, when an electrolyte is added to a charged micellar solution, the original charge distribution is swamped and the associated repulsions are screened. This can result in a salt-induced CP of the charged micellar solution (Kumar et al., 2002).

The role of temperature increase and salt concentration on CP depression of a non-ionic surfactant solution consists of increasing hydrophobicity of non-ionic amphiphiles in aqueous media. Conversely, increasing hydrophilicity by adding an ionic surfactant in such solutions results in a dramatic CP increase (Figure 20) (Sharma and Bahadur, 2002). The incorporation of ionic surfactants far below their cmc in a non-ionic surfactant solution leads to the formation of mixed micelles, thus charging non-ionic micelles. This introduces electrostatic repulsion between the micelles, thus hindering their clustering in a coacervate phase formation and raising CP (Marszall, 1988).

To reduce the CP of such a mixed ionic/non-ionic surfactant solution, the uncompensated charge on the micellar surfaces or in the micellar core must be eliminated. Indeed, once the charged surfactant is added, the CP of the system becomes sensitive to the addition of salt. Once again, the addition of electrolytes to an ionic/non-ionic micellar solution swamps the original charge distribution of mixed micelles and the corresponding repulsions are screened,

resulting in a CP depression whose extent depends on the electrolyte concentration and the ionic/non-ionic surfactant ratio (Figure 21) (Marszall, 1988).

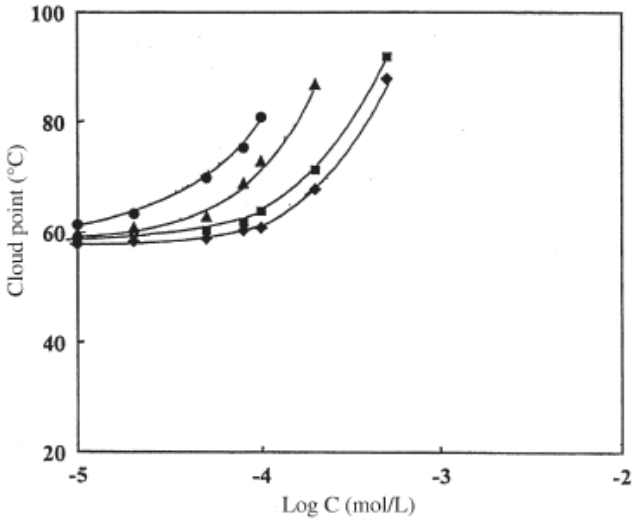

Figure 20. CP of Pluronic L64 in the presence of anionic surfactants. ●: sodium dodecyl sulfate, ▲: sodium decyl sulfate, ■: sodium decane sulfonate and ◆: sodium dodecyl benzene sulfonate (Sharma and Bahadur, 2002).

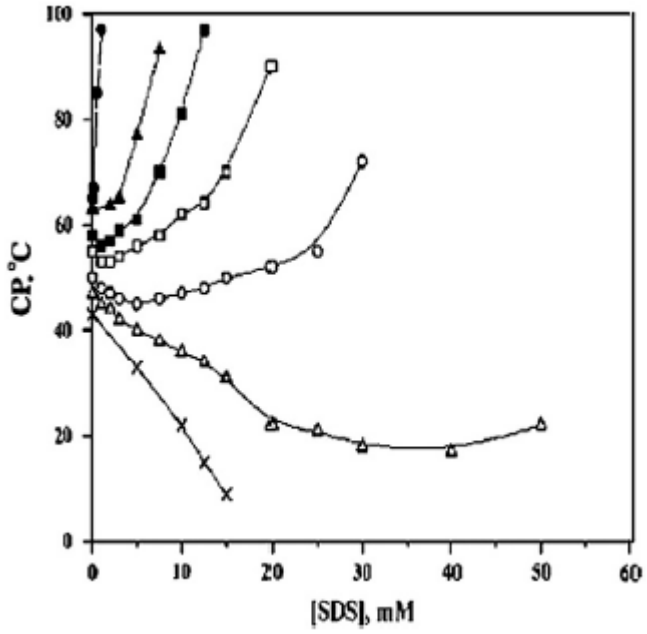

Figure 21. CP of TX-100 (1 wt.%) in the presence of various concentrations of NaCl as a function of SDS concentration. ●: 0.0 M, ▲: 0.25 M, ■: 0.5, ◇: 0.75, □: 1.00 M, △: 1.25 M, +: 1.5 M (Mukherjee et al., 2011).

Since the emulsion coalescence process is a highly related CP phenomenon (Johnson et al., 1990b), every single CP consideration developed in this section applies entirely to the emulsion

coalescence process. The role of additives in this process through their ability to modify water structure reinforces the importance of studying them separately.

2.5.2 Ions' effect on water structure: Structure making and breaking electrolyte

To understand the effect of salt on emulsion stability, water structure in itself must be deepened, in addition to analysis of surfactant and polymeric surfactant aggregation behaviour. Due to its extensive hydrogen bond network, water is set aside from other liquids as a very structured liquid. This structure affects the number of ion properties and makes water a universal solvent and a liquid of reference.

The notion of liquid structure encompasses the concepts of "stiffness", "openness" and "order" in the bulk, and in the case of water, it also includes extent of hydrogen bonding (Marcus, 2009). The stiffness of a liquid is defined as the necessary work to create a cavity in the liquid, in order to accommodate a solute particle or a liquid to condense into it from the vapour phase. In the following equation, it is expressed as the difference between the cohesive energy density and the internal pressure (Marcus, 1999):

$$\delta_H^2 - P_i = \left[\Delta_{Vap}H - RT\right]/V - [T\alpha_P/k_T - p], \qquad (2.22)$$

in which δ_H is the Hildebrand solubility parameter, P_i is the internal pressure, $\Delta_{Vap}H$ is the enthalpy of vapourization, V is the molar volume, α_P is the isobaric expansibility, k_T is the isothermal compressibility, p is the vapour pressure, and T the temperature of interest, all of which being thermodynamic quantities available and tabulated in many monographs. Water is found to be very stiff with $\delta_H^2 - P_i$ equal to $219\ MPa$ at 25℃, which is beyond most liquid and categorises water among the stiffest of liquids.

The "openness" of a fluid is related to its free volume, i.e., the difference between its bulk molar volume and the intrinsic molar volume (Marcus, 2009). There is no unique definition of intrinsic molar volume. More often, the van der Waals molar volume is used for this purpose, but it has the shortcoming of not taking into account the exclusion volume adjacent to a given molecule which another particle cannot penetrate (Marcus, 2009).

The McGowan intrinsic volume corrects this default and for water it is found to be $V_X = 16.7\ Cm^3mol^{-1}$ (Marcus, 2012), which is lower than its molar volume at 25℃, $V = 18.07\ Cm^3mol^{-1}$. The fraction of free volume according to this measure is then $(1 - V_X/V) = 0.092$. It can be seen that water is a packed and dense liquid, comparable to solvents like

glycerol and formamide. Indeed, these two solvents also have their free volumes $(1 - V_X/V) < 0.1$, contrasting with some other solvents like Dimethyl Sulfoxide (DMSO) and nitromethane, whose this quantity is 0.14 and 0.41, respectively.

A liquid order is evaluated in terms of the deficit of its molar entropy compared to the same quantity in the ideal gas phase. It can be estimated as

$$\Delta_{Vap}S(T_b) = \Delta_{Vap}H(T_b)/T_b, \qquad (2.23)$$

in which T_b is the normal boiling point at atmospheric pressure (0.101325 Mpa). A liquid is said to be ordered when $\Delta_{Vap}S(T_b) > 12$. With a value of 13.15, water as with many other solvents, is an ordered liquid (Marcus, 1992).

Some quantities related to the structure of water are reported in Table 7 and, as can be seen, water is a very structured liquid, among the most structured. For many organic substances, the cohesive interaction in water between its molecules as expressed by its strong stiffness, small openness and relatively high order, is more important than the adhesive energy between water and them. Its ability to dissolve inorganic electrolytes should therefore come from an additional component of structure, which is its high polarity as evidenced by its extended and dense hydrogen bond network.

Most of the inorganic electrolytes promote hydrogen bonding in bulk water and consequently extend and strengthen it in structuring water further, contrary to many organic cosolvents. This strengthening of water structure corresponds to ion hydration, which occurs during the interaction of water with other polar substance. The extent of hydration depends on the polarity of the solute.

Table 7. Measures of the structuredness of water: "stiffness" and "order"(Marcus, 2009).

t/°C	$(\delta_H^2 - P_i)$	$\Delta\Delta_{vap}S/R$
0		8.35
20	2179	8.01
30	2078	7.87
50	1877	7.63
70	1686	7.43
90	1508	7.28
120	1274	7.12
160	956	7.00
200	772	6.93
240	608	6.88

It has been suggested that the entropy of hydration of ions provides a relevant approach to decide on their structure making (salting out) or breaking (salting in) ability (Frank and Evans, 1945). In fact, these concepts of salting out and salting in are amenable to quantitative expression in terms of structural entropy derivable from experimental standard molar entropy of hydration (Marcus and Loewenschuss, 1984). On a general finding basis, cations have a less pronounced effect on water structure than anions. The structural entropy of an ion is expressed as (Krestov, 1984)

$$\Delta S_{struc} = \Delta_{hydr}S^{\infty} - 0.615S^{\circ}_{transl} - \eta S_{rot}, \qquad (2.24)$$

where $\Delta_{hydr}S^{\infty}$ stands for the entropy of hydration, S°_{transl} is the translational entropy, η is the viscosity and S_{rot} is the rotational entropy. The higher the value of ΔS_{struc}, the more structure breaking is the anion of interest. Table 8 lists some tabulated values for selected ions. One can see that polyvalent anions are more effective in enhancing water structure.

Table 8. Water structural entropy, effects of representative ions (Marcus, 2009).

Ion	ΔS_{Struct}
F^-	-57
Cl^-	20
Br^-	41
I^-	68
NO_3^-	23
ClO_4^-	44
CO_3^{2-}	-160
SO_4^{2-}	-100
PO_4^{3-}	-319

In non-ionic surfactant or uncharged block copolymer solutions, this strong water structure making property of polyvalent anions such as PO_4^{3-} results in a notable strengthening of water structure which, becoming poor solvent for surfactants, causes the prevalence of surfactant-surfactant interaction and the growth of the surfactant aggregates leading to their coalescence and phase separation (Mukherjee et al., 2011). In small concentrations, this anion is found to halve CP of Pluronic F127 (Fig. 22) and can go up to allowing it to occur at room temperature.

In comparison, much more NaCl is required to achieve comparable reduction. In many surfactants and PEO-based copolymers solutions, CP depends strongly on the amphiphile composition, with higher values for those containing a higher percentage of EO units (da Silva and Loh, 1998, Xiuli et al., 2004). For such surfactants particularly, utilisation of salt in addition to increasing temperature is essential to achieve very good performance in phase

separation via CP if desired. Another feature observed in polymer clouding phenomenon is that it displays very little dependence on polymer concentration, as shown in Figure 23.

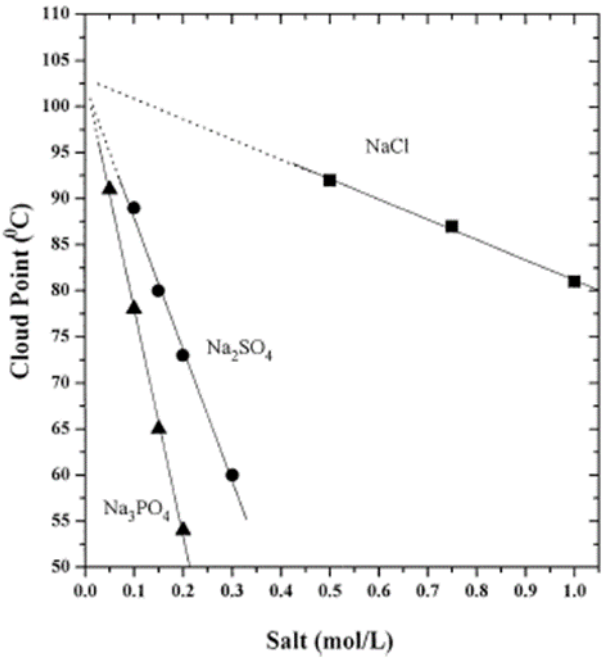

Figure 22. Schematic representation of changes in solution behaviour of surfactant organisation with the HLB of surfactant (Pandit et al., 2000).

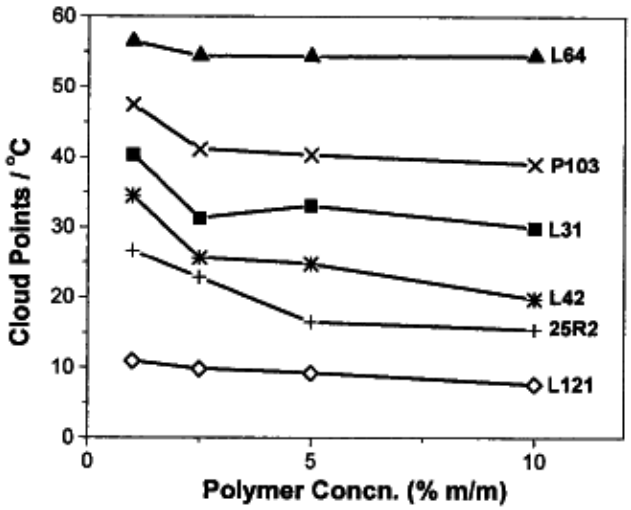

Figure 23. Clouding temperature of aqueous copolymer solutions (da Silva and Loh, 1998).

In many situations, as evidenced in Figure 22, CP shifting has been found to follow a linear trend and given known essential empirical constants, it can be predicted using the following equation for structure breaking anions, combining constants, a linear term and Langmuir isotherm

$$T = T_0 + c[M] + \frac{B_{max}K_A[M]}{1 + K_A[M]} \quad (2.25)$$

And for structure making ions

$$T = T_0 + C[M], \quad (2.26)$$

where T_0 is the CP of polymer in pure water, $[M]$ stands for molar concentration of salt, c is a constant of temperature/molarity unit, K_A is the apparent binding constant of the anion to the polymer and B_{max} is the maximum cloud point increase at saturation binding of ion (Zhang and Cremer, 2010, Deyerle and Zhang, 2011). In many of these publications and others, the CP is stated as the "lower concentration solution temperature" (LCST). For structure breaking ions, shifting of CP starts becoming exponential at high concentrations of salt, while it remains linear at all concentrations for salting out ions.

2.5.3 Thermodynamics of Emulsion Stability

Emulsion stability is led by a balance between forces favouring and opposing aggregation of dispersed droplets in the continuous medium. These forces at the interface of thickness δ between two immiscible bulk phases are the hydrodynamic friction also called Marangoni-Gibbs effect (Akbari and Nour, 2018), the attractive van der Waals and the repulsive double layer or electrostatic interactions, which form the basis of the DLVO theory (Gómez-Merino et al., 2007), and steric interaction (Tadros, 2013).

Stability of emulsions primarily depends on the presence of interfacial barrier preventing coalescence of the dispersed droplets (Mosayebi and Abedini, 2013). As dispersed droplets get close along together, they experience distortion and their surface area increases (Figure 24). This distortion causes them to flatten, creating a convective flux or drainage of the continuous phase thin film between them, which in the absence of any hydrodynamic friction, can disrupt the droplet interfacial barrier. This hydrodynamic friction is brought by surfactant adsorption which through mechanical enhancement of the droplet interfacial barrier, opposes and slows down such drainage.

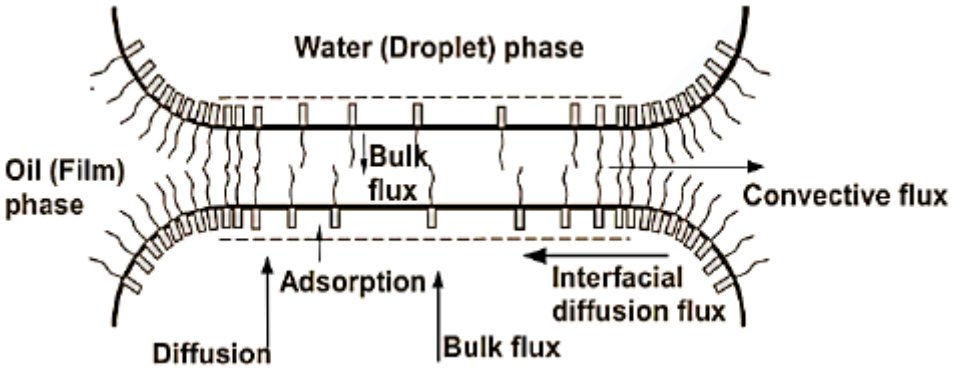

Figure 24. Schematic representation of Marangoni-Gibbs stabilization mechanism (Akbari and Nour, 2018).

London dispersion forces arising from charge fluctuation in atoms or molecules (such as in ether oxygen group in PEO) is the main, but not the only, component of van der Waals attraction (Gao and Eisenberg, 1993, Tadros, 2006b). The two other components, Keesom (dipole-dipole) and Debye (dipole-induced dipole) tend to cancel each other out. In accordance with electrostatic law, the Coulombic attractive force between two particles or droplets increases with decreasing their separation distance and becomes very high at a short distance. This type of van der Waals attraction between two droplets is given by:

$$V_A = -\frac{AR}{12h}, \tag{2.27}$$

where R is the radius of the two droplets, h stands for surface-to-surface separation distance between two droplets and A is the Hamaker constant given by:

$$A = \left(A_{11}^{1/2} - A_{22}^{1/2}\right)^2, \tag{2.28}$$

where $A_{11}^{1/2}$ and $A_{22}^{1/2}$ are the Hamaker constants of droplets and continuous phase respectively. For any given material, the Hamaker constant A is given by:

$$A = \pi q^2 \beta, \tag{2.29}$$

where q is the number of atoms or molecules per unit volume and β is the London dispersion constant, depending on the polarisability of the atoms or molecules.

To counterbalance this aggregation force, which in absence of any counteraction will lead to droplet merging, one of the opposing forces is the electrostatic repulsion. This force arises between droplets containing electrical charges or when using ionic surfactants, and results in the formation of electrical double layers. When charged dispersed colloidal droplets approach

a distance of separation smaller than twice the double-layer extension, double layer begins to overlap and repulsion occurs (Tadros, 2008). This repulsive force is given by the expression:

$$V_{el} = \frac{4\pi\varepsilon_r\varepsilon_0 R^2\psi_0^2 exp(-\kappa h)}{2R + h}, \tag{2.30}$$

where ε_r is the relative permittivity (78.6 for water at 25℃), ε_0 is the permittivity of free space, R is the droplet radius, ψ_0 is the surface potential (approximately equal to the measurable zeta potential) and κ is the Debye-Huckel parameter which is related to the number of ions n_0 per unit volume and the valency of the ions Z_i. The thickness of the double-layer $1/\kappa$ is expressed as:

$$\frac{1}{\kappa} = \left(\frac{\varepsilon_r\varepsilon_0 kT}{2n_0 Z_i^2 e^2}\right)^{1/2}, \tag{2.31}$$

where k is the Boltzmann's constant and T is the absolute temperature.

The magnitude of repulsion decreases drastically when increasing electrolyte concentration. Indeed, adding electrolyte to the ionic micellar solution swamped the original ionic charge distribution and the corresponding repulsions are screened (Marszall, 1988), resulting in the occurrence of emulsion breakdown via induced CP process.

The most important repulsive force which is more effective in stabilising emulsions is steric interaction. This force arises when non-ionic surfactants or polymers are adsorbed at the liquid-liquid interface. When in a dispersion two droplets containing adsorbed polymer layers (with adsorbed layer thickness of δ) approach a distance of separation h whereby these layers begin to overlap, i.e., when $h < 2\delta$, repulsion occurs as a result of two main effects (Tadros, 2013), namely the unfavourable mixing of the solvated chains and the reduction of configurational entropy of the chains.

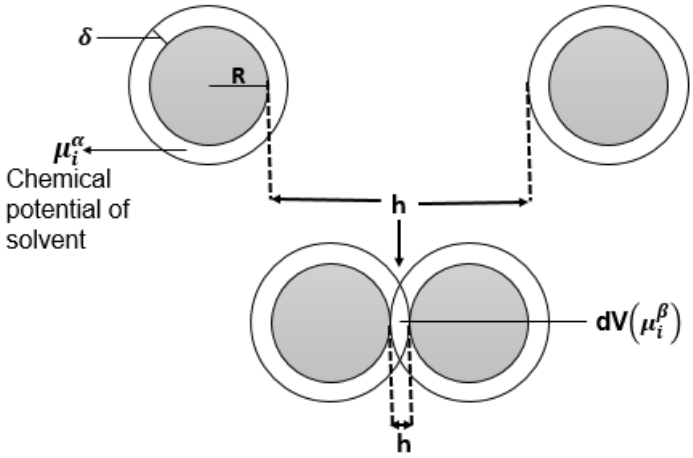

Figure 25. Schematic representation of the overlap of two polymer layers (Tadros, 2006a).

The unfavourable mixing of polymer layers arises when these are in good solvent, meaning that the chains are strongly solvated by the medium. Figure 25 shows two droplets covered by polymer layers approaching each other at a distance $h < 2\delta$, and forced to form an overlap region of volume element dV. The chains volume fraction before overlap is φ_2 and the solvent chemical potential is μ_1^α. In the overlap region, the volume fraction of the chain becomes $\varphi_2' > \varphi_2$ and the solvent chemical potential becomes $\mu_1^\beta < \mu_1^\alpha$. The relations between initial and final chains volume fraction and solvent chemical potential express the increase in the osmotic pressure of the overlap region. Consequently, the solvent diffuses from the bulk to the overlap region and the two droplets separate because of the strong mutual repulsion. From Flory theory, the free energy of mixing G_{mix} due to unfavourable overlap is:

$$\frac{G_{mix}}{kT} = \frac{4\pi}{3V_1}\emptyset_2^2 N_{av}\left(\frac{1}{2}-\chi\right)\left(\delta-\frac{h}{2}\right)^2\left(3R+2\delta+\frac{h}{2}\right), \qquad (2.32)$$

where k is Boltzmann's constant, T is the absolute temperature, V_1 is the molar volume of the solvent, N_{av} is the Avogadros' constant and χ is the dimensionless *Flory-Huggins polymer-solvent interaction parameters* giving the indication of solvation of chains by the molecules of the medium.

From the above equation, it can be seen that when a polymer chain interaction parameter χ is less than 0.5, G_{mix} is positive, the chains are in good solvent and the interaction is repulsive, increasing rapidly with increasing h when the latter is lower than 2δ. If however $\chi > 0.5$, the medium becomes poor solvent for the chains, G_{mix} is negative and the interaction becomes attractive. In the case $\chi = 0.5$, the polymer mixing behaves ideally. This condition is referred to as θ-condition and represents the onset of change from repulsive to attractive interaction.

Thus, to grant steric stabilisation via an unfavourable chain mixing mechanism, one has to ensure that the chains are continuously kept under θ-conditions.

The reduction in configurational chains entropy, also referred to as elastic interaction G_{el}, arises when chains overlap. As can be seen in Figure 26 where the polymer chain is represented by a simple rod attached to the surface, when the two surfaces are separated by an infinite distance, each chain will have a number of configurations, Ω_∞, that are determined by the volume of the hemisphere swept by the rod (Tadros, 2006a). When the two surfaces approach a distance h that is smaller than the radius of the hemisphere swept by the rod, the volume available to the chains becomes smaller and this leads to reduction in the configurational entropy to a value $\Omega < \Omega_\infty$. This gives rise to a strong repulsion and the effect is referred to as elastic repulsion, which is given by the expression:

$$G_{el} = 2v' ln \frac{\Omega}{\Omega_\infty}, \tag{2.33}$$

in which v' is the number of polymer chains per unit area of the surface. One must note that G_{el} is always positive and gets very high on the considerable overlap of the polymer layers.

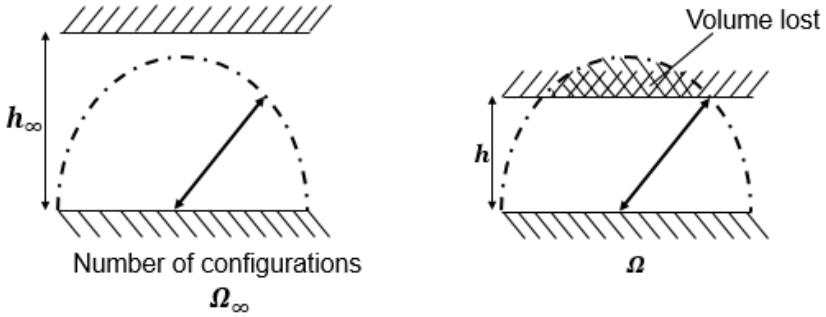

Figure 26. Schematic representation of the entropic, volume restriction or elastic interaction (Tadros, 2006a).

It is clear from the above development that increasing salt concentration in the dispersion will impoverish hydration of water for the PEO chain by strengthening water structure and salting this polymer chain out. This will result in increasing of χ value beyond θ-condition, causing droplet aggregation and emulsion breakdown. This is an important point, because it demonstrates how emulsion coalescence process is a surfactant CP related phenomenon. The value of $(1/2 - \chi)$ in Equation 2.32 determines the sign of G_{mix}. If $(1/2 - \chi)$ is positive, $\chi < 0.5$, G_{mix} is positive and the interaction is repulsive. In the other case, the interaction becomes attractive.

The χ is therefore related to the hydration of water for both PEO and PPO chains. In water, only PEO is strongly hydrated by water molecules, with χ being less than 0.5 at normal temperature and in the absence of electrolytes. At a critical electrolyte concentration and temperature, χ will change the value from less than 0.5 to more than 0.5, resulting in dehydration of the chain, its salting out, and ultimate emulsion coalescence.

2.5.4 Kinetics of Emulsions Stability

If droplets are growing, then it can be predicted when emulsion breakdown will take place. This growth can be denoted as coalescence or Ostwald ripening rate. It is a constant which quantitatively measures the time required for the initial concentration of particles to be reduced to a critical value, immediately preceding phase separation (Florence and Rogers, 1971).

Coalescence rate of emulsions displaying monomodal distribution has been recognised to largely follow a first-order kinetic process occurring between adjacent drops in dispersion, independently of the number of droplets in that dispersion. In a homoaggregation system where colloidal particles are suspended in water (which is the case for emulsions), DLVO theory states that the suspension stability can be quantified by considering the kinetics of formation of particle dimers, according to the reaction $A + A \rightarrow A_2$, where A refers to the individual particle monomer, and A_2 is the particle dimer aggregate (Trefalt and Borkovec, 2014). The rate of coalescence can then be represented as (Ye et al., 2004)

$$N_t/N_0 = e^{-K_c t}, \tag{2.34}$$

where N_t is the number concentration of droplets at time *t*, N_0 is the number concentration of freshly formed droplets at time zero and K_c is the apparent coalescence rate constant. In the absence of oiling-off in the emulsion, i.e., when the volume of emulsion droplets remains constant, the relationship between the emulsion droplet number N and the mean volume average droplet diameter, $d_{30} = (\sum nd^3/\sum n)^{1/2}$, where n_1, n_2, n_3 …, are the number of droplets with diameters d_1, d_2, d_3 …, is given by (Rodea-González et al., 2012)

$$\frac{4}{3}\pi\left(\frac{d_{30}}{2}\right)^3 N = constant \tag{2.35}$$

The relative number of emulsion droplets can then be obtained from (Das and Chattoraj, 1982)

$$\frac{N_t}{N_0} = \left[\frac{(d_{30})_{t=0}}{(d_{30})_{t=t}}\right]^3 \tag{2.36}$$

Kinetic plots of $ln(N_t/N_0)$ versus storage time *t* gives a straight line whose the slope is k_c.

This model becomes less effective when two or more populations of droplets are present in the emulsion, making it multimodal. In addition, the irreversible increase in droplet size in this case, can proceed from additional mechanisms such as Ostwald ripening. Ostwald ripening is generally modelled with the well-known Lifshitz-Slyozov-Wagner (LSW) theory (Ariyaprakai and Dungan, 2010, Santos et al., 2017), based on the assumption that diffusion of oil through the water determines the overall ripening rate. This theory predicts that, at an asymptotically long time, there is a constant ripening rate ω_T which is determined by the growth in the cube of the number-weighted mean droplet radius $\bar{r}$:

$$\omega_T \equiv \frac{d\bar{r}^3}{dt} = \frac{8\gamma C_w^{eq} D_O V_o}{9kT}, \tag{2.37}$$

where, γ is the interfacial tension between the oil and aqueous phase at the droplet surface, V_o is the molecular volume of the oil, C_w^{eq} is the aqueous oil solubility, D_O is the diffusivity of the oil molecule, k is the Boltzmann constant and T is absolute temperature.

Coalescence is modelled by the following general equation (Santos et al., 2017):

$$\frac{1}{D_0^2} - \frac{1}{D^2} = \frac{2\pi}{3}\omega_C t, \tag{2.38}$$

where, D_0 is the initial diameter, D is the diameter at time t and ω_c is the coalescence rate.

2.6 Conclusion

Diverse aspects of surfactants, polymers, and their simultaneous presence in aqueous solutions have been reviewed. It appeared that polymer-surfactants interactions and aggregation behaviour are best studied with surface tensiometry. Similarly to low molecular surfactants, block copolymers are found to display micellisation behavior in the aqueous medium. Their interaction when simultaneously present in aqueous solutions is dependent on their association states.

Surfactants and polymers' behaviours and their interactions have been found to be critically dependent on their molecular constitutions. External macroscopic factors influencing polymers and amphiphilic behaviour in solutions have also been considered. Many of them have direct impact on micellar solutions behaviours. In particular, electrolytes, due to their ability to influence micellar solutions both sterically and electrostatically, are of considerable importance in ionic/non-ionic surfactant systems.

The emulsion breakdown processes (Ostwald ripening and coalescence) of block copolymer based emulsion are CP related phenomena, and they are determined by micelles entrapping droplet interactions: steric or electrostatic. The influence of electrolytes on amphiphiles behaviours in the aqueous phase is extended to emulsion stability where they are found to play a key role in coalescence and Ostwald ripening through their role on the variation of CP. This influence was found to be dependent on electrolyte nature (salt valance) and it is closely related to the alteration of the solvency property of the medium.

Chapter 3 Materials and Methods

This chapter sets out the experimental methods used for characterisations of F127/surfactants aqueous solutions and oil in water emulsions. These characterisations consisted of monitoring aqueous solutions surface and interfacial tensions, and emulsions stability.

Surface tension was recorded as surfactants concentrations were varied for fixed F127 concentrations. Concentration ranges of the three surfactants were chosen to suit each aggregation state of F127 in solution and for both non-associated and associated F127, they were selected so as to cover the range from their monomers to micelles.

Oil in water emulsion stability was monitored as surfactant concentrations were changed for fixed F127 and salt concentrations. Sodium phosphate salt was chosen according to its strength in the Hofmeister series (Table 8) and its concentration was chosen according to its ability to lower F127 CP (Figure 22). It must be kept in mind that reduction of the CP cannot take place at same extent as for pure copolymer solution since, as shown in section 2.5.1, the presence of an ionic surfactant induces a substantial increase of the CP beyond that of the pure non-ionic surfactant solution.

3.1 Materials

Sodium dodecyl surface (SDS) (95% purity) and Cetyltrimrthylammonium bromide (CTAB) (99% purity) were purchased from Sigma-Aldrich and used as received. Tetraethylene glycol monododecyl ether ($C_{12}E_4$) was purchased from Rebound Chemical and used as received.

Poly(ethylene oxide)$_{100}$-poly(propylene oxide)$_{65}$-poly(ethylene oxide)$_{100}$ (average molecular weight 12600 g.mol^{-1}) was generously provided by BSAF and used without further purification. For the purpose of this study, Pluronic will be designated according to BSAF nomenclature and shall be referred to as F127.

Light mineral oil (density 0.838 g.mL^{-1}) was purchased from Fourchem and used as received. Analytical grade sodium phosphate (Na_3PO_4) (95% purity) purchased from Associated Chemical Enterprises (ACE) company was used to prepare all emulsions.

3.2 Methods

3.2.1 Surface Tension

Surface tension is due to the difference in cohesive forces between liquid molecules at the interface and in the bulk. Whereas molecules are interacting equally with each other in the bulk, at the surface they are not surrounded by like neighbours on all sides. Consequently, they interact strongly with the like molecules that are directly surrounding them, creating an inward force which pulls them toward the bulk (Kronberg et al., 2014). This situation applies to both liquid-gas and two immiscible liquid interfaces. When two immiscible liquids are in contact, interfacial tension arises from differences between the intermolecular forces at the two liquids' surfaces in contact with each other.

Surface tensions of aqueous solutions were measured by the pendant drop method using a drop shape analyser (Kruss, model DSA 100) (Figure 27). The accuracy of measurements was checked by frequent calibration measurement of pure water ($\sigma = 72$ mN. m^{-1} for water-air interface and $\sigma = 51.83 - 0.103 \times T$[℃] for water-light mineral oil (Stan et al., 2009)]). Each surface tension value was an average of triplicated measurements. The measurements were made at varying surfactant concentrations and constant F127 content. Two series of constant F127 concentrations ($10 - 50 - 100$ µM and $3.5 - 4 - 4.5$ mM) below and above F127 cmc were used for varying surfactant concentrations. The concentration ranges of the three surfactants were chosen to suit each aggregation state of F127 in solution. For both F127 non-associated and associated states, they were selected so as to cover the range from their monomers to micelles. All solutions were prepared by mixing appropriate amounts of polymer and surfactant stock solutions. They were then equilibrated at room temperature for at least 24 hours before surface tension measurements took place.

Figure 27. Drop shape analyser (KRUSS DSA 100 Tensiometer) used for determining surface tension.

When using the pendant drop method, interfacial tension is measured from a fluid droplet suspended to a needle. Surface tension is determined by fitting the shape of the drop (in a captured video image) to the Young-Laplace Equation which relates interfacial tension to drop shape. More precisely, at equilibrium, the droplet obeys the Young-Laplace equation, relating the Laplace pressure across an interface to the curvature of the interface and the interfacial tension γ (Berry et al., 2015):

$$\gamma\left(\frac{1}{R_1}+\frac{1}{R_2}\right)=\Delta P\equiv\Delta P_0-\Delta\rho gz, \tag{3.1}$$

where R_1 and R_2 are the principal radii of curvature, $\Delta P\equiv P_{in}-P_{out}$ is the Laplace pressure across the interface, $\Delta\rho=\rho_d-\rho$ is the density difference between the drop phase and the continuous phase respectively, g is the acceleration of gravity, z is the height at which the liquid droplet is raised, and ΔP_0 is the reference pressure at $z=0$.

Technological progress due to the advent of high-precision cameras and high power computing desktops has automated this method and made it a widely used technique. The essential components of the pendent drop method apparatus are: a needle, a camera to capture the drop image, a light source, and a computer for data analysis (Figure 28a). Although the experimental setup is of relative simplicity, care must be taken to ensure good image quality for accurate determination of interfacial tension. Principally, light quality is of critical importance. The light source must be diffused to eliminate any optical aberration at the drop periphery and spurious reflections from the drop interface arising from other sources (Berry et al., 2015, Woodward,

2013). In the same way, the drop image captured by the camera sensor must be undistorted by the lensing effect. Finally, software analysis is greatly simplified by a homogeneous image background. An ideal image for accurate analysis is shown in Figure 28b.

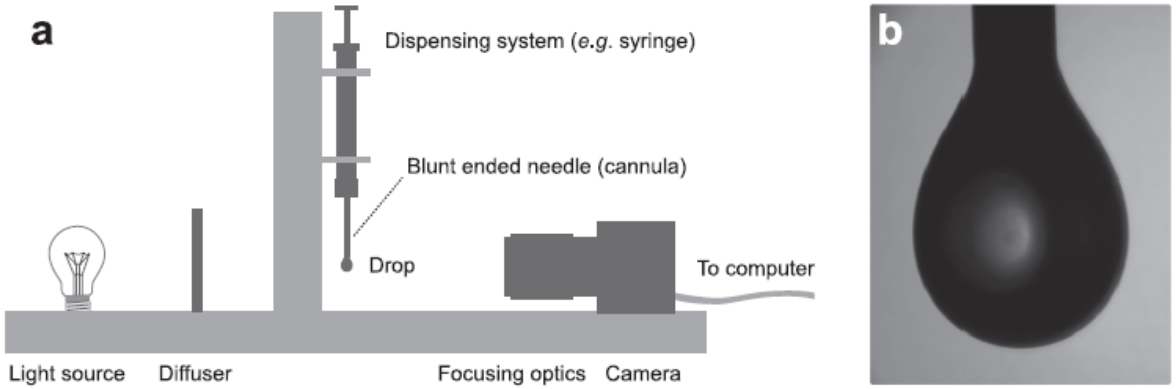

Figure 28. (a) Essential components of a drop shape analyzer; (b) typical drop image required for accurate analysis (Berry et al., 2015).

Apart from electronic settings issues, the needle must be absolutely vertical, i.e., parallel to gravity. The drop generated from the needle must be of adequate size to ensure that the gravitational effect is non-negligible (Berry et al., 2015). If the gravitational effect is negligible, the surface tension is overestimated in virtue of Equation 2.39. Finally, the oscillation of the droplet which can be induced by the air currents must be minimised. When measuring liquid/liquid interfacial tension, this vibration is avoided by performing the measurement in a cuvette (Figure 29). In the case of water/air surface tension measurement, this effect is minimised with an anti-vibration table (Woodward, 2013, Berry et al., 2015).

The needle (diameter ~ 1.8 mm) attached to the syringe containing the aqueous emulsifiers' mixture and attached to the goniometer was suspended in air or placed in a cuvette filled with mineral oil. The water drop was then generated at the bottom of the needle in the air or oil phase. The drop shape was then monitored via Drop Shape Analysis (DSA) software provided by Kruss and interfacial tension was given according to Equation 2.39. The only required input by the software for oil-water interfacial tension measurements is the density of both liquids (mineral oil and water). The densities of the water and oil phases were taken as 0.998 and 0.84 $g.mL^{-1}$, respectively and they were assumed to remain constant in the presence of emulsifiers. A cuvette made of quart was used to contain the oil phase. The cell was initially cleaned and soaked with soap. It was then rinsed with distilled water and dried.

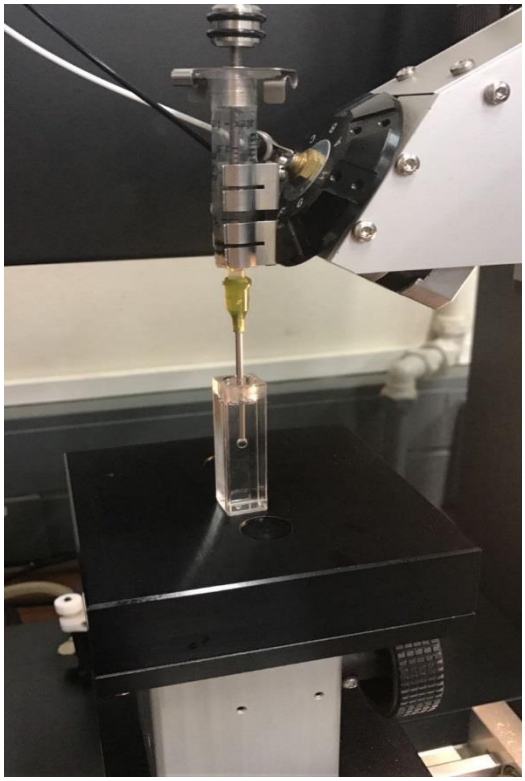

Figure 29. Water-oil surface tension measurement.

3.2.2 Emulsion Preparation

One to one volume ratio (50 v/v %) light mineral oil in water emulsions were prepared. Surfactants and F127 concentrations were chosen as a result of surface tension measurements. All emulsions' aqueous phases were made of 3.5 mM of F127, 0.37 M of Na_3PO_4 and varying surfactant concentrations: 30, 40, 50, 60 mM for SDS and CTAB and 5, 10, 20 and 30 mM for $C_{12}E_4$. Emulsions were duplicated and stored at 60℃. A Silverton L5M-A laboratory mixer (Figure 30) was used to prepare them. Light mineral oil was heated in a beaker at 70℃ on a hot plate. Aqueous phases were stirred at 200 rpm with a magnetic stirrer beforehand. A 3000 rpm shear was then applied to the aqueous phase while slowly adding oil for one minute. The mixture of water and oil was then sheared for anothers two minutes before increasing shear to 7500 rpm for an additional ten minutes. The formed emulsion was then removed from the homogeniser, and slowly stirred until it cooled to roomed temperature.

Masses of surfactants and F127 were calculated as follows:

$$M_{surfactant} = x \times CMC \times M_m \times V_w, \quad (3.2)$$

where x is a cmc multiplicative coefficient, M_m is the molar mass of surfactant and V_w is the volume of the phase in which surfactant is dissolved (water).

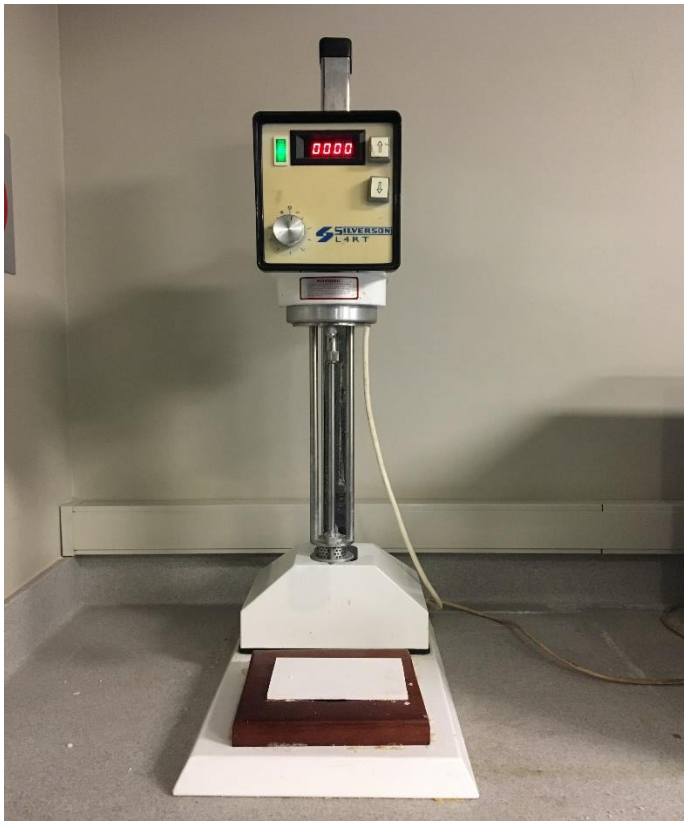

Figure 30. Silverson L5M-A Laboratory Mixer

3.2.3 Droplet Size Distribution Measurements

The interest of approaching both the interactions between amphiphiles and the influence of salts on their behavior from a molecular point of view determines the question of emulsion stability as closely related to the variations of the individual aspects of dispersed phase droplets in the continuous medium. It follows that particle size distribution is among the best-fitted methods to study kinetic stability of emulsion.

Due to its wide dynamic range (from submicron to millimetre), its rapid measurements (results generated in less than a minute), the lack of calibration for the equipment and the repeatability (large numbers of particles are sampled in each measurement), laser diffraction is one of the most widely used methods to measure dispersion and emulsion particle size distribution (Goodarzi and Zendehboudi, 2019). In this technique, a laser beam is directed through a dispersed particulate sample, and the angular variation in the intensity of the scattered light is measured. Large particles scatter light at small angles relative to the laser beam whereas small particles scatter light at large angles (Figure 31). To determine the size of the particles scattering the light, the angular scattered intensity data are analysed according to the Mie theory (Kusters et al., 1991). The particle size is reported as a volume equivalent sphere diameter.

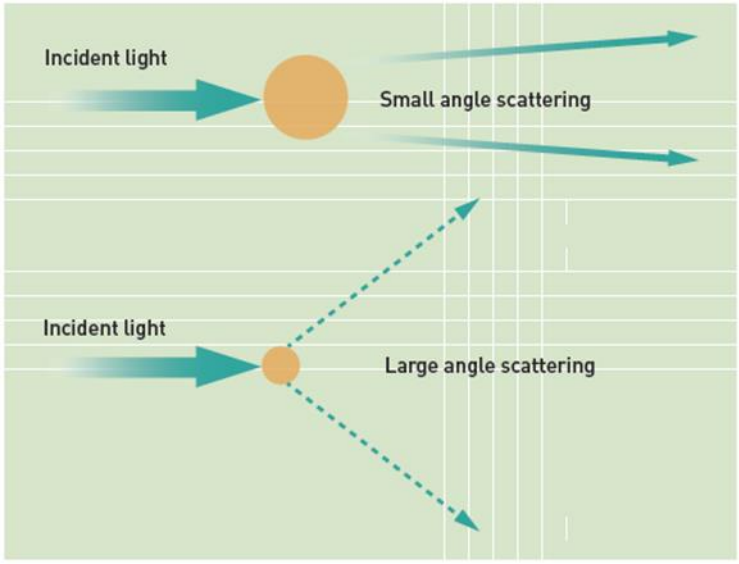

Figure 31. Angular light scattering in the function of particle diameter (Instruments, 2012).

A DSD apparatus is composed of four parts (Malvern, 2013): the optical bench, the dispersion units, the measurement cell (wet cell in Figure 32) and application software. The optical bench has the purpose of transmitting red and blue lights through a sample and then using its detectors to generate data about the scattering pattern caused by the particles in the sample. The data are then interpreted by the application software to provide particle size information.

The dispersion unit can be of two types: wet and dry. Wet units (Hydro MV/LV/EV/SM) deal with the dispersion of a sample suspended within a liquid dispersant. Contrarily, the dry units have the function of ensuring that a dry sample is dispersed and evenly fed to the measurement cell within a continuous stream of air. The measurement cell is intercalated between the dispersion unit and the optical unit. The sample is led between measurement windows in the cell so that the laser can pass through it in order to perform the measurement.

Finally, the application software controls the optical and the dispersion units hardware and also processes the raw data gathered by the system, providing data analysis (mainly diverse types of diameter) and reporting features (size distribution). The informations required by the DSD software about the physical properties of the emulsion are the refractive and adsorption indices of the continuous medium which are 1.33 and 0.1, respectively, and the refractive index of the dispersed medium which is 1.52.

To evaluate the emulsion stability versus time, an accelerated ageing technique was employed namely heat exposure. Emulsions were stored at 60℃ for days. DSD and mean diameters of oil droplets were evaluated by the Malvern MasterSizer 3000 instrument (Figure 32). Particle

size distribution was determined immediately after emulsions were prepared and at regular time intervals. Determinations were conducted in duplicates and values of standard deviations were significantly low. Weighted mean diameters were obtained from DSD expressed as differential surface area and the volume-weighted mean diameter (D4.3) is found to be more sensitive to changes in particle size involving emulsion irreversible breakdown processes (coalescence and Ostwald ripening) than the surface weighted mean diameter or Sauter mean diameter (D3.2) (Relkin and Sourdet, 2005).

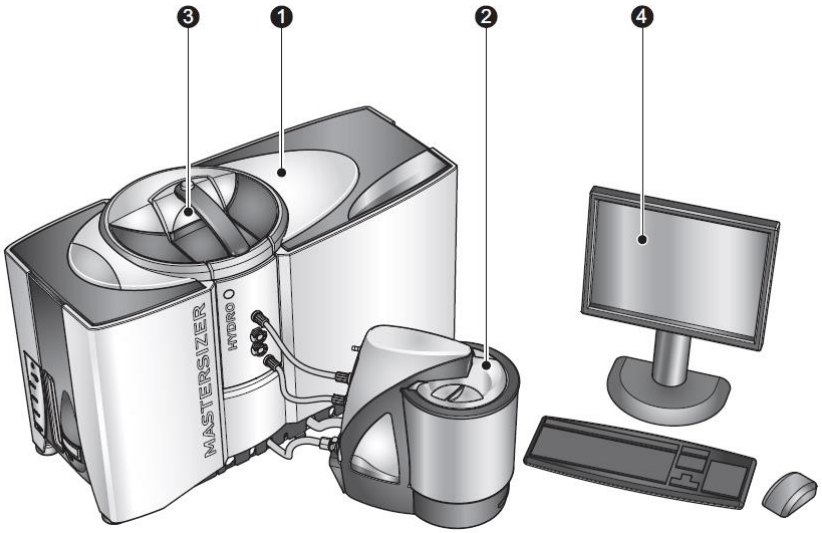

Figure 32. Malvern Mastersizer 3000 with emulsion loading unit: 1) Optical unit; 2) Wet dispersion unit; 3) Wet cell; 4) Computer running the Mastersizer application software (Malvern, 2013).

3.2.5 Rheological Measurements

The rheological behaviours or flow properties of emulsions significantly affect their quality (Hu et al., 2017). The rheology of fluid emulsions can be characterized in terms of the dependence of their apparent viscosity on shear rate (Mcclements, 2007). Viscosity can be defined as the internal resistance of a fluid to flow. Factors that can affect emulsions viscosity include their chemical composition (typically the ratio of dispersed and continuous phase) and droplet−droplet interaction.

For dilute emulsions (with dispersed phase volume fraction $\emptyset < 0.1$), the viscosity is said to be Newtonian and is independent of the applied shear rate. However, for most practical emulsions (with $\emptyset > 0.1$) or shear thinning system, the viscosity is decreased with an increase in shear rate, reaching a Newtonian value above a critical shear rate (Tadros, 2004).

Viscosity is a bulk property that can give information on the droplet-droplet interaction (whether attractive or repulsive). It can be used to qualitatively follow the change of the emulsion on storage. However, to apply it in a quantitative manner, one must know the nature of the interaction forces between droplets (Tadros, 2004). For this reason, viscosity alone cannot account for a destabilising mechanism of an emulsion.

Proving the system does not undergo any flocculation, the viscosity increase monotonically with increase in the average droplet size. Thus, in the absence of any flocculation, reduction of viscosity is significant of coalescence occurring in the emulsion. This is the consequence of the general trends regarding the effect of the particle size on the viscosity of the dispersion (Rámirez et al., 2002). The smaller the particle size, the more viscous the dispersion, and the wider the range of particle size, i.e, the more polydispersed the emulsion, the lower the viscosity.

Similarly, viscosity measurement can be used as a guide for flocculation assessment only in the case where coalescence and Ostwald ripening are absent. One of the power-law models (the *Bingham model*) can be used to illustrate this. In the equation $\sigma = \sigma_\beta + \eta_{Pl}\dot{\gamma}$, the σ_β parameter is the extrapolated yield value (obtained by extrapolation of the shear stress-shear rate curve to $\dot{\gamma} = 0$) and η_{Pl} is the slope of the linear portion of the $\sigma - \gamma$ curve. Both of these parameters may be related to the emulsion flocculation (Tadros, 2004). Given any volume fraction of the emulsion and at any DSD, the higher the values of these parameters the more the flocculated the emulsion is.

Thus, in storing the emulsion at any given temperature and in making sure that the DSD remains constant (i.e. no Ostwald ripening or coalescence take place), the least increase in the above parameters indicates flocculation of the emulsion. Contrarily, in the case that Ostwald ripening and/or coalescence occur simultaneously, it is possible that σ_β and η_{Pl} may change in a complex manner with storage time. Indeed, Ostwald ripening and coalescence resulting in a shift of the DSD to higher diameters, this has the effect of reducing σ_β and η_{Pl}, which conflicts with flocculation.

Consequently, only in the absence of the latter processes (which can be ascertained by particle size distribution), the viscosity measurements can be used as a guide to assess flocculation. Rheological measurements were limited to intact emulsion samples. They were performed on a Physica MCR 301 instrument (Figure 33) using the cone-and-plate geometry in the controlled

shear rate mode. The gap was 0.051 mm and the cone angle was 1.007°. The emulsion samples were hand-shaken before measurements. The shear rate was varied from 0.1 to 1000 s^{-1}. The viscosity vs. shear rate flow curves were obtained at ambient temperature, approximately 25°C.

Figure 33. Physica Messtechnik GmbH laboratory rheometer.

3.2.6 Optical Microscopy

Optical Microscopy (OM) is used to obtain structural information on emulsion under scale limit where unaided eyes are inoperative. This technique provides information about structurally complex systems in the form of images that are often relatively easy to perceive and understand by human beings (Mcclements, 2007). Due to its inexpensiveness, its ease of operation and its availability in most research facilities, OM is the most used type of microscopy.

Three fundamental qualities have to be warranted if OM is to be used to examine the structure of a microscopic object: resolution, magnification and contrast. *Resolution* is the ability to distinguish between two or more objects that are close together. *Magnification* is the number of times that the image is greater than the examined objects. *Contrast* determines how well an object can be distinguished from its background (Mcclements, 2007).

One of the major shortcomings of OM is that optical images of the emulsion microstructure require flat sample preparation (Hu et al., 2017). This preparation consists of spreading an emulsion across a slide and covering it with a coverslip. This procedure can alter emulsion structural properties and should therefore, be carried out carefully and reproducibly. OM can also be subjective and to overcome this disadvantage, it is often necessary to observe a large number of different regions in the sample spread on the slide to obtain reliable statistical data.

Modern optical microscopes are connected to computers that can capture and store a digital image of emulsion, which can then be processed using software to obtain information about microstructure. Optical micrographs of the F127/surfactant stabilised O/W emulsions were captured by a Zeiss (Axio Imager 2) optical microscope fitted with a digital camera. The emulsions samples were 10 times diluted and the diluted samples were placed directly on a microscope slide and covered with a coverslip. The emulsions were observed with differential interference contrast light (DIC).

Chapter 4 Results and Discussion

The scope of this chapter is to investigate aqueous block copolymer-surfactant mixtures and stability of emulsions formulated with mixed emulsifiers and salt. Mixed micellar and interfacial properties of SDS, CTAB and $C_{12}E_4$ with F127 are examined. The behaviours of the mixed emulsifiers and their ability to stabilise emulsions formulated with salt are investigated and discussed as a function of surfactant concentration. The mechanisms involved in emulsion stabilisation by polymeric surfactants have been investigated before and are quite well understood (Tadros, 2008). However, the ability of copolymer-surfactants mixture systems to stabilise emulsions depends strongly on their adsorption and association behaviours in the aqueous phase. In this Chapter, the surface properties of mixed emulsifiers are discussed, as well as the application of these properties to oil and water dispersions.

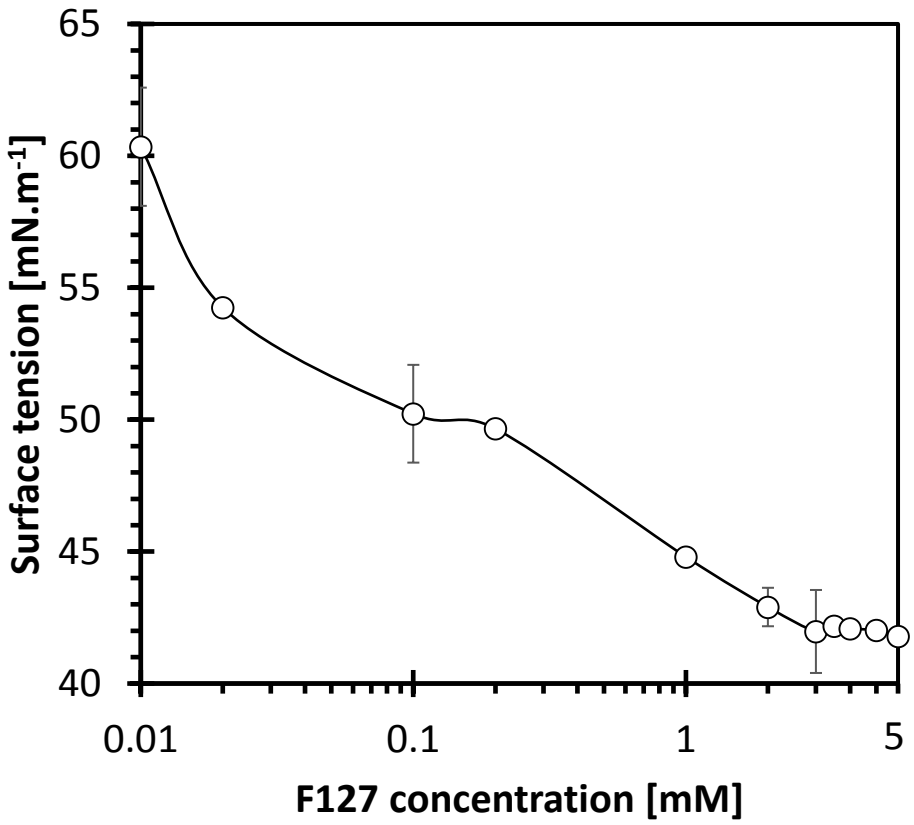

Figure 34. Surface tension of F127 at 20° C.

To ascertain surface-active and aggregating properties of F127 in the aqueous phase, surface tension measurements have been performed. Figure 34 shows a decrease of F127 solution surface tension as a function of its concentration. The decrease of surface tension indicates that the copolymer molecules have surface activity and wetting action (Thummar et al., 2011). The

break point represents the concentration beyond which F127 micelles are formed. Our observed cmc value of 3 mM at 20° C is in good agreement with the literature value (Alexandridis et al., 1994b). In contrast to the reported results of commercial Pluronics which usually show two break points (Alexandridis et al., 1994a), the occurrence of a single break in our F127 suggests that the other break is probably the effect of polydispersity (Zheng and Davis, 2000). It can be seen that the variation in surface tension caused by F127 is relatively low compared to the three low molecular surfactants. This is due to the high molecular weight of the copolymer hydrophobic moiety which quickly saturates the interface and leads to low cmc value (Bahadur et al., 1988).

Table 9. Outstanding aggregation concentrations detected by surface tension measurements at solution-air interface.

F127 (mM)	**SDS**		**CTAB**		**C12E4**	
	cac (mM)	**cmc** (mM)	**cac** (mM)	**cmc** (mM)	**cac** (mM)	**cmc** (mM)
0	—	9 (**8.12**)	—	1.62	—	0.06
0.01	0.4 (**0.4**)	9 (**9.12**)	—	3.54	—	1
0.05	0.4 (**0.4**)	13 (**13**)	—	3.54	—	3.54
0.1	0.2 (**0.2**)	20 (**25**)	—	7.58		—
3.5	1.25 (**2.04**)	180 (**181**)	1	30.1 (**35**)	—	~0.81
4	1.25 (**2.04**)	250 (**251**)	1	35.4 (**35**)	—	2.04
4.5	1.25	280	1	81	—	7.58

Note. When F127 present in solution, non-expressed cac concentrations are an indication of almost instantaneous binding of concerned surfactant to F127. The values in brackets and bold referred to outstanding aggregation concentration at water-oil interface.

The experimental results must be discussed while keeping in mind that surface activity of all mixed emulsifiers systems displayed equivalent behaviour at water/air and water/mineral oil interfaces (Figure 35). As can be seen in Table 9, cmc and other outstanding concentrations in both cases do not show systematic variation with changing fluid pairs. The essential distinguishing feature is definitely the gap between surface tension at the two interfaces, due to the difference in polarity at the two interfaces, inducing a difference in the magnitudes of hydrophobicity between the two pairs of fluids.

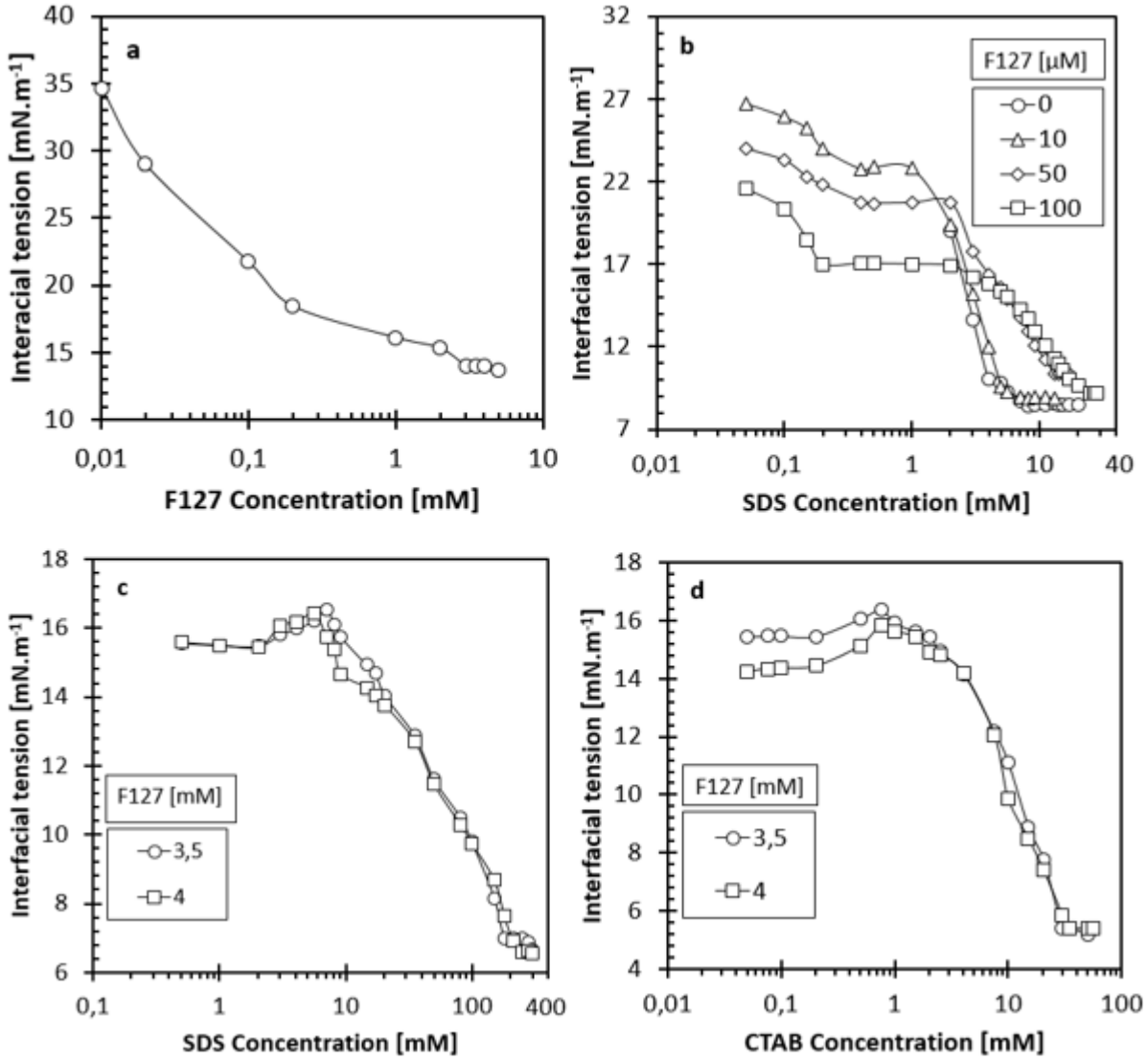

Figure 35. Water/Oil interfacial tension measurements at 25° C: a) F127; b) F127/SDS mixture below F127 cmc; c) F127/SDS mixture above F127 cmc; d) F127/CTAB mixture above F127 cmc.

Due to its low density of intermolecular interactions, air is a particularly nonpolar phase with very weak adhesive energy to a very cohesive interacting solvent such as water. The cohesive interaction in water between its molecules as expressed by its strong stiffness, small openness and relatively high order (see Section 2.5.2) is more important than the adhesive energy between water and air. Mineral oil in comparison has relatively greater adhesive energy, hence, its relative solubility in water phase allowing it to penetrate into the interfacial film is higher than air. The mutual repulsion is thus less pronounced at water-mineral oil than at water-air interface, giving rise to higher interfacial tension in the second case. The equivalence of surface-active behaviours at water/air and water/mineral oil interfaces show that the same

interaction mechanisms at the two interfaces are relevant for the understanding of emulsion stability.

Emulsions stability is best studied by following the variation of droplets size on which surfactant forming micelles are adsorbed (See Figure 17). For this reason, the interaction between surfactants and copolymers in the aqueous phase is of crucial importance for understanding of emulsion stability. The progressive emulsion breakdown process is best monitored by particle size distribution. The results obtained from Malvern Mastersizer as a function of surfactants concentration for freshly prepared emulsions are shown in Figures 40−48−53. Contrary to emulsions prepared with neat surfactants (i.e. 10 mM and 20 mM $C_{12}E_4$, 50 mM and 60 mM CTAB and 50 mM and 60 mM SDS) (Appendices 1 − 3) which (except those prepared with SDS) showed great instability, all emulsions stabilised with mixed F127/Surfactant emulsifiers exhibited monomodal distributions. This indicates that no re-coalescence phenomenon took place during the emulsification process, despite the high kinetic energy involved during the processing (7500 rpm), and susceptibility to the partial break up of interface of some droplets. Indeed, during emulsification process, the enhancement of collisions among newly formed droplets can lead them to re-coalesce if their interface is not completely covered by emulsifier molecules (Jafari et al., 2008).

Emulsification produces a substantial increase in the interfacial area, and for a fixed emulsion composition, there is a maximum interfacial area at a certain particle distribution size, which can be completely covered by the emulsifier. With further emulsification and below the limiting particle size distribution, emulsifier content becomes insufficient to cover the newly formed droplet interfaces completely and consequently, these droplets tend to coalesce with their neighbours.

Excessive energy input during emulsification can significantly enhance re-coalescence phenomenon (Torkkeli, 2003). High-intensity turbulence due to excessive energy input during emulsification (excessive mechanical energy in rotor-stator emulsification system for example) can lead to collisions between droplets. The role of adsorbed surfactant molecules on droplets interfaces is to prevent their re-coalescence in case they collide. If the colliding droplets are insufficiently covered by emulsifier, their collision results in re-coalescence.

Two scenarios can be the origins of incomplete covering of droplets interfaces by an emulsifier. The first one is the low content of surfactant in a continuous phase. The second and the more

related to energy input is the timescale of surfactant adsorption. In the case that emulsification energy exceeds a certain limit (typically 5000 rpm in rotor-stator system) by producing excessive turbulence and high susceptibility of droplets collision, the timescale of surfactant adsorption could be longer than the timescale of collision. The fresh droplet interfaces will be incompletely covered and re-coalescence will take place. This leads to the paradoxical conclusion that high emulsification energy which is supposed to produce a fine emulsion can rather generate one with bigger particle size distribution.

In this study, the presence of only one peak in the droplet distributions of freshly prepared emulsions stabilized with mixed emulsifiers shows that no re-coalescence occurs even at high processing energy. It can be thought that highly extended F127 PEO blocks formed multilayers around droplets entrapped in mixed micelles, covering the interface sufficiently to prevent re-coalescence (Jafari et al., 2008). In the cases of F127/ionic surfactants mixed micelles, it is presumable that Na_3PO_4 had efficiently screened repulsive charges inside mixed micelles, impeding disruption of F127 aggregates, thus maintaining effective coverage of entrapped droplets by mixed micelles and avoiding re-coalescence.

Stability of O/W emulsions formulated with F127 as stabilisers are substantially enhanced by the addition of low molecular surfactants. When these low molecular surfactants are ionic, to the steric repulsion of the droplets induced by unfavourable mixing of PEO hydrophilic chains is added the electrostatic repulsion of alike charges incorporated in the F127 micelle. A synergistic combination of these two stabilising mechanisms increases the CP of the aqueous phase further, the channel by which coalescence and Ostwald ripening proceed. However, even without input of any additional emulsifier, because of its high hydrophilic character (70 % of EO content) inducing a CP beyond 100 ℃ (see section 2.5.1, Table 6; and section 2.5.2, Figure 22), F127-based emulsions would be very resistant to irreversible breakdown processes when durably exposed to heat in absence of a water structure making electrolytes.

Figure 35 shows the influence of ageing treatment and Na_3PO_4 on the DSD of mineral oils in water emulsions stabilised by F127. In the absence of an ionic surfactant, the interaction between droplets containing adsorbed F127 is exclusively controlled by unfavourable mixing of its solvated chains. In the Equation 2.32 governing this free energy of mixing, it can be seen that the determining factor of emulsion stability is the $1/2 - \chi$ quantity, by which solvation conditions are good for chains or not, depending on whether χ gives rise to positive G_{mix} or not. In the presence of the high Na_3PO_4 valance salt, F127 could not retain its hydration at 60

℃ for more than four weeks and χ changed to > 0.5, shifting steric interaction of hydrated PEO from repulsive to attractive. As can be seen in Figure 36, growing of emulsion droplets started after 28th day of heat exposure, highlighting determining influence of Na_3PO_4 on coalescence of O/W emulsion stabilised by F127.

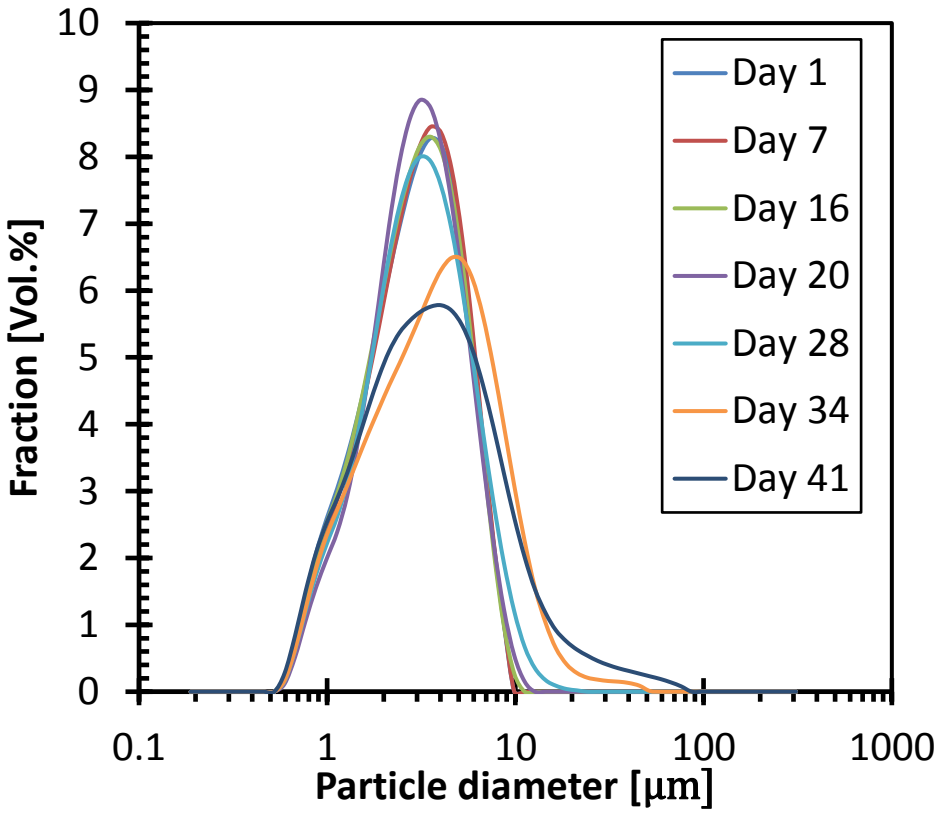

Figure 36. Droplets size distribution for F127 based emulsion.

4.1 SDS interaction with F127

The concentrations of F127 were investigated below and above 3 mM and F127 is respectively non-associated and in the micellar form on the two sides of this concentration according to surface tension results (Figure 34) and reference (Alexandridis et al., 1994b). Below this concentration, the aggregation behaviour of SDS in the presence of diluted F127 was studied by surface tension in the concentration range from 10 µM to 100 µM. The cmc value for the individual SDS was found to be 8.1 mM and agrees well with the reported literature values (8.3 mM (Ruiz, 1999)).

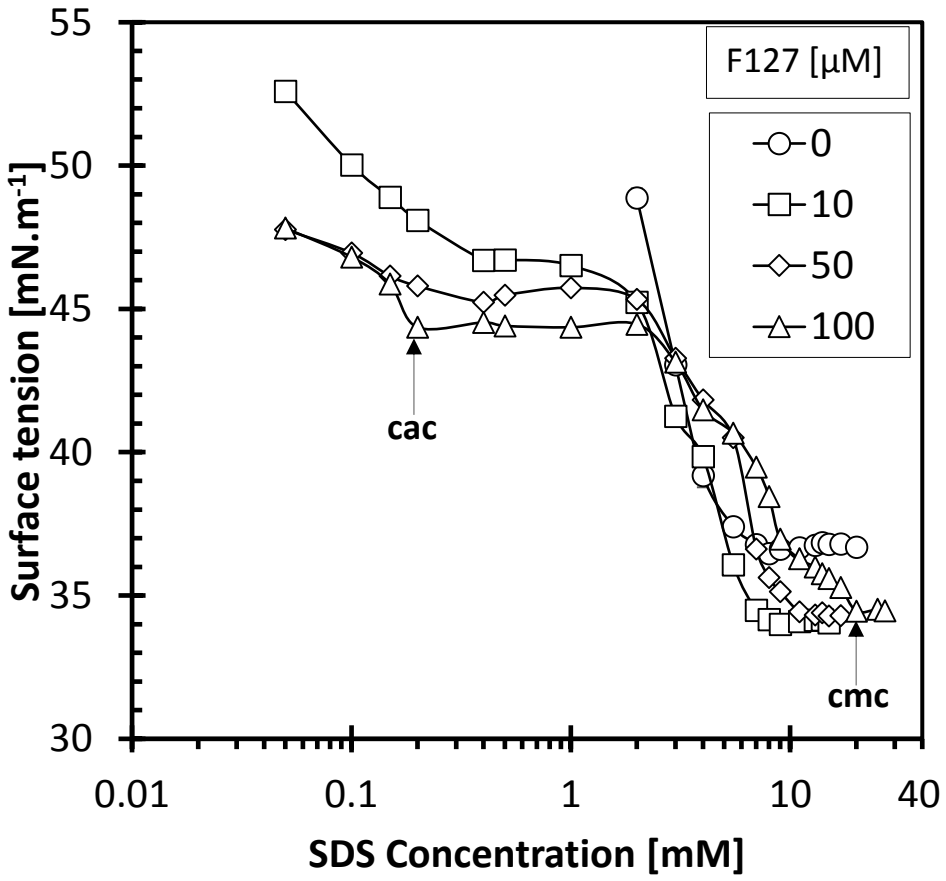

Figure 37. Surface tension versus concentration plots for SDS solution in the presence of non-associated F127.

The surface tension isotherms for the F127/SDS system are displayed in Figure 37. Before the addition of SDS in solution, the surface activity is due to the exclusive presence of the surface-active F127 monomers at the air/water interface. The subsequent decrease in surface tension when adding SDS is due to SDS partitioning between the bulk solution and its adsorption at air/water interface where F127 is also present. As further SDS is added, the decrease in surface tension is followed by a first plateau beyond cac of SDS. The cac is lower than the cmc of pure SDS. A marginal dependence of cac on F127 concentration is observed.

Interactions between anionic SDS and F127 in its diluted non-associated state can be viewed in some respects as analogous to the interaction of anionic surfactant with water-soluble homopolymers. In this case, the concept of competitive formation of polymer-free surfactant aggregates and polymer-surfactant association complexes relevant to homopolymer-surfactant systems (Section 2.4.1) can be applied to interactions with F127 non-associated block copolymer as well. The main factor controlling this competitive interaction is the flexibility of

the copolymer main chain, dictating the magnitude of polymer shielding area a_{pol}. For complexation-aggregation of SDS on the copolymer backbone to occur preferentially to surfactant self-micellisation, the copolymer must be of an overall relative high flexibility resulting from an average of the flexibilities of its two blocks.

Polyethylene oxide block in F127 is known to be very flexible as evidenced by its relatively high shielding area (Nagarajan, 1985). However, complete analysis of the interaction between F127 and SDS through their mass balance equation (Equation 2.16) is hampered by the absence of any quantitative data on the Polypropylene oxide shielding area. Although no data are available regarding this quantity for Polypropylene oxide block in order to deduce the overall flexibility of the F127 copolymer, the flexibility of PPO can be estimated through the constitution of its main chain.

The nature of the chemical groups constituting the polymer main chain determines its flexibility or its stiffness by the ease with which rotation can take place about the chemical bonds along the main chain upon glass transition or melting (Young and Lovell, 2011). Presence of bulky groups such as $p-$ phenylene in the main chain makes rotation difficult and increases polymer stiffness. Presence of polar groups such as amide linkage ($-CONH-$) that allows intermolecular hydrogen bonding to take place also increases stiffness and reduces flexibility. Finally, a third factor increasing polymer main chain stiffness is the type and size of any side groups present in the polymer backbone.

Alternatively, the incorporation of linking groups such as $-O-$ or $-CO-O-$ in the main chain increases polymer flexibility, lowering both glass transition temperature and melting point. This is the case for ethylene oxide (EO) whose main chain contains an oxygen linking group (Figure 38). Although propylene oxide (PO) contains a methyl $-CH_3$ side group which can be expected to increase chain stiffness, its presence is offset by the oxygenated $-O-$ linking group (Figure 39) whose role is to promote chain flexibility. From the comparison of Figures 38 and 39, it can be said that the PPO block in the F127 copolymer is of comparable flexibility to the hydrophilic PEO chain, so that overall F127 shielding can be said to be an average of its respective blocks.

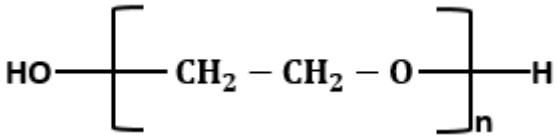

Figure 38. PEO monomer chemical structure.

In this case, F127 should display a global a_{pol} value characteristic of polymer-surfactant intrinsic-equilibrium constants (K_f and K_b) and aggregation numbers (g_f and g_b) indicative of complexation-aggregation occurrence in preference to micellisation. One should remember that in case $K_f < K_b$ and $g_b \sim g_f$, free micelles only form upon saturation of the polymer after completion of complexation-aggregation. Thus, overall flexibility of the F127 backbone allows it to completely wrap around the SDS micelle (Figure 15), decreasing the positive interfacial free energy of the anionic head groups lying at the micellar surface, hence promoting complexation in preference to the formation of free micelles.

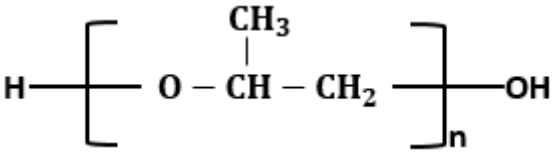

Figure 39. PPO monomer chemical structure.

Figure 37 shows the characteristic isotherms related to diluted block copolymer/surfactant interaction (Li et al., 2011, Ortona et al., 2006) for the F127/SDS system. Surface tension starts by decreasing smoothly, even at low SDS concentration without indication of any aggregation between SDS and F127 in solution. This surface tension decrease is due to surfactant partitioning between the bulk solution and its adsorption at the water/air interface where F127 is also present. As further SDS is added, a decrease in surface tension is followed by the first plateau beyond cac of SDS, which is lower than cmc.

In the composition range of the first plateau, surfactants aggregate on the copolymer backbone led by hydrophobic and ion-dipole interaction with F127 (Li et al., 2011). In this range of surfactant concentrations, the hydrophobic interaction between SDS and F127 is sufficient to give rise to the formation of bulk complexes. At this stage, PPO dehydrates from water phase followed by PEO segments (regions A and B in Figure 15). The dehydration of the PEO segment also takes place through hydrophobic interaction. In this same range of SDS concentration, the dehydration of F127 is followed by a reorganisation of F127/SDS aggregation complex to form a complete ion-dipole association complex, where PEO segments first rehydrate followed by PPO.

Thus, the formation of bulk complexes in solution on the first plateau above cac goes through dehydration of F127 backbone led by polymer induced micellisation, followed by its rehydration led by ion-dipole interaction. Beyond the first plateau, increase in SDS

concentration results in increasing concentration of surfactant at the water/air interface (surface excess concentration). Upon saturation of water/air interface, SDS starts aggregating in the bulk. One can see that self-aggregation of SDS in the presence of polymer is actually an extended critical micelle concentration (cmc_e) due to increasing of adsorption domain. This accretion of adsorption domain is also the cause of the continual increase of SDS cmc with the increasing of F127 concentration, leading to a greater increase of adsorption domain each time.

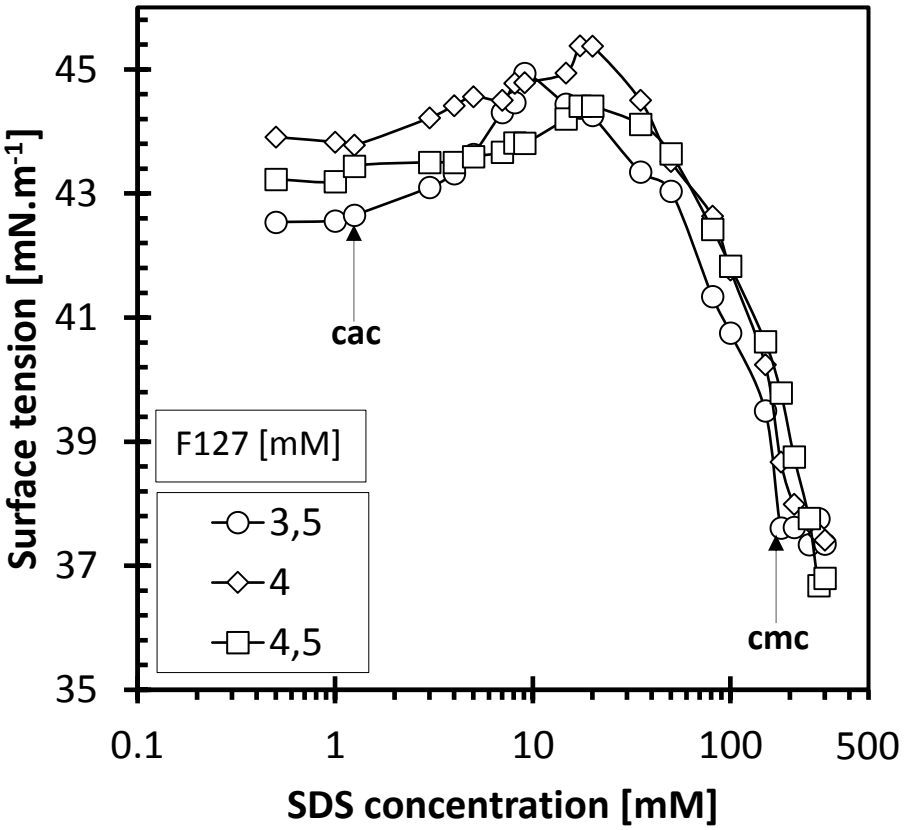

Figure 40. Surface tension versus concentration plots for SDS solution in the presence of micellar F127.

The salient feature of isotherm in mixed F127/SDS systems when the former is concentrated or in micellar structure (Figure 40) is the decrease of surface activity with increasing surfactant concentration. Several studies on F127/ionic surfactant systems carried out using different techniques (Sastry and Hoffmann, 2004) showed that F127 and other Pluronics micelles are destabilised and suppressed by ionic surfactants. At F127 concentrations beyond its cmc and at room temperature, its micelles are in equilibrium with its monomers in bulk as well as at interface. Indeed, at F127 cmc and beyond, F127 monomers dominate at the interface and inhibit SDS adsorption.

Initially, monomeric concentrations of F127 and ionic surfactants at water/air interface do not change significantly enough to affect surface tension. Beyond cac, SDS starts binding substantially to polymeric monomers both at the interface and in the bulk. The polyelectrolyte-like complexes formed being less hydrophobic than the nude surfactants and copolymer (Couderc-Azouani et al., 2005), sink from the interface into the bulk, leaving the water/air interface unsaturated with respect to both F127 and surfactants. As a consequence, surface tension increases during the course of the binding process up to a maximum, beyond which it starts decreasing.

Since F127 micelles are in equilibrium with its monomers at room temperature, SDS can theoretically bind to both micelles and monomers. Although surface tension cannot probe bulk properties, we have good reason to think that the range of surface tension increase also corresponds to binding with copolymer micelles and to the subsequent shifting of *copolymer micelle* ↔ *monomer* equilibrium in favour of the latter as evoked in literature by using other methods (Li et al., 2001b, Thummar et al., 2011). Since hydrophobicity is the first driving force of block copolymer-surfactant complexation, it is likely that in the mixed micelles (as for interaction with monomeric block copolymer), ionic surfactants first bind to PPO blocks in the core of F127 micelle. Therefore, the destabilisation of F127 micelles by SDS is most likely to be largely due to high charge density of head groups in the hydrophobic core of the ionic F127/SDS mixed micelles, which by mutual repulsion leads to disruption of the micelle.

However, as shown by Hetch and Hoffmann (Hecht and Hoffmann, 1994), this electrostatic repulsion between head groups cannot be the only mechanism underlying micelle destabilisation, otherwise, the addition of electrolytes supposed to screen alike charges should reverse or at least inhibit micelle disruption. Additional mechanisms are probably changes in PPO and PEO state of hydration, as evidenced for monomeric F127. By binding to PPO in the F127 inner hydrophobic core, the former becomes saturated with surfactant and is less hydrophobic. For SDS, as its concentration increases and after completion of PPO binding, it also binds to the fully hydrated PEO chains in the outer shell of the copolymer micelle. This process results in PEO dehydration. Combination of these two processes leads to disequilibrium of F127 HLB and alteration of its aggregation capacity. As SDS concentration increases beyond the maximum of surface tension increase, copolymer micelles are disrupted and its monomers are saturated in the bulk. Beyond this point, surfactant monomers start populating interface, inducing surface tension decrease. This decrease in surface tension

continues until the interface is completely saturated and normal surfactant micelles start forming.

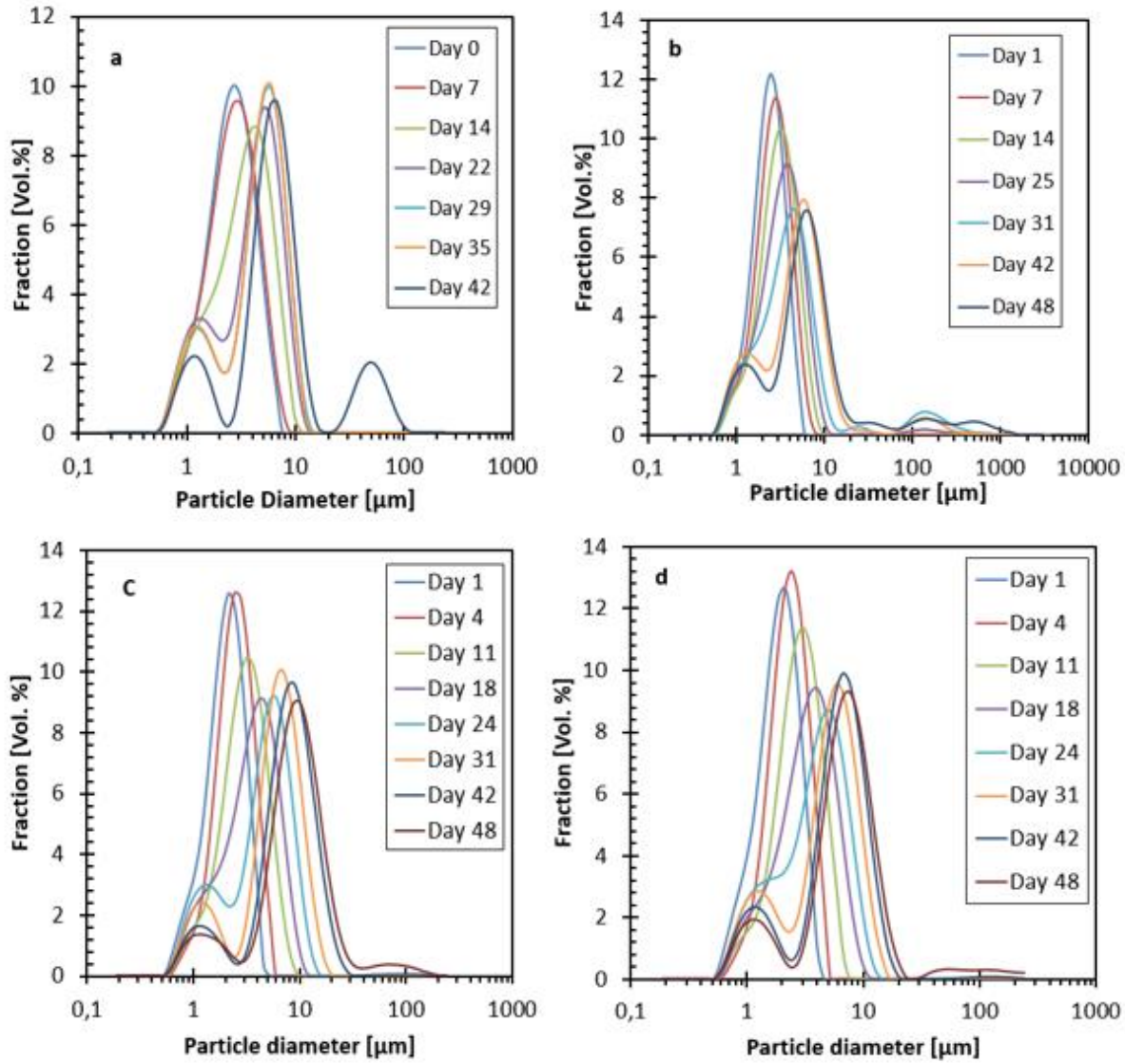

Figure 41. DSD for emulsions containing different SDS concentrations: a) 30 mM, b) 40 mM, c) 50 mM, d) 60 mM.

The presence of electrolytes in surface-active systems has been found to exert remarkable influence on their surface tension and aggregation behaviour (Corrin and Harkins, 1947, HAQ et al., 2017, Bharatiya et al., 2008). In this study, their ability to influence micellar characteristics by altering surfactant interactions is leveraged in the understanding of emulsion stability formulated with mixed emulsifiers. Figure 41 shows the influence of ageing treatment on the DSD of emulsions stabilised by F127/SDS mixed emulsifiers. They all display progressive broadening of DSD, shifting to larger droplets with accentuation of the shoulder

towards a bimodal distribution as surfactant concentration increases and heat exposure is pursued in time.

The interaction of PEO solvated chains giving rise to unfavourable mixing is hampered by the binding effect of SDS surfactant to F127 chain. In this condition, the usual Flory-Huggins polymer-solvent interaction parameter, χ, giving the measure of polymer-solvent interaction (Tadros, 2008) is insufficient to account for emulsion stability behaviour, and electrostatic effect must be included. As a consequence, the main stabilising mechanism is not steric anymore but it is now due to electrostatic repulsion of F127/SDS mixed micelles induced by the presence of SDS electric charges at the mixed micellar surface (Manohar and Kelkar, 1990, Mata et al., 2004). As temperature changes do not affect appreciably charged emulsifier solutions' CP (Shinoda and Lindman, 1987), the presence of sodium phosphate becomes the main factor accountable for the emulsion breakdown processes. By swamping original charge distribution and screening the corresponding electrostatic repulsion, the high valance of sodium phosphate allows droplets' merging resulting in coalescence.

The shifting of droplets size distributions to bimodality as surfactant concentration increases and heat exposure is pursued reveals consecutive activities of two distinct types of droplet populations. According to F127/SDS isotherms when F127 is in the micellar state (Figure 40), no pure SDS micelle occurs at used SDS concentrations for preparation of our emulsions. However, taking into account the effect of high valence sodium phosphate salt which considerably reduces cmc of both F127 and SDS, it is likely that the whole process from complexation with unassociated F127 to the formation of pure SDS micelles fit in the used concentrations of our emulsions.

One should remember that the onset of SDS binding to F127 is associated with the occurrence of F127/micellar SDS complexes whose formation increases interfacial tension and decreases surface activity. When F127 micelles are completely disrupted and free monomers fully bounded, the polyelectrolyte-like micelles are rearranged in a complete ion-dipole complex as in region D of Figure 15, with F127 chain wrapped around SDS micellar heads. On the other hand, the excess concentration of SDS pursues interfacial activity until pure SDS micelles entrapping oil droplets are formed (Figure 15). Consequently, two different populations of oil droplets are entrapped in SDS micelles: the first being entrapped in SDS micelles fully bounded to F127 chains wrapped around SDS micellar heads, and the second being entrapped in SDS micelles free of F127 chains wrapped around them. As a consequence, in the early days of

exposure, only unwrapped droplets aggregate (those entrapped in SDS pure micelles) while the wrapped ones are unaffected by clouding due to protective F127 monolayer shielding SDS ionic heads from sodium phosphate screening effect.

It could be expected that with further exposure to heat, the F127 monolayer should dehydrate and sink from droplet interface, leaving screened charged micelles unshielded and exposed to clouding, which would result in droplets merging and coalescence. However, the constancy of the size of a portion of the droplets as appearing in Figure 41 (and in appendix 5 for 20 mM SDS), shows that F127 monolayer of wrapped droplets never sink and its shielding action from Na_3PO_4 screening effect is very effective.

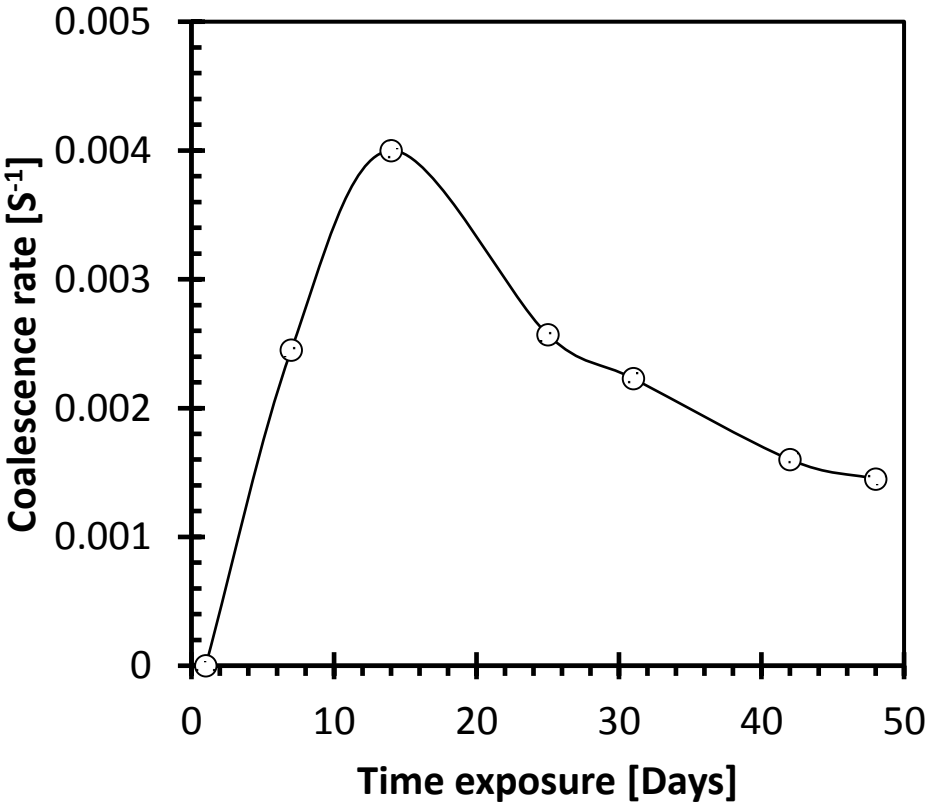

Figure 42. Variation of coalescence rate of emulsion containing 40 mM SDS

At a small SDS concentration (10 mM in appendix 5), F127/SDS aggregation complexes are probably not fully reorganised yet (or just a few of them are) to form a complete ion-dipole association complex where the F127 chain is completely wrapped around the SDS micelle. At this concentration and below, although SDS micelles might not be free of any binding to F127 (region C of Figure 15), they are not completely shielded from the salt screening effect. As a consequence, only one population of droplets exist, those entrapped in relatively free SDS

micelles. This is why the appearance of shoulder and shifting to bimodality only starts becoming evident at long-term exposure with a further increase in surfactant concentrations, concentrations at which complete ion-dipole association complexes are in equilibrium with free SDS micelles.

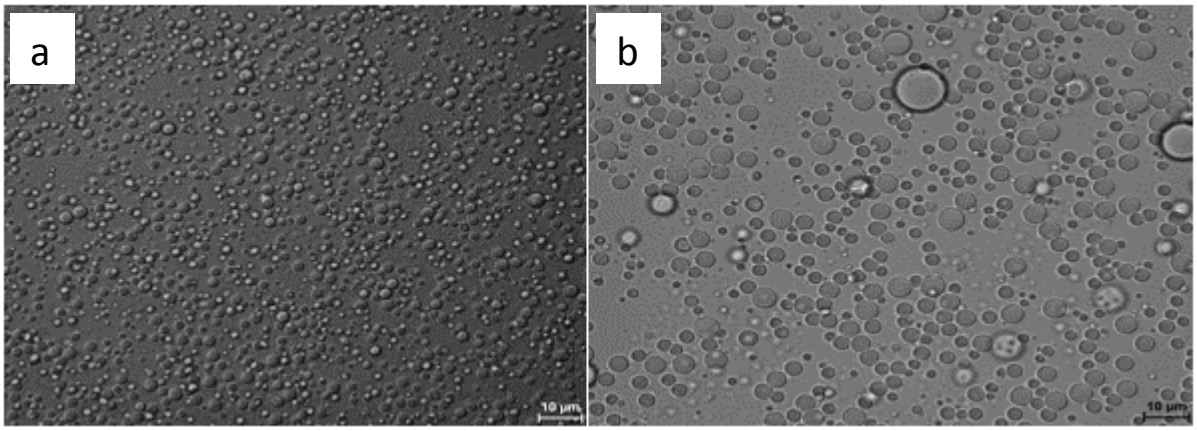

(A)

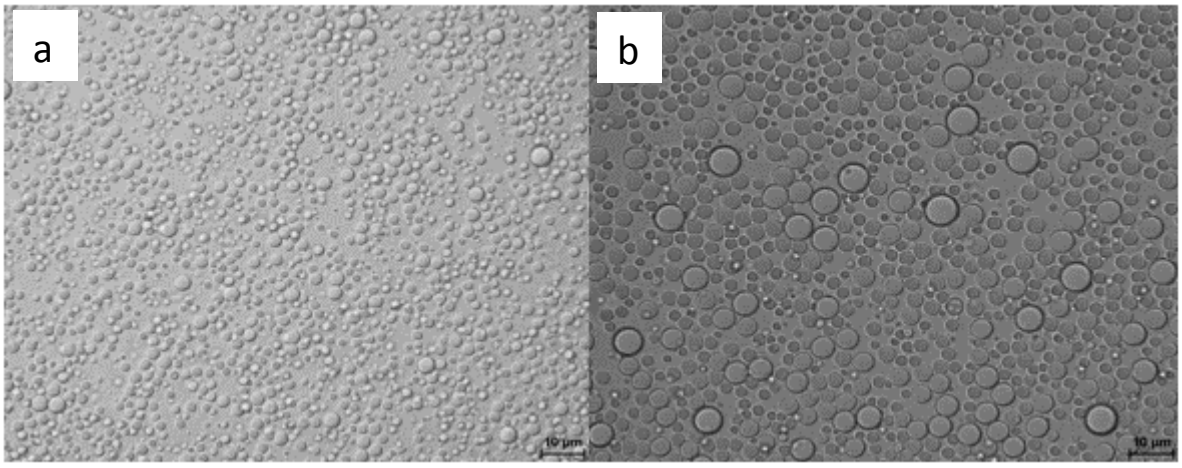

(B)

Figure 43. Optical micrographs of 10 times diluted emulsions for first (a) and 37th day (b): (A) 40 mM SDS and (B) 50 mM SDS.

The preceding interpretation is corroborated by Figures 42 and 43. After the fast increase of droplets diameter in the early days of exposure, coalescence rate (calculated through Equation 2.38) of SDS shows a net decrease tending towards a stabilisation. This lowering of coalescence rate can be viewed as a shifting of droplets activity from one population of droplets to another, from unstable unshielded droplets to stable shielded ones. Indeed, SDS micrographs show clear evidence of the considerable number of particles whose diameters have remained

constant next to those whose diameters are considerably increased. The decrease of the total number of droplet causing decrease of collision rate is an additional aspect regarding the lowering of coalescence rate.

Figure 44 displays variation of freshly prepared 30 mM SDS emulsions' viscosity with increase of shear rate. All emulsions showed shear-thinning behaviour, i.e., decrease of the apparent viscosity with increasing shear rate applied. Shear-thinning behaviour in Figure 44 could be due to the gradual orientation of the F127 macromolecule in the direction of flow in order to reduce the frictional resistance and their deformation by hydration in the direction of flow (BREWER et al., 2016).

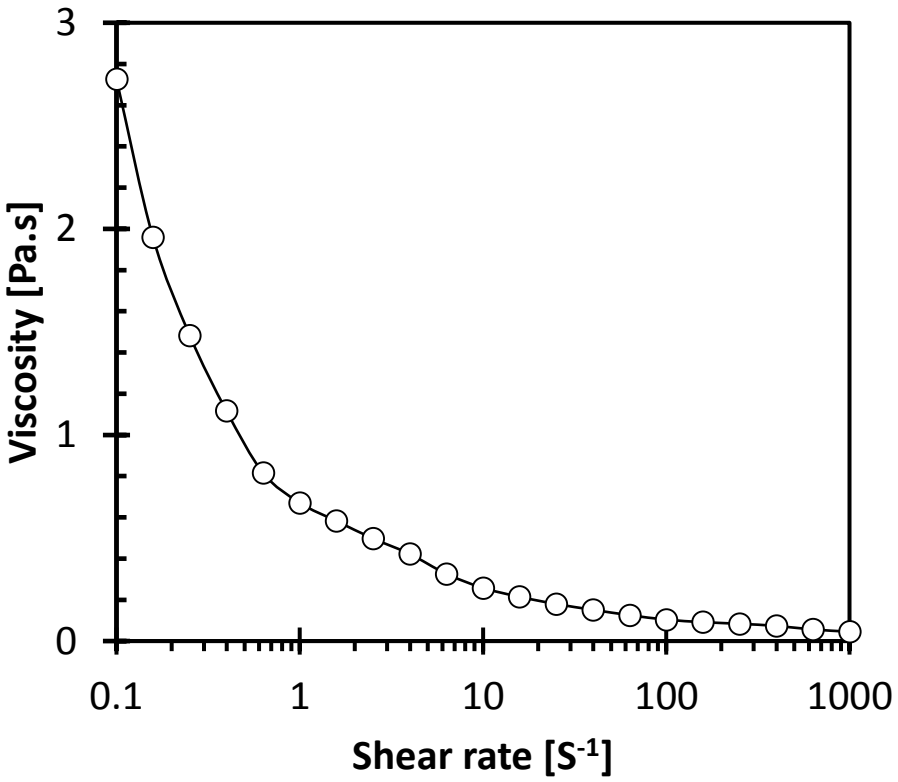

Figure 44. Variation of freshly prepared 30 mM SDS emulsion viscosity with increasing shear rate

The decrease in viscosity in Figure 44 upon the increase in shear rate is strongly connected with the movement of the droplets of the dispersed phase (Zhang et al., 2018). At low shear rate, the motion state of the droplets is not severely affected. As they are not deformed, the droplets are less likely to move in the direction of the action of the external force. As shear rate increases, the deformation of the droplets happens, leading them to move totally along the direction of the action of the external force.

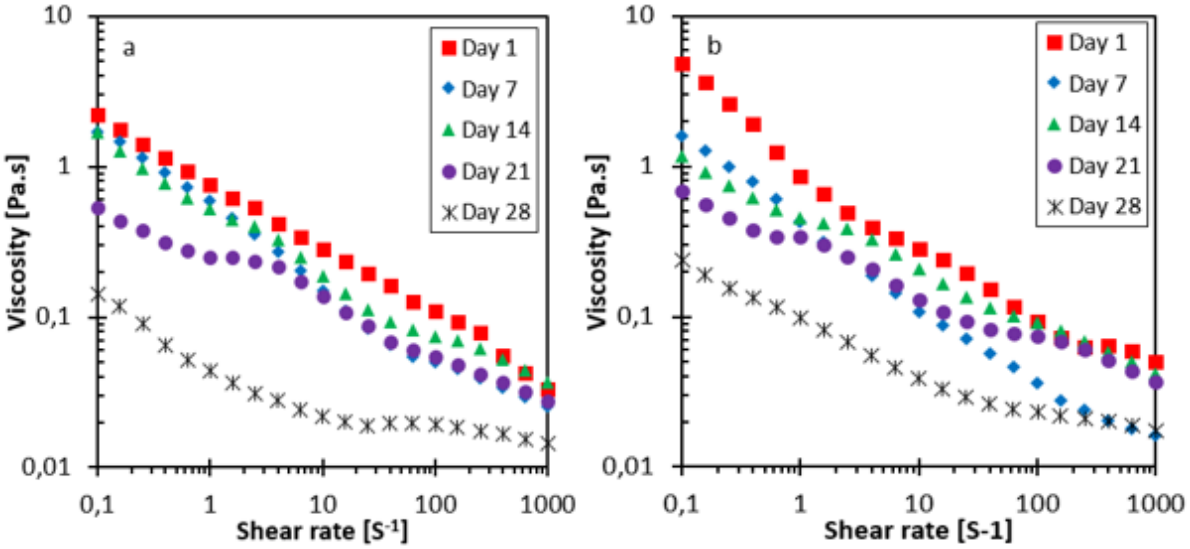

Figure 45. Variation of viscosity for emulsion containing 40 mM SDS and 50 mM SDS

It is well known that particle size has a direct effect on dispersion viscosity (Rámirez et al., 2002): the smaller the particle size distribution, the more viscous the dispersion, the wider the range of particle size (i.e., the more polydispersed the system), the lower viscosity. As a consequence, a shifting of particle size distribution to bimodality is associated with large reduction in viscosity. Figure 45 shows the evolution of viscosity with ageing. In absence of any flocculation (as evidenced by Figure 43) and at any volume fraction of oil, increase in droplet size results in reduction of viscosity and coalescence of the emulsion is ascertained by the decrease of its viscosity (Tadros, 2004). Thus, the large reduction of viscosity for ionic SDS containing systems is significant of salt strong activity in screening repulsive electrostatic interaction between charged droplets, bringing them closer for thinning and disruption of the liquid film.

4.2 CTAB interaction with F127

Below F127 cmc, the aggregation behaviour of CTAB in the presence of diluted F127 was studied by surface tension in the concentration range from 10 µM to 100 µM. The cmc value for the individual CTAB was found to be 1.6 mM and agrees well with the reported literature values (1.66 mM (Alawi, 2010)).

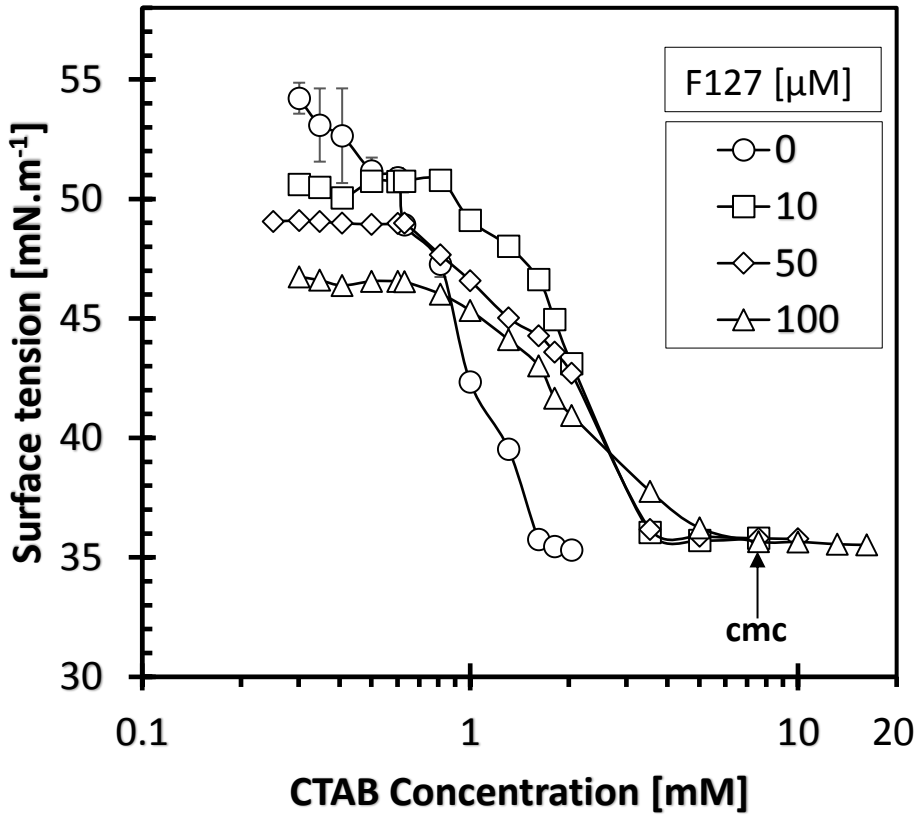

Figure 46. Surface tension versus concentration plots for CTAB solution in the presence of non-associated F127.

The same pattern of thermodynamic association with an individual block of F127 used for SDS can apply for CTAB. Figure 46 shows the evolution of surface tension as a function of CTAB concentration at different F127 concentrations. The F127/CTAB isotherms show a marked difference compared to SDS/F127 mixture. Surface tensions start by remaining constant, with values quite similar to those of pure surfactant solutions, which is a reliable indication of low CTAB activity at water/air interface where F127 is also present.

In these first regions of isotherms, the trends suggest that after CTAB weak activity at the interface, interaction with F127 occurs almost spontaneously as surfactant concentration increases, to form complexes with the compatible segment of a block copolymer. Upon further increase of surfactants concentration, surface tensions reach points where they start decreasing dramatically, indicating an increase of surface activity at water/air interface, consecutive to F127 monomers saturation in bulk. Surface tension continues to decrease with increasing CTAB concentration until a second plateau is reached, significant of the surfactants extended critical micelle concentration (cmc_e).

Contrary to SDS, one can see that at low concentrations, CTAB does not display a decrease in surface tension when simultaneously present in solution with F127. This is significant of the fact that the adsorbed F127 monomers inhibit its surface activity when it is in small concentrations in the solution. This provides an indication of the relative binding strength of the two surfactants to F127. In this respect, and as compared to SDS, CTAB seems to interact less strongly with F127. The reason for this difference relies in the structural difference between the three surfactant head groups. While CTAB should also be found rehydrating the hydrophilic PEO segment through the ion-dipole mechanism, it is restricted to do so by its cationic nature, exposing it to repulsion from the protonated hydrophilic PEO block (Nagarajan, 1985). The only interaction mechanism of CTAB with F127 is thus through polymer-induced micellisation, which in these cases is the only mechanism underlying the F127/CTAB association complex. Consequently, complete ion-dipole association complex cannot occurs (region D of Figure 15) since ion-dipole interaction with PEO is not cooperative. SDS is not subjected to any of these restrictions.

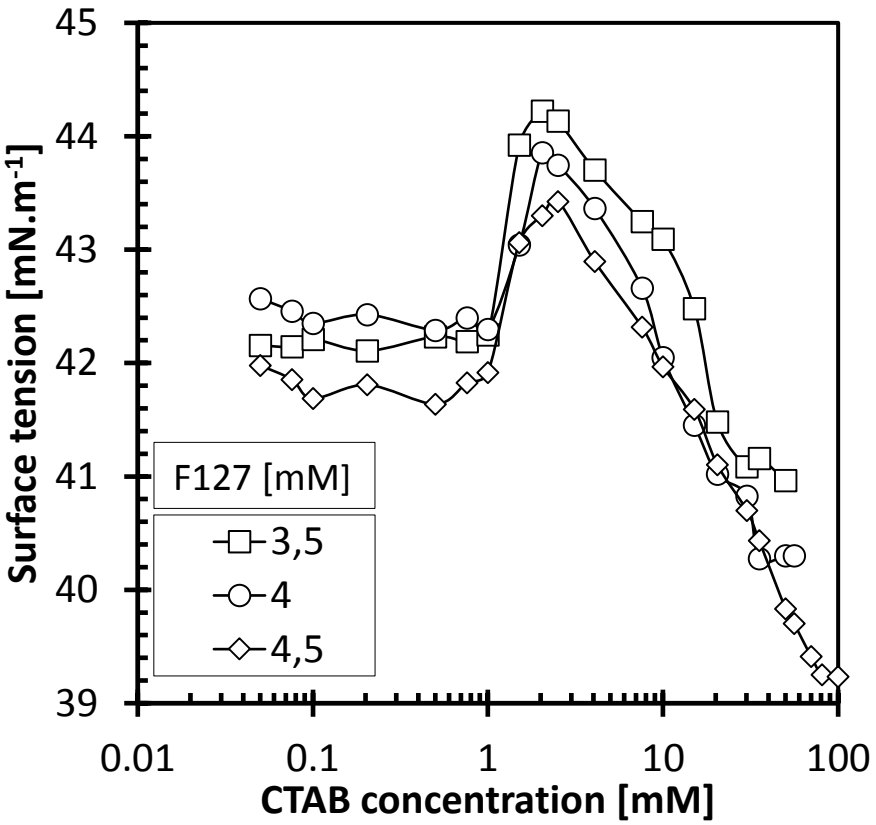

Figure 47. Surface tension versus concentration plots for CTAB solution in the presence of micellar F127.

When simultaneously present in solution with micellar F127, similarly to SDS, F127/CTAB displays a shifting of *copolymer micelle* ↔ *monomer* equilibrium in favour of the latter (Figure 47). Beyond cac, CTAB starts binding substantially to monomeric F127 both at interface and in the bulk, forming hydrophobic polyelectrolyte-like complexes which are less hydrophobic than nude surfactant and copolymer. Consequently, these polyelectrolyte complexes sink from interface, causing increase in surface tension due to unsaturation of air/water interface.

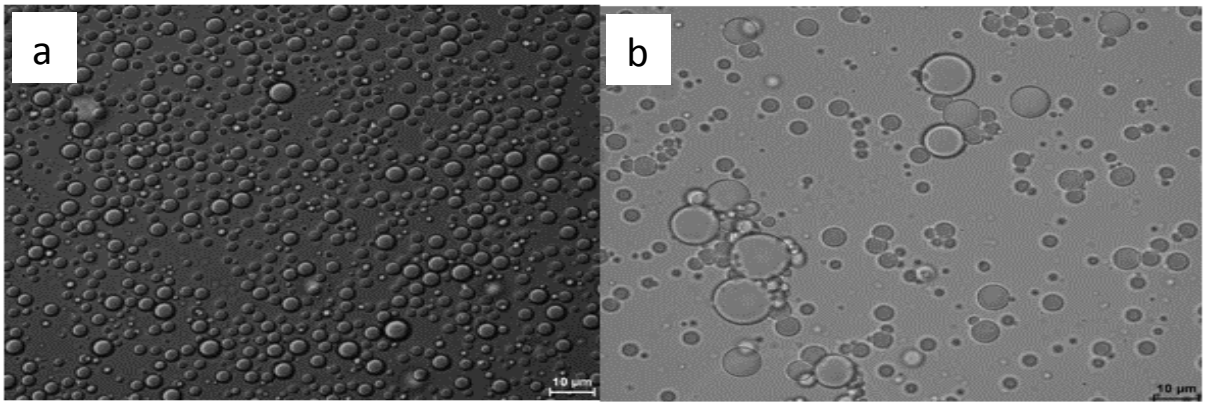

(A)

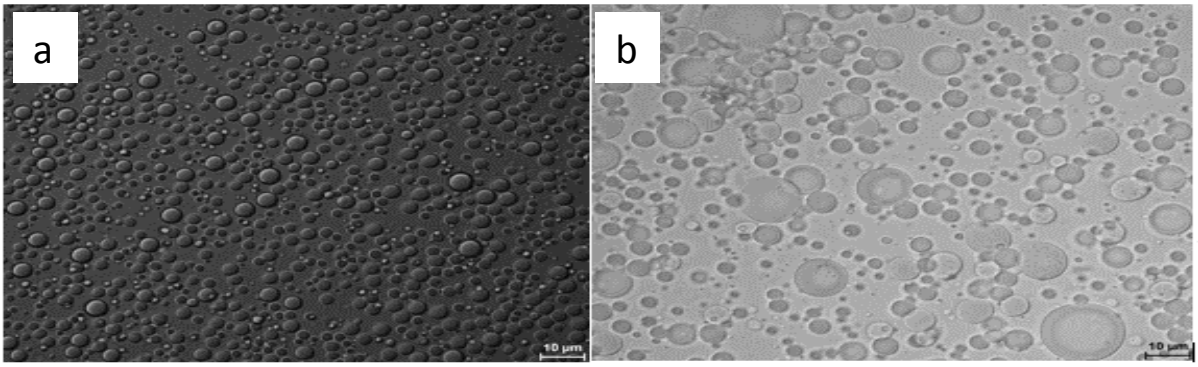

(B)

Figure 48. Optical micrographs of 10 times diluted emulsions containing: (A) 30 mM CTAB for first (a) and 28th (b) day. (B) 40 mM CTAB for first (a) and 35th (b) day

Figure 48 shows optical micrograph images of CTAB containing emulsions. Evidence of coalescence droplets can be observed, with small flocculated droplets hooked on the coalesced ones. The simultaneous presence of flocculation and coalescence in CTAB emulsion tends to indicate that Ostwald ripening could have proceeded from flocculation before resulting in monodispersed droplets undergoing coalescence. Thus, two consecutive breaking down mechanisms could have taken place in CTAB containing emulsions, contrary to SDS emulsions which only displayed coalescence.

Figure 49 shows the influence of ageing on emulsion stabilised by mixed F127/CTAB emulsifiers. The primary DSD of the emulsion only showed a very small increase with increase of the storage time, indicating that coalescence is insignificant. Coalescence started becoming substantial only on the 22th day for the two least concentrated emulsions, and 30th day for the two most concentrated ones. However, the absence of any increase in droplet size in the early days of heat exposure might be significant of weak flocculation induced by the reduction of solvency for F127 PEO chain upon the presence of salt (Tadros, 2004). The weak flocculation is strengthened over time as heat exposure is pursued and becomes incipient when the solvency of water for PEO chain becomes very poor, i.e. above θ-condition.

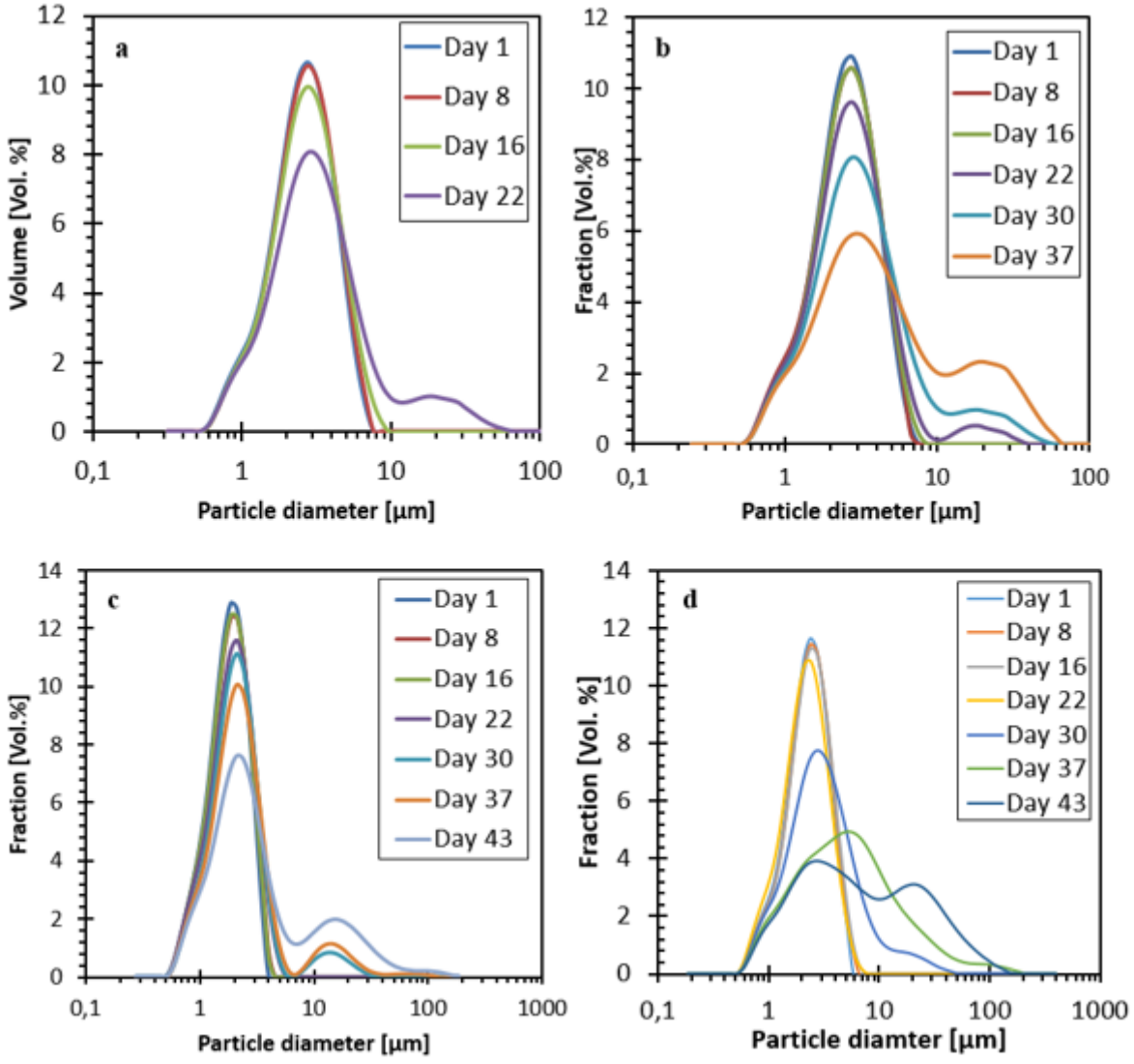

Figure 49. DSD for emulsions containing different CTAB concentrations: a) 30 mM, b) 40 mM, c) 50 mM, d) 60 mM

Indeed, CTAB, due to its cationic nature, undergoes electrostatic repulsion with protonated PEO blocks of F127. Therefore, full binding of CTAB to F127 chain cannot occur, since ion-dipole interaction with PEO is not cooperative. In this situation, reorganisation of the F127/CTAB system to form ion-dipole association complex is unable to lead to the complete wrapping of the F127 chain around CTAB ionic micelles (as in phase D of Figure 15). As a consequence, there are entire non-interacting blocks of F127 which are pending in the aqueous phase. It is likely that unwrapped blocks of F127 molecules pending in aqueous phase give rise to entanglements between hydrophilic chains linked to neighbouring droplets, which may promote flocculation and, subsequently, Ostwald ripening by reducing the path length of flocculated oil droplets brought in contact (Santos et al., 2017). As ripening proceeds in time and CTAB concentration is increased further, the emulsions become roughly monodispersed and "diffusion-solubilisation" of smaller droplets in bigger ones is stopped. Beyond this point, coalescence takes over and becomes the dominant destabilising mechanism. The combination of these two mechanisms can be the reason why CTAB-containing systems broke down so quickly compared to SDS.

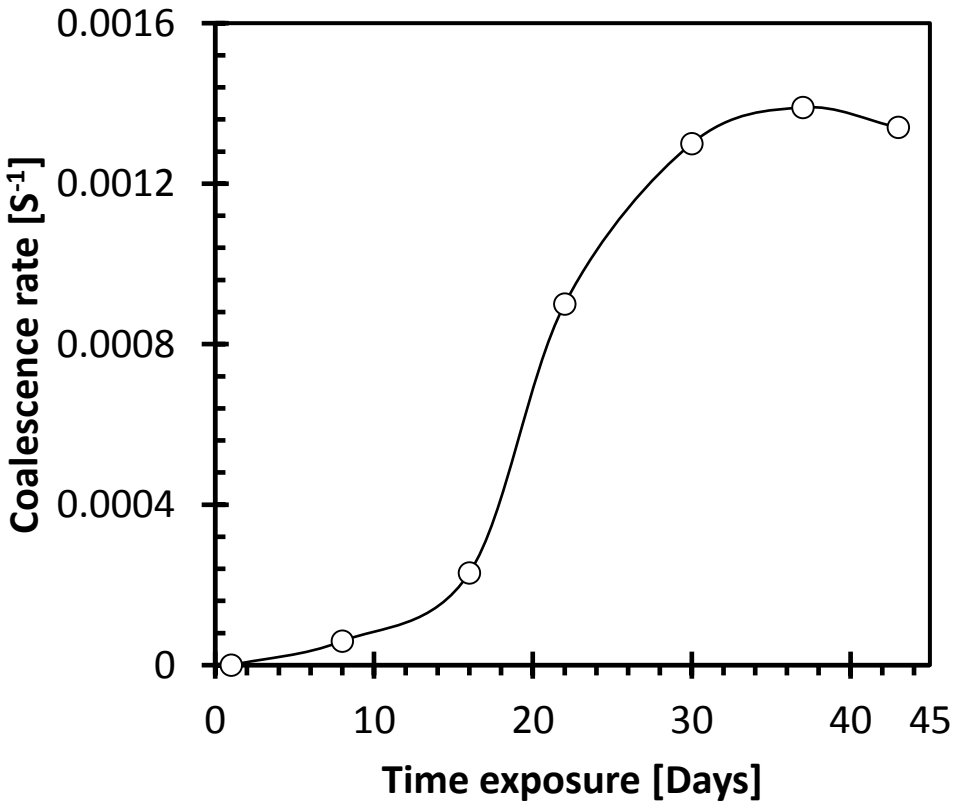

Figure 50. Variation of coalescence rate of emulsion containing 40 mM CTAB

Due to the complex structure of mineral oil, molecular quantities composing the LSW equation are difficult to estimate (especially molecular volume V_o and aqueous solubility C_w^{eq} which are easily estimated from group contributions when the molecular structure is well known (Durchschlag and Zipper, 1994, Polak and Lu, 1973, Tsonopoulos and Wilson, 1983, Heidman et al., 1985, Economou et al., 1997); unfortunately this makes Equation 2.37 difficult to use for estimation of Ostwald ripening. However, contrary to the SDS coalescence rate which displays a rapid increase followed by sharp decrease, CTAB containing emulsions shows a continuous increase of coalescence rate followed by relative stabilisation (Figure 50).

It is well known that Ostwald ripening by its own cannot lead to phase separation because the rate of droplets growth decreases as the droplet size increases, i.e. as the emulsion becomes monodispersed (Tadros et al., 2004). Although mineral oil is very low soluble in water and droplets are too big for the pressure gradient inside droplets of different sizes to be significant and substantial, there is still one mechanism which can potentially lead to Ostwald ripening before emulsion becomes roughly monodispersed and coalescence takes over as the main breaking down process. This mechanism is the entanglement taking place between protonated PEO blocks which undergo repulsion from CTAB headgroups and pend in the aqueous phase. Although the distances between droplets are not very long, as has been shown by Santos *et al.* (2017), the entanglement taking place could be the promoting mechanism of flocculation, which would subsequently result into Oswald ripening. In addition, the fact that emulsions are stored at high temperature could be the reason of incipient flocculation taking place as stated above, which generally is accompanied by a large increase of flocculated structure's cohesive energy E_C (Tadros, 2004).

In short, the conditions for an incipient flocculation are met since the solvency of the medium is deeply affected by the presence of sodium phosphate and the high storage temperature. Moreover, E_C is increased by the strong attraction between the droplets which is promoted by PEO blocks entanglement. The high E_C have the ultimate effect of leading to Ostwald ripening which would subsequently lead to coalescence. It is therefore plausible to think that increase in coalescence rate on Figure 50 could be significant of coalescence taking over as main breaking down process after completion of Ostwald ripening.

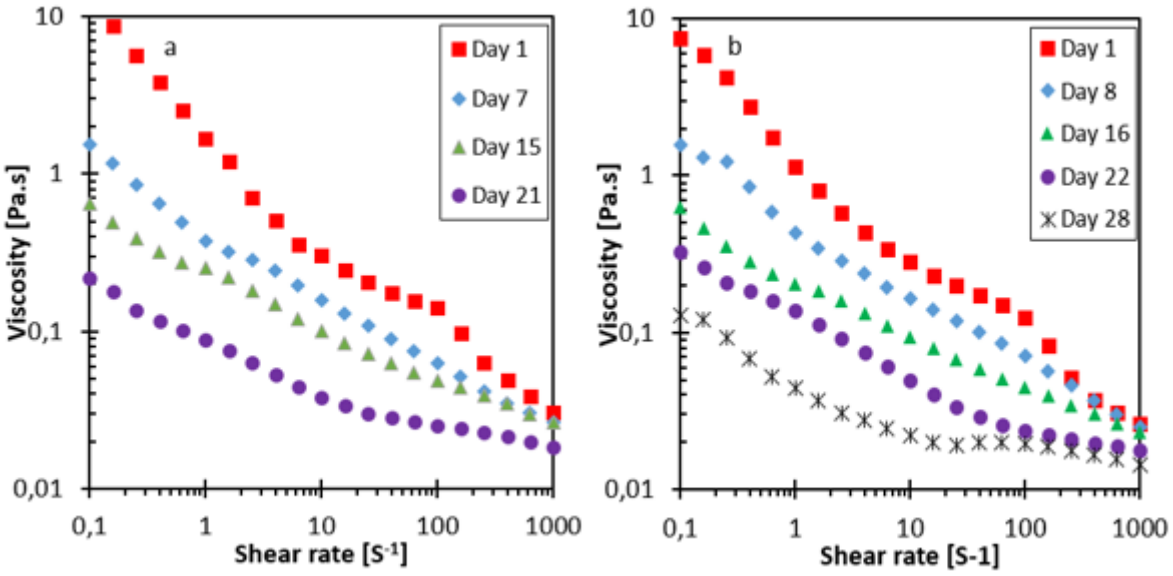

Figure 51. Variation of viscosity for emulsion containing 30 mM CTAB and 40 mM CTAB

Figure 51 shows the evolution of viscosity with the ageing of CTAB containing emulsions. Similarly to SDS, shear-thinning behaviour is observed for CTAB containing system viscosity measurement. The observed decrease of viscosity from the early storage time shows that, as stated for particle size distribution, coalescence was not completely absent, though no increase in droplet size was observed suggesting the presence of weak flocculation (Tadros, 2004). Thus, F127/CTAB stabilised emulsions are found to undergo consecutive flocculation, Ostwald ripening and coalescence, which is accountable for their quick break down.

4.3 $C_{12}E_4$ interaction with F127

Under F127 cmc, the aggregation behaviour of $C_{12}E_4$ in the presence of diluted F127 was studied by surface tension in the concentration range from 10 µM to 50 µM. The cmc value for the individual $C_{12}E_4$ was found to be 0.06 mM and agrees well with the reported literature values (0.0064 mM (Rosen et al., 1982)) .

Once again, similarly to SDS, the same pattern of thermodynamic association with individual blocks of F127 can apply for $C_{12}E_4$. Surface tension in Figure 52 starts by remaining constant, with values lower than those of pure surfactant solutions, indicating inexistent $C_{12}E_4$ activity at water/air interface where F127 is also present. After surfactant inexistent activity at the interface, the interaction between F127 and $C_{12}E_4$ occurs almost spontaneously as $C_{12}E_4$ concentration increases, to form complexes with the compatible segment of block copolymer. Upon further increase of $C_{12}E_4$ concentration, surface tensions reach points where they start

decreasing dramatically, indicating an increase of surface activity at the water/air interface, consecutive to F127 monomers' saturation in bulk. Surface tension continues to decrease with increasing $C_{12}E_4$ concentration until a second plateau is reached, significant of cmc_e.

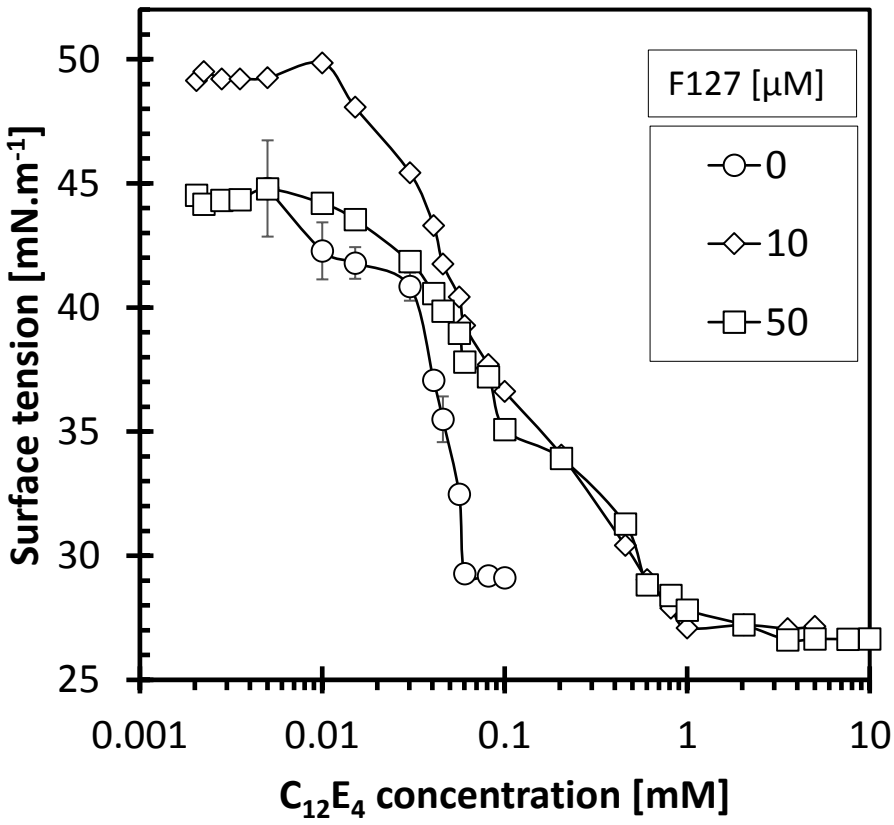

Figure 52. Surface tension versus concentration plots for $C_{12}E_4$ solution in the presence of non-associated F127

Similarly to CTAB and contrary to SDS, $C_{12}E_4$ does not display a decrease in surface tension when simultaneously present in solution with F127. The reason for this difference lies in the structural difference between the three surfactant head groups. The neutral nature of $C_{12}E_4$ head group prevents it from interacting with PEO polar groups through the ion-dipole mechanism. The only interaction mechanism of $C_{12}E_4$ with F127 is thus through polymer-induced micellisation, which in these cases is the only mechanism underlying F127/Surfactant association complex. Consequently, a partial or complete ion-dipole association cannot take place and complex formation is limited to regions A and B in Figure 15.

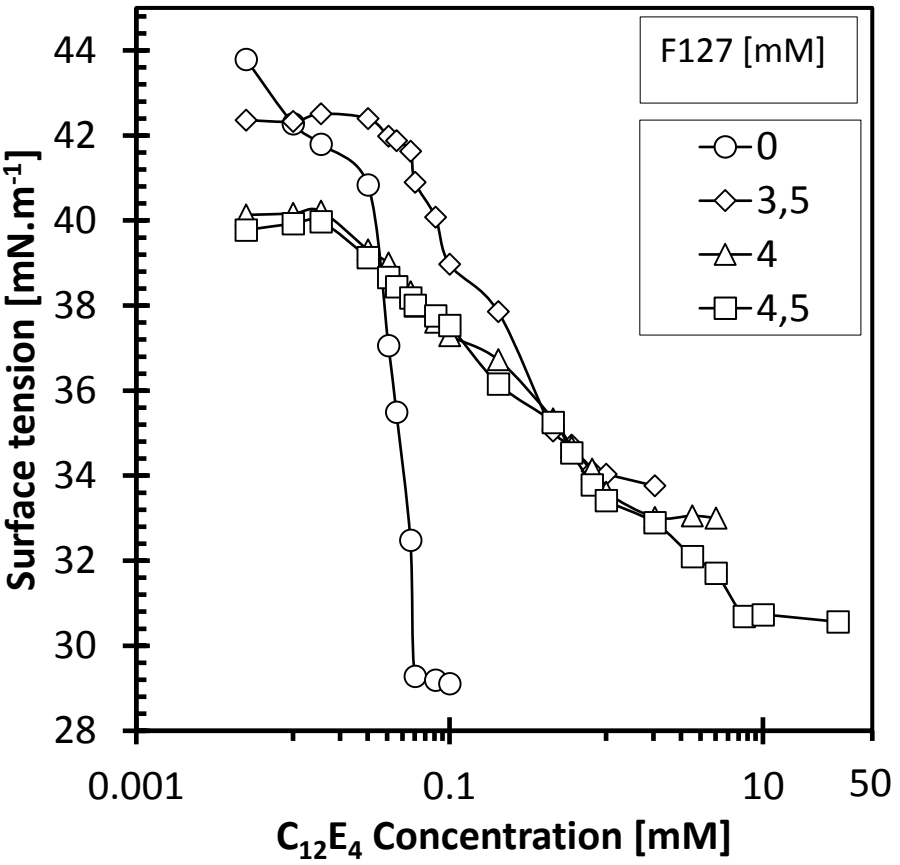

Figure 53. Surface tension versus concentration plots for $C_{12}E_4$ in the presence of micellar F127

Interaction of micellar F127 with neutral $C_{12}E_4$, as shown in Figure 53, displays different trend from CTAB and SDS and no decrease in surface activity is detected. Two break points instead of three can be seen that divide the surface tension curve into three distinct regions. The isotherms remain similar to those of mixture with unassociated F127 (Figure 52). At the beginning of interaction, surface tension values are quite similar to those of pure $C_{12}E_4$ solutions, indicating weak activity of $C_{12}E_4$ at water/air interface. Therefore, most of the added $C_{12}E_4$ at that stage must be associating with F127 micelles in bulk solution. This trend clearly shows spontaneous interaction with F127 micelles, occurring as a result of the surface activity of F127 which promotes the formation of mixed micelles with $C_{12}E_4$.

This ready association of the two uncharged amphiphilic compounds to form mixed micelles is favoured by the presence of the hydrated EO chains in contact with water in both $C_{12}E_4$ and F127 amphiphiles, assuring their complete miscibility in mixed micelles (Couderc et al., 2001). With further increase in $C_{12}E_4$ concentration, copolymer micelles become saturated and surface tension starts decreasing substantially, indicating renewed activity of $C_{12}E_4$ at water/air

interface. A continuing increase in $C_{12}E_4$ concentration decreases further interfacial tension until the second plateau significant of water/air interface saturation occurs. At this point, normal surfactant micelles start forming. Thus, no loss in interfacial activity is observed. It should be noticed that surfactants' cmc in the presence of associated F127, as shown in Figure 53, increases much more extensively than in non-associated F127 solutions. This is due to the fact that, in addition to natural accretion of hydrophobic microdomains due to the presence of surface-active F127, the latter (when aggregated), increases these microdomains even further in producing a mixed hydrophobic core, which reduces the free monomer concentration of $C_{12}E_4$ (Tadros, 2006b).

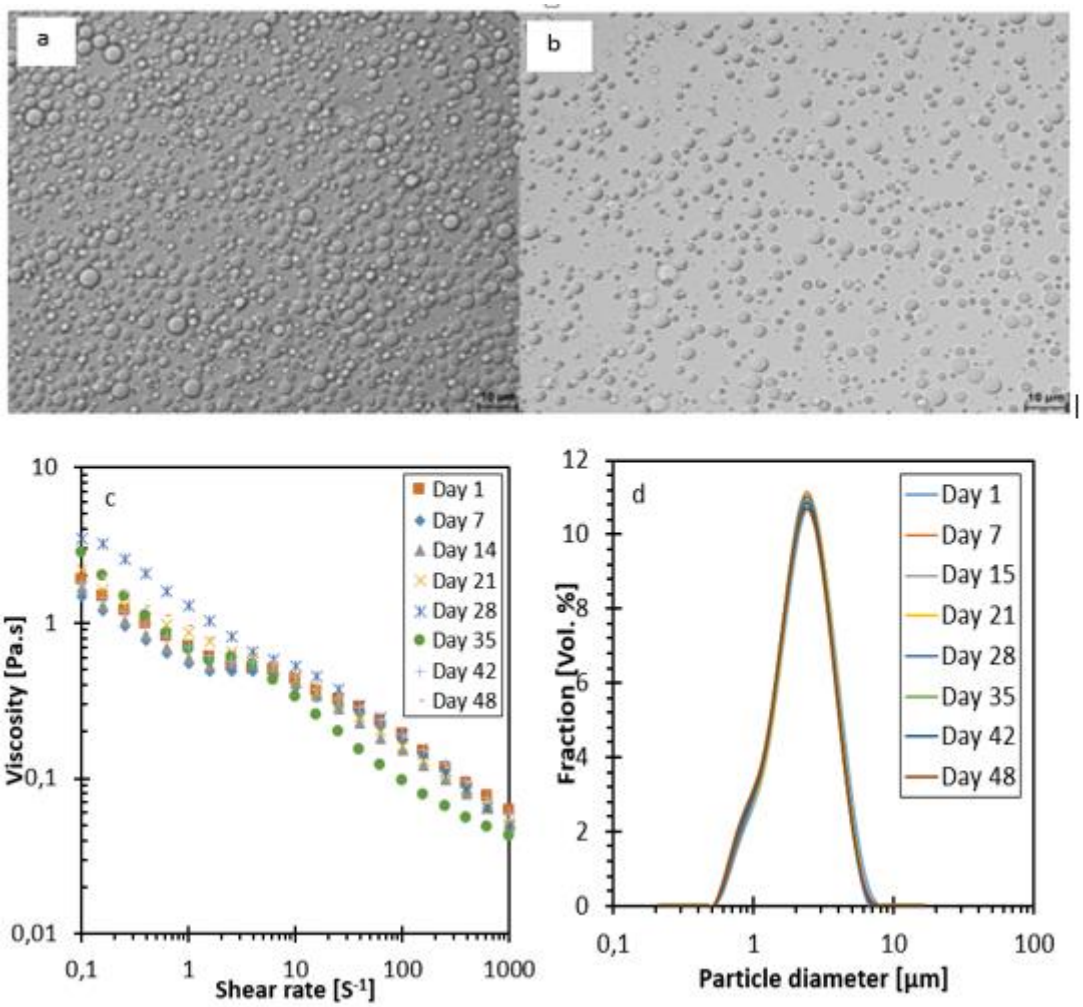

Figure 54. Influence of ageing on emulsions stabilised by 10 mM $C_{12}E_4$ containing systems: a) and b) Optical micrographs of 10 times diluted emulsions for first and 42th day respectively, c) Flow curves, d) particle size distribution.

Figure 54 exhibits stability of $C_{12}E_4$ containing emulsions as established through the three testing methods. Figure 54d is representative of $C_{12}E_4$ droplets size constancy over the range of its concentrations and time exposure. This stability is perfectly corroborated by

corresponding viscosity measurement and optical micrograph photography. No significant variation in viscosity was observed. Likewise, no apparent increase in droplet size can be detected from OM, and this was taken as the final evidence of $C_{12}E_4$ stability against coalescence.

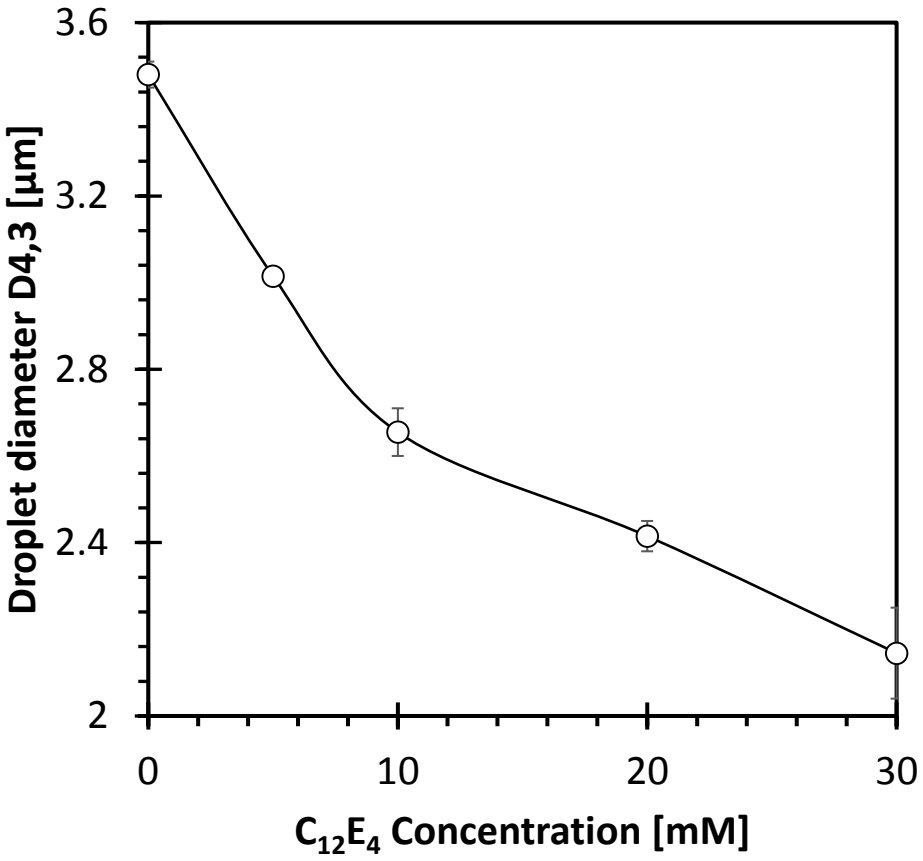

Figure 55. Influence of $C_{12}E_4$ concentration on freshly prepared emulsions

This stability shows that sodium phosphate salt combined to heat supposedly to reverse solvency of the medium for a polar compound has no detectable effect on the neutral mixed micelle. As has been detected with surface tension, $C_{12}E_4$ does not cause disruption of F127 micelles. Contrariwise, their ready association reinforces and stabilises their formed mixed micelles. The strong resistance to coalescence for droplets entrapped in the F127/$C_{12}E_4$ mixed micelles is thus favoured by the complete miscibility of $C_{12}E_4$ and F127 in mixed micelles, due to the presence of the hydrated EO chains in contact with water in both emulsifiers. Since no disruption of F127 micelles is observed in the presence of $C_{12}E_4$ cosolute, the observed decrease of emulsion droplets diameter accompanying reduction of the corresponding micelle hydrodynamic radius (Figure 55) means that the strong cohesion of F127/$C_{12}E_4$ mixed micelles

conferring remarkable stability to their corresponding entrapped droplets is corroborated by the continuous increase of its density. Taking into account these results, the emulsion formulated with $C_{12}E_4$ as cosurfactant showed best physical stability.

4.3 Conclusion

Surfactants and F127 aggregation behaviour in aqueous solution has been examined. Existence of extended cmc in all cases of surfactant used provided proof of interaction taking place between these low molecular amphiphiles and F127. While variations of cac for interaction between SDS and F127 can be mitigated, the extension of all surfactants cmc with an increasing F127 concentration provided a real indication of microdomain accretion in solution on all the range of F127 concentrations. Absence of cac for CTAB and $C_{12}E_4$ in their interactions with F127 and the evidence of low and inexistent interfacial activities when mixed with F127 suggested their spontaneous binding at low concentration with F127.

On the other hand, ionic surfactants have been found to reduce F127 hydrophobic activity when presented in solution in equilibrium conditions between its micellar and monomeric species. This was not the case for $C_{12}E_4$ whose cooperation with F127 in the formation of mixed micelles was found to be effective on all ranges of $C_{12}E_4$ concentrations. This difference in the complex behaviour between ionic and non-ionic surfactants when binding to F127 suggested differences between polyelectrolyte-like complexes, nude surfactants and copolymer micelles regarding their hydrophobicity. Finally, the only difference between surfactants and copolymer surface activities at water/air and water/mineral oil interfaces have been found to be the magnitude of surface tension, being higher in the first case because of the gap in the difference of polarities at water-air and water-oil interfaces.

When applied to colloidal dispersions, the gathered informations on adsorption and aggregation behaviour of the above-mixed emulsifiers in aqueous solutions provided essential aspects of understanding of oil in water emulsions' stability and destabilisation. Highly extended F127 multilayers formed around droplets and efficient screening effects of sodium phosphate were found to impede re-coalescence in freshly prepared emulsions. High valance of sodium phosphate in conjunction with heat exposure played key roles in accelerating ageing of prepared emulsions. While F127/$C_{12}E_4$-based emulsions exhibited great stability to coalescence for all $C_{12}E_4$ concentrations, F127/ionic surfactants underwent destabilisation. F127/CTAB-based emulsions displayed consecutive Ostwald ripening and coalescence and because of this, phase-separated quicker than F127/SDS-based emulsions. Due to complete

cooperation of ion-dipole interaction between SDS and F127 backbone, F127/SDS-based emulsions were the seat of coalescence shifting between two populations of droplets, namely the unstable ones entrapped in pure SDS micelles, and the very stable ones caught in F127/SDS complexes.

Chapter 5 General Conclusion

The outcomes of this study on the alteration of synergism between F127 and low molecular surfactants (SDS, CTAB and $C_{12}E_4$) in enhanced ionic strength aqueous media provided molecular insights on sequences of stabilisation and destabilisation mechanisms of emulsions. The kinetic study of emulsion stability was preceded by investigation on surface activities of aqueous mixtures of F127 and surfactants (ionic and neutral) in which critical parameters were surfactants concentration, F127 concentration, and fluid pairs interface.

Surface activities were studied in order to infer aggregation behaviours, essential for an understanding of emulsion stability mechanisms. Apart from surface tension magnitude, it was found that every mixed emulsifier systems displayed equivalent adsorption behaviours at water/air and water/mineral oil interfaces. Relevantly to emulsion stabilisation, surface tensions were found to be lower at water/mineral oil interfaces than at their water/air counterparts. A deep understanding of the interactions between surfactants and F127 involved distinguishing between the monomeric and micellar states of the latter. In every cases, the existence of extended surfactant critical micelle concentrations has proven interactions taking place between the low molecular surfactant and amphiphilic F127.

When simultaneously present in solution with dilute monomeric F127, SDS behaviour suggested a complex association with the polymer before aggregating as a pure micelle. Conversely, CTAB and $C_{12}E_4$ displayed, respectively, weak and inexistent interfacial activity at low concentrations and were ready to interact with F127 even at their lowest concentrations. Every surfactant was found to be subjected to different interaction mechanisms and thermodynamic association patterns depending on the involved individual block of the copolymer. Association of ionic surfactants with micellar F127 gave rise to mixed micelle formation followed by a decrease of interfacial activity significant of monomeric F127 replacement at the interface before pure micelle formation took place upon subsequent increase of surfactant concentration. $C_{12}E_4$ showed cooperative association with F127 to form mixed micelle without loss of interfacial activity.

Stability mechanisms of oil in water emulsions were found to fundamentally rely on emulsifiers' molecular interactions and adsorption behaviours in the aqueous phase. The highly extended F127 PEO block multilayer covering oil droplets entrapped in mixed emulsifiers aggregates and the sodium phosphate screening effect in ionic mixed emulsifiers-based emulsions, constituted a bulwark against re-coalescence during the emulsification process.

Sodium phosphate was the accelerating shifting agent of solvation of the hydrophilic PEO block toward solvophobic character at high temperature in pure F127-based emulsions. Coalescence could then proceed due to the subsequent shifting of hydrated PEO steric interaction from a repulsive to attractive one.

Salt and heat effects had no influence on F127/$C_{12}E_4$-based emulsions and they showed great stability to both coalescence and Ostwald ripening. F127/CTAB-based emulsions displayed consecutive Ostwald ripening and coalescence destabilisation mechanisms and they showed great instability compared to F127/SDS-based emulsions. Entanglements between PEO non-interacting blocks of F127 with CTAB ionic micelles were found to subsequently result in flocculation and ripening of droplets entrapped in F127/CTAB complexes. This ripening destabilisation mechanism reached saturation points beyond which coalescence took over.

F127/SDS emulsifying systems gave rise to two populations of droplets in emulsion, namely those entrapped in SDS micelles covered by a wrapped F127 monolayer and those caught in simple and unwrapped SDS aggregates, respectively related to F127/SDS complex aggregations and SDS pure micelles. These two categories of droplets displayed different resistances to coalescence. Oil droplets entrapped in pure SDS micelles were very sensitive to coalescence, while the protective F127 monolayer wrapped around SDS micelles provided great stability to the droplets entrapped in complete F127/SDS ion-dipole complexes. Hence, the progressive shifting of DSD to bimodality was the result of the transition of coalescence destabilisation mechanism from the first population of droplets to the second.

Recommendations

Aggregate structures in mixed emulsifiers systems have been inferred from surface tensiometry and adsorption behaviours. It is advised that they should be quantitatively investigated in presence of salt using fluorescence quenching and DLS methods.

It is suggested that CPs of all mixed emulsifier systems should be measured in the presence of salt to provide more insight into Ostwald ripening and coalescence break-down mechanisms.

Stability of F127/surfactants-based emulsions has been studied in the presence of Na_3PO_4. It is suggested that the effect of additives on these mixed emulsifiers' ability to stabilise O/W emulsions is extended to other salts for comparative reasons.

Surface and interfacial tension measurements have been performed in the aqueous phase without the presence of any additives. It is suggested that these measurements are performed in presence of salt.

Emulsions have been cooled to room temperature immediately after their preparation. It is advised that conductivity measurements versus temperature of $C_{12}E_4$ containing emulsions should presented to be sure that no phase inversion occurs during the cooling process.

To better understand occurrence of coalescence and Ostwald ripening, it is advised to present results of particles size versus time, and try to fit the data to some models.

It is advised that flocculation and coalescence should be check with oscillatory rheological measurements to better understand the interactions forces for each surfactant systems.

References

ABISMAıL, B., CANSELIER, J. P., WILHELM, A. M., DELMAS, H. & GOURDON, C. 1999. Emulsification by ultrasound: drop size distribution and stability. *Ultrasonics sonochemistry*, 6**,** 75-83.

AKBARI, S. & NOUR, A. H. 2018. Emulsion types, stability mechanisms and rheology: A review. *International Journal of Innovative Research and Scientific Studies (IJIRSS)*, 1.

ALAWI, S. M. 2010. Thermodynamics studies of cetyltrimethylammonium bromide (CTAB) in N, N-dimethyl acetamide-water mixtures. *Oriental Journal of Chemistry*, 26**,** 1235.

ALEXANDRIDIS, P., ATHANASSIOU, V., FUKUDA, S. & HATTON, T. A. 1994a. Surface activity of poly (ethylene oxide)-block-poly (propylene oxide)-block-poly (ethylene oxide) copolymers. *Langmuir*, 10**,** 2604-2612.

ALEXANDRIDIS, P. & HATTON, T. A. 1995. Poly (ethylene oxide)□ poly (propylene oxide)□ poly (ethylene oxide) block copolymer surfactants in aqueous solutions and at interfaces: thermodynamics, structure, dynamics, and modeling. *Colloids and Surfaces A: Physicochemical and Engineering Aspects*, 96**,** 1-46.

ALEXANDRIDIS, P., HOLZWARTH, J. F. & HATTON, T. A. 1994b. Micellization of poly (ethylene oxide)-poly (propylene oxide)-poly (ethylene oxide) triblock copolymers in aqueous solutions: thermodynamics of copolymer association. *Macromolecules*, 27**,** 2414-2425.

ARIYAPRAKAI, S. & DUNGAN, S. R. 2010. Influence of surfactant structure on the contribution of micelles to Ostwald ripening in oil-in-water emulsions. *Journal of colloid and interface science*, 343**,** 102-108.

AVEYARD, R., BINKS, B. P. & CLINT, J. H. 2003. Emulsions stabilised solely by colloidal particles. *Advances in Colloid and Interface Science*, 100**,** 503-546.

BAHADUR, P., SASTRY, N., RAO, Y. & RIESS, G. 1988. Interaction studies of styrene—ethylene oxide block copolymers with ionic surfactants in aqueous solution. *Colloids and Surfaces*, 29**,** 343-358.

BANCROFT, W. D. 2002. The theory of emulsification, VI. *The Journal of Physical Chemistry*, 19**,** 275-309.

BANIPAL, T. S. & SOOD, A. K. 2013. Mixed micellar and interfacial interactions of a triblock polymer (EO37PO56EO37) with a series of monomeric and dimeric surfactants. *Journal of Surfactants and Detergents*, 16**,** 881-891.

BERRY, J. D., NEESON, M. J., DAGASTINE, R. R., CHAN, D. Y. & TABOR, R. F. 2015. Measurement of surface and interfacial tension using pendant drop tensiometry. *Journal of colloid and interface science,* 454**,** 226-237.

BHARATIYA, B., GHOSH, G., BAHADUR, P. & MATA, J. 2008. The effects of salts and ionic surfactants on the micellar structure of tri- block copolymer PEO- PPO- PEO in aqueous solution. *Journal of Dispersion Science and Technology,* 29**,** 696-701.

BHATTACHARYA, S. & HALDAR, J. 2004. Thermodynamics of micellization of multiheaded single-chain cationic surfactants. *Langmuir,* 20**,** 7940-7947.

BINKS, B. P. 2002. Particles as surfactants—similarities and differences. *Current opinion in colloid & interface science,* 7**,** 21-41.

BINKS, B. P. & CLINT, J. H. 2002. Solid wettability from surface energy components: relevance to Pickering emulsions. *Langmuir,* 18**,** 1270-1273.

BINKS, B. P. & LUMSDON, S. 2000. Influence of particle wettability on the type and stability of surfactant-free emulsions. *Langmuir,* 16**,** 8622-8631.

BRACKMAN, J. C. 1990. *The interaction between water-soluble polymers and surfactant aggregates.* Rijksuniversiteit Groningen.

BREWER, D. R., FRANCO, J. M. & GARCIA-ZAPATEIRO, L. A. 2016. Rheological properties of oil-in-water emulsions prepared with oil and protein isolates from sesame (Sesamum Indicum). *Food Science and Technology,* 36**,** 64-69.

CACACE, M., LANDAU, E. & RAMSDEN, J. 1997. The Hofmeister series: salt and solvent effects on interfacial phenomena. *Quarterly reviews of biophysics,* 30**,** 241-277.

CALDERÓ, G. & SOLANS, C. 2013. Polymeric O/W nano-emulsions obtained by the phase inversion composition (PIC) Method for biomedical nanoparticle preparation. *Edited by Tharwat F. Tadros*.

CHEVALIER, Y. & BOLZINGER, M.-A. 2013. Emulsions stabilized with solid nanoparticles: Pickering emulsions. *Colloids and Surfaces A: Physicochemical and Engineering Aspects,* 439**,** 23-34.

CORRIN, M. & HARKINS, W. D. 1947. The effect of salts on the critical concentration for the formation of micelles in colloidal electrolytes1. *Journal of the American Chemical Society,* 69**,** 683-688.

COSTA, C., MEDRONHO, B., FILIPE, A., MIRA, I., LINDMAN, B., EDLUND, H. & NORGREN, M. 2019. Emulsion Formation and Stabilization by Biomolecules: The Leading Role of Cellulose. *Polymers,* 11**,** 1570.

COUDERC-AZOUANI, S., SIDHU, J., THURN, T., XU, R., BLOOR, D. M., PENFOLD, J., HOLZWARTH, J. F. & WYN-JONES, E. 2005. Binding of sodium dodecyl sulfate and hexaethylene glycol mono-n-dodecyl ether to the block copolymer L64: electromotive force, microcalorimetry, surface tension, and small angle neutron scattering investigations of mixed micelles and polymer/micellar surfactant complexes. *Langmuir,* 21**,** 10197-10208.

COUDERC, S., LI, Y., BLOOR, D. M., HOLZWARTH, J. F. & WYN-JONES, E. 2001. Interaction between the nonionic surfactant hexaethylene glycol mono-n-dodecyl ether (C12EO6) and the surface active nonionic ABA block copolymer pluronic F127 (EO97PO69EO97) formation of mixed micelles studied using isothermal titration calorimetry and differential scanning calorimetry. *Langmuir,* 17**,** 4818-4824.

DA SILVA, R. C. & LOH, W. 1998. Effect of additives on the cloud points of aqueous solutions of ethylene oxide–propylene oxide–ethylene oxide block copolymers. *Journal of colloid and interface science,* 202**,** 385-390.

DAI, S. & TAM, K. 2001. Isothermal titration calorimetry studies of binding interactions between polyethylene glycol and ionic surfactants. *The Journal of Physical Chemistry B,* 105**,** 10759-10763.

DAI, S., TAM, K. & LI, L. 2001. Isothermal titration calorimetric studies on interactions of ionic surfactant and poly (oxypropylene)− poly (oxyethylene)− poly (oxypropylene) triblock copolymers in aqueous solutions. *Macromolecules,* 34**,** 7049-7055.

DANOV, K. D., KRALCHEVSKY, P. A. & ANANTHAPADMANABHAN, K. P. 2014. Micelle–monomer equilibria in solutions of ionic surfactants and in ionic–nonionic mixtures: A generalized phase separation model. *Advances in colloid and interface science,* 206**,** 17-45.

DAS, K. & CHATTORAJ, D. 1982. Kinetics of coalescence of polar oil/water emulsion stabilised by ionic detergents and proteins. *Colloids and Surfaces,* 5**,** 75-78.

DEYERLE, B. A. & ZHANG, Y. 2011. Effects of Hofmeister anions on the aggregation behavior of PEO–PPO–PEO triblock copolymers. *Langmuir,* 27**,** 9203-9210.

DICKINSON, E. 2009. Hydrocolloids as emulsifiers and emulsion stabilizers. *Food hydrocolloids,* 23**,** 1473-1482.

DURCHSCHLAG, H. & ZIPPER, P. 1994. Calculation of the partial volume of organic compounds and polymers. *Ultracentrifugation.* Springer.

DZULKEFLY, K., KHOH, H., AHMAD, F. & AHMAD, S. A. 2010. Solvent-free esterification process for the synthesis of glucose bolaform surfactants. *Oriental Journal of Chemistry*, 26**,** 747.

EASTOE, J. Surfactant chemistry and general phase behavior. *Surfactant Chemistry*.

ECONOMOU, I., HEIDMAN, J., TSONOPOULOS, C. & WILSON, G. 1997. Mutual solubilities of hydrocarbons and water: III. 1- hexene; 1- octene; C10? C12 hydrocarbons. *AIChE Journal*, 43**,** 535-546.

FLORENCE, A. & ROGERS, J. 1971. Emulsion stabilization by non- ionic surfactants: experiment and theory. *Journal of Pharmacy and Pharmacology*, 23**,** 233-251.

FORGIARINI, A., ESQUENA, J., GONZALEZ, C. & SOLANS, C. 2001. Formation of nano-emulsions by low-energy emulsification methods at constant temperature. *Langmuir*, 17**,** 2076-2083.

FRANK, H. S. & EVANS, M. W. 1945. Free volume and entropy in condensed systems III. Entropy in binary liquid mixtures; partial molal entropy in dilute solutions; structure and thermodynamics in aqueous electrolytes. *The Journal of Chemical Physics*, 13**,** 507-532.

GAO, Z. & EISENBERG, A. 1993. A model of micellization for block copolymers in solutions. *Macromolecules*, 26**,** 7353-7360.

GILANYI, T. & WOLFRAM, E. 1981. Interaction of ionic surfactants with polymers in acqueous solution. *Colloids and Surfaces*, 3**,** 181-198.

GODDARD, E. 2018. Polymer-surfactant interaction: Part I. Uncharged water-soluble polymers and charged surfactants. *Interactions of surfactants with polymers and proteins*. CRC Press.

GODDARD, E., TURRO, N., KUO, P. & ANANTHAPADMANABHAN, K. 1985. Fluorescence probes for critical micelle concentration determination. *Langmuir*, 1**,** 352-355.

GÓMEZ-MERINO, A., RUBIO-HERNÁNDEZ, F., VELÁZQUEZ-NAVARRO, J., GALINDO-ROSALES, F. & FORTES-QUESADA, P. 2007. The Hamaker constant of anatase aqueous suspensions. *Journal of colloid and interface science*, 316**,** 451-456.

GOODARZI, F. & ZENDEHBOUDI, S. 2019. A comprehensive review on emulsions and emulsion stability in chemical and energy industries. *The Canadian Journal of Chemical Engineering*, 97**,** 281-309.

GRIFFIN, W. C. 1949. Classification of surface-active agents by" HLB". *J. Soc. Cosmet. Chem.*, 1**,** 311-326.

HADGIIVANOVA, R. & איבנובה'חדג, ר. 2009. *Aggregation of Amphiphilic Molecules in Solution: Thermodynamics, Metastability, and Kinetics*, University of Tel-Aviv.

HAMLEY, I. W. 2005. *Block copolymers in solution: fundamentals and applications*, John Wiley & Sons.

HAQ, Z., REHMAN, N., ALI, F., KHAN, N. M. & ULLAH, H. 2017. Effect of Electrolyte (NaCl) and Temperature on the Mechanism of Cetyl Trimethylammonium Bromide Micelles. *Sains Malaysiana,* 46**,** 733-741.

HECHT, E. & HOFFMANN, H. 1994. Interaction of ABA block copolymers with ionic surfactants in aqueous solution. *Langmuir,* 10**,** 86-91.

HEIDMAN, J., TSONOPOULOS, C., BRADY, C. & WILSON, G. 1985. High- temperature mutual solubilities of hydrocarbons and water. Part II: Ethylbenzene, ethylcyclohexane, and n- octane. *AIChE journal,* 31**,** 376-384.

HIERREZUELO, J., AGUIAR, J. & RUIZ, C. C. 2005. Micellar properties of a mixed surfactant system constituted by n-octyl-β-D-thioglucopyranoside and sodium dodecyl sulphate. *Colloids and Surfaces A: Physicochemical and Engineering Aspects,* 264**,** 29-36.

HU, Y.-T., TING, Y., HU, J.-Y. & HSIEH, S.-C. 2017. Techniques and methods to study functional characteristics of emulsion systems. *journal of food and drug analysis,* 25**,** 16-26.

INSTRUMENTS, M. 2012. A basic guide to particle characterization. *MRK1806-01*.

JAFARI, S. M., ASSADPOOR, E., HE, Y. & BHANDARI, B. 2008. Re-coalescence of emulsion droplets during high-energy emulsification. *Food hydrocolloids,* 22**,** 1191-1202.

JOHANSSON, I. & SOMNASILIIDARALL, P. 2007. Formulation of Carpet Cleaners. *Handbook for cleaning/decontamination of surfaces***,** 103.

JOHNSON, O., WASHINGTON, C. & DAVIS, S. 1990a. Long-term stability studies of fluorocarbon oxygen transport emulsions. *International Journal of Pharmaceutics,* 63**,** 65-72.

JOHNSON, O., WASHINGTON, C. & DAVIS, S. 1990b. Thermal stability of fluorocarbon emulsions that transport oxygen. *International Journal of Pharmaceutics,* 59**,** 131-135.

KIM, J. W., LEE, D., SHUM, H. C. & WEITZ, D. A. 2008. Colloid surfactants for emulsion stabilization. *Advanced materials,* 20**,** 3239-3243.

KLEVENS, H. 1953. Structure and aggregation in dilate solution of surface active agents. *Journal of the American Oil Chemists' Society,* 30**,** 74-80.

KRESTOV, G. 1984. Thermodynamics and structure of solutions. *Journal of Structural Chemistry,* 25**,** 252-258.

KRONBERG, B., HOLMBERG, K. & LINDMAN, B. 2014. *Surface chemistry of surfactants and polymers*, John Wiley & Sons.

KUMAR, S., SHARMA, D., KHAN, Z. A. & KABIR-UD-DIN* 2002. Salt− Induced Cloud Point in Anionic Surfactant Solutions: Role of the Headgroup and Additives. *Langmuir,* 18**,** 4205-4209.

KUSTERS, K. A., WIJERS, J. G. & THOENES, D. 1991. Particle sizing by laser diffraction spectrometry in the anomalous regime. *Applied optics,* 30**,** 4839-4847.

KWAŚNIEWSKA, D., WIECZOREK, D. & ZIELIŃSKI, R. WATER NUMBER OF SELECTED SURFACTANTS. *CURRENT TRENDS IN COMMODITY SCIENCE***,** 62.

LAD, K., BAHADUR, A., PANDYA, K. & BAHADUR, P. 1995. Clouding and aggregation behaviour of ethylene oxide/propylene oxide/ethylene oxide block copolymers in aqueous media in the presence of sodium dodecyl sulphate.

LI, Y., BAO, M., WANG, Z., ZHANG, H. & XU, G. 2011. Aggregation behavior and complex structure between triblock copolymer and anionic surfactants. *Journal of Molecular Structure,* 985**,** 391-396.

LI, Y., XU, R., COUDERC, S., BLOOR, D. M., HOLZWARTH, J. F. & WYN-JONES, E. 2001a. Binding of tetradecyltrimethylammonium bromide to the ABA block copolymer Pluronic F127 (EO97 PO69 EO97): electromotive force, microcalorimetry, and light scattering studies. *Langmuir,* 17**,** 5742-5747.

LI, Y., XU, R., COUDERC, S., BLOOR, M., WYN-JONES, E. & HOLZWARTH, J. F. 2001b. Binding of sodium dodecyl sulfate (SDS) to the ABA block copolymer Pluronic F127 (EO97PO69EO97): F127 aggregation induced by SDS. *Langmuir,* 17**,** 183-188.

LINSE, P. 1993. Micellization of poly (ethylene oxide)-poly (propylene oxide) block copolymers in aqueous solution. *Macromolecules,* 26**,** 4437-4449.

LINSE, P. 1994. Micellization of poly (ethylene oxide)-poly (propylene oxide) block copolymer in aqueous solution: effect of polymer impurities. *Macromolecules,* 27**,** 2685-2693.

LINSE, P. & MALMSTEN, M. 1992. Temperature-dependent micellization in aqueous block copolymer solutions. *Macromolecules,* 25**,** 5434-5439.

MANOHAR, C. & KELKAR, V. 1990. Model for the cloud point of mixed surfactant systems. *Journal of Colloid and Interface Science,* 137**,** 604-606.

MARCUS, Y. 1992. The structuredness of solvents. *Journal of solution chemistry,* 21**,** 1217-1230.

MARCUS, Y. 1999. The structuredness of water at elevated temperatures along the saturation line. *Journal of molecular liquids,* 79**,** 151-165.

MARCUS, Y. 2009. Effect of ions on the structure of water: structure making and breaking. *Chemical reviews,* 109**,** 1346-1370.

MARCUS, Y. 2012. *Ions in water and biophysical implications: from chaos to cosmos,* Springer Science & Business Media.

MARCUS, Y. & LOEWENSCHUSS, A. 1984. . Standard entropies of hydration of ions. *Annual Reports Section" C"(Physical Chemistry),* 81**,** 81-135.

MARSZALL, L. 1988. Cloud point of mixed ionic-nonionic surfactant solutions in the presence of electrolytes. *Langmuir,* 4**,** 90-93.

MATA, J., JOSHI, T., VARADE, D., GHOSH, G. & BAHADUR, P. 2004. Aggregation behavior of a PEO–PPO–PEO block copolymer+ ionic surfactants mixed systems in water and aqueous salt solutions. *Colloids and Surfaces A: Physicochemical and Engineering Aspects,* 247**,** 1-7.

MCCLEMENTS, D. J. 2007. Critical review of techniques and methodologies for characterization of emulsion stability. *Critical reviews in food science and nutrition,* 47**,** 611-649.

MCCLEMENTS, D. J. 2015. *Food emulsions: principles, practices, and techniques,* CRC press.

MILNER, S. T., LACASSE, M.-D. & GRAESSLEY, W. W. 2009. Why χ is seldom zero for polymer− solvent mixtures. *Macromolecules,* 42**,** 876-886.

MOHAJERI, E. & NOUDEH, G. D. 2012. Effect of temperature on the critical micelle concentration and micellization thermodynamic of nonionic surfactants: polyoxyethylene sorbitan fatty acid esters. *Journal of Chemistry,* 9**,** 2268-2274.

MOROI, Y., SUGII, R., AKINE, C. & MATUURA, R. 1985. Anionic surfactants with methylviologen and cupric ions as divalent cationic gegenion (II): Effect of alkyl chain length on solubility and micelle formation. *Journal of colloid and interface science,* 108**,** 180-188.

MOSAYEBI, A. & ABEDINI, R. 2013. USING DEMULSIFIERS FOR PHASE BREAKING OF WATER/OIL EMULSION. *Petroleum & Coal,* 55.

MUKHERJEE, P., PADHAN, S. K., DASH, S., PATEL, S. & MISHRA, B. K. 2011. Clouding behaviour in surfactant systems. *Advances in colloid and interface science,* 162**,** 59-79.

NAGARAJAN, R. 1980. Thermodtnamics of surfactant-polymer interactions in dilute aqueous solutions. *Chemical Physics Letters,* 76**,** 282-286.

NAGARAJAN, R. 1985. Thermodynamics of nonionic polymer—micelle association. *Colloids and surfaces,* 13**,** 1-17.

NAGARAJAN, R. 2001. Solubilization of "guest" molecules into polymeric aggregates. *Polymers for Advanced Technologies,* 12**,** 23-43.

NAGARAJAN, R., CHAIKO, M. A. & RUCKENSTEIN, E. 1984. Locus of solubilization of benzene in surfactant micelles. *The Journal of Physical Chemistry,* 88**,** 2916-2922.

NAGARAJAN, R. & GANESH, K. 1989a. Block copolymer self-assembly in selective solvents: theory of solubilization in spherical micelles. *Macromolecules,* 22**,** 4312-4325.

NAGARAJAN, R. & GANESH, K. 1989b. Block copolymer self- assembly in selective solvents: Spherical micelles with segregated cores. *The Journal of Chemical Physics,* 90**,** 5843-5856.

NAGARAJAN, R. & WANG, C.-C. 1996. Solution behavior of surfactants in ethylene glycol: probing the existence of a CMC and of micellar aggregates. *Journal of colloid and interface science,* 178**,** 471-482.

NAGARAJAN, R. & WANG, C.-C. 2000. Theory of surfactant aggregation in water/ethylene glycol mixed solvents. *Langmuir,* 16**,** 5242-5251.

NIKAS, Y. & BLANKSCHTEIN, D. 1994. Complexation of nonionic polymers and surfactants in dilute aqueous solutions. *Langmuir,* 10**,** 3512-3528.

ORTONA, O., D'ERRICO, G., PADUANO, L. & VITAGLIANO, V. 2006. Interaction between cationic, anionic, and non-ionic surfactants with ABA block copolymer Pluronic PE6200 and with BAB reverse block copolymer Pluronic 25R4. *Journal of colloid and interface science,* 301**,** 63-77.

PANDIT, N., TRYGSTAD, T., CROY, S., BOHORQUEZ, M. & KOCH, C. 2000. Effect of salts on the micellization, clouding, and solubilization behavior of pluronic F127 solutions. *Journal of colloid and interface science,* 222**,** 213-220.

PAREKH, P., YERRAMILLI, U. R. & BAHADUR, P. 2013. Cloud point and thermodynamic parameters of a non-ionic surfactant heptaoxyethylene dodecyl ether (C 12 E 7) in presence of various organic and inorganic additives.

PIACENTINI, E. 2016. Emulsion. *Encyclopedia of Membranes***,** 679-682.

PICKERING, S. U. 1907. Cxcvi.—emulsions. *Journal of the Chemical Society, Transactions,* 91**,** 2001-2021.

POLAK, J. & LU, B. C.-Y. 1973. Mutual solubilities of hydrocarbons and water at 0 and 25 C. *Canadian Journal of Chemistry,* 51**,** 4018-4023.

QIU, Q., SOMASUNDARAN, P. & PETHICA, B. A. 2002. Hydrophobic complexation of poly (vinyl caprolactam) with sodium dodecyl sulfate and dodecyltrimethylammonium bromide in solution. *Langmuir,* 18**,** 3482-3486.

RÁMIREZ, M., BULLÓN, J., ANDÉREZ, J., MIRA, I. & SALAGER, J.-L. 2002. Drop size distribution bimodality and its effect on O/W emulsion viscosity. *Journal of dispersion science and technology,* 23**,** 309-321.

RELKIN, P. & SOURDET, S. 2005. Factors affecting fat droplet aggregation in whipped frozen protein-stabilized emulsions. *Food Hydrocolloids,* 19**,** 503-511.

RODEA-GONZÁLEZ, D. A., CRUZ-OLIVARES, J., ROMÁN-GUERRERO, A., RODRÍGUEZ-HUEZO, M. E., VERNON-CARTER, E. J. & PÉREZ-ALONSO, C. 2012. Spray-dried encapsulation of chia essential oil (Salvia hispanica L.) in whey protein concentrate-polysaccharide matrices. *Journal of Food Engineering,* 111**,** 102-109.

ROSEN, M. J. 1989. Selection of surfactant pairs for optimization of interfacial properties. *Journal of the American Oil Chemists' Society,* 66**,** 1840-1843.

ROSEN, M. J., COHEN, A. W., DAHANAYAKE, M. & HUA, X. Y. 1982. Relationship of structure to properties in surfactants. 10. Surface and thermodynamic properties of 2-dodecyloxypoly (ethenoxyethanol) s, C12H25 (OC2H4) xOH, in aqueous solution. *The Journal of Physical Chemistry,* 86**,** 541-545.

ROSEN, M. J. & KUNJAPPU, J. T. 2004. *Surfactants and interfacial phenomena,* Wiley Online Library.

RUCKENSTEIN, E. 1999. Surfactant aggregation in nonionic polymer solutions. *Langmuir,* 15**,** 8086-8089.

RUCKENSTEIN, E., HUBER, G. & HOFFMANN, H. 1987. Surfactant aggregation in the presence of polymers. *Langmuir,* 3**,** 382-387.

RUIZ, C. C. 1999. Micelle formation and microenvironmental properties of sodium dodecyl sulfate in aqueous urea solutions. *Colloids and Surfaces A: Physicochemical and Engineering Aspects,* 147**,** 349-357.

SAITO, S. 1969. Salt effect on polymer solutions. *Journal of Polymer Science Part A- 1: Polymer Chemistry,* 7**,** 1789-1802.

SANTOS, J., CALERO, N., TRUJILLO-CAYADO, L., GARCIA, M. & MUÑOZ, J. 2017. Assessing differences between Ostwald ripening and coalescence by rheology, laser

diffraction and multiple light scattering. *Colloids and Surfaces B: Biointerfaces,* 159**,** 405-411.

SARKAR, B., RAVI, V. & ALEXANDRIDIS, P. 2013. Micellization of amphiphilic block copolymers in binary and ternary solvent mixtures. *Journal of colloid and interface science,* 390**,** 137-146.

SARMORIA, C., PUVVADA, S. & BLANKSCHTEIN, D. 1992. Prediction of critical micelle concentrations of nonideal binary surfactant mixtures. *Langmuir,* 8**,** 2690-2697.

SASTRY, N. & HOFFMANN, H. 2004. Interaction of amphiphilic block copolymer micelles with surfactants. *Colloids and Surfaces A: Physicochemical and Engineering Aspects,* 250**,** 247-261.

SEVCIKOVA, P., VLTAVSKA, P., KASPARKOVA, V. & KREJCI, J. Formation, characterization and stability of nanoemulsions prepared by phase inversion. Proceedings of the 13th WSEAS international conference on Mathematical and computational methods in science and engineering, 2011. World Scientific and Engineering Academy and Society (WSEAS), 132-7.

SHARMA, R. & BAHADUR, P. 2002. Effect of different additives on the cloud point of a polyethylene oxide-polypropylene oxide-polyethylene oxide block copolymer in aqueous solution. *Journal of Surfactants and Detergents,* 5**,** 263-268.

SHARMA, T., DOHARE, N., KUMARI, M., SINGH, U. K., KHAN, A. B., BORSE, M. S. & PATEL, R. 2017. Comparative effect of cationic gemini surfactant and its monomeric counterpart on the conformational stability and activity of lysozyme. *Rsc Advances,* 7**,** 16763-16776.

SHAW, D. 1992. *Introduction to colloid and surface chemistry (colloid and surface engineering),* Oxford Butterworth-Heinemann.

SHILOACH, A. & BLANKSCHTEIN, D. 1997. Prediction of critical micelle concentrations and synergism of binary surfactant mixtures containing zwitterionic surfactants. *Langmuir,* 13**,** 3968-3981.

SHILOACH, A. & BLANKSCHTEIN, D. 1998. Predicting micellar solution properties of binary surfactant mixtures. *Langmuir,* 14**,** 1618-1636.

SHINODA, K. & LINDMAN, B. 1987. Organized surfactant systems: microemulsions. *Langmuir,* 3**,** 135-149.

SHIRAHAMA, K. 1974. The binding equilibrium of sodium dodecyl sulfate to poly (ethylene oxide) in 0.1 M sodium chloride solution at 30 C. *Colloid and Polymer Science,* 252**,** 978-981.

SHIRAHAMA, K., TSUJII, K. & TAKAGI, T. 1974. Free-boundary electrophoresis of sodium dodecyl sulfate-protein polypeptide complexes with special reference to SDS-polyacrylamide gel electrophoresis. *The Journal of Biochemistry*, 75**,** 309-319.

SHUKLA, D. & TYAGI, V. 2006. Cationic gemini surfactants: a review. *Journal of oleo science*, 55**,** 381-390.

SOLANS, C. & SOLÉ, I. 2012. Nano-emulsions: formation by low-energy methods. *Current Opinion in Colloid & Interface Science*, 17**,** 246-254.

SOUTHALL, N. T., DILL, K. A. & HAYMET, A. 2002. A view of the hydrophobic effect. ACS Publications.

STAN, C. A., TANG, S. K. & WHITESIDES, G. M. 2009. Independent control of drop size and velocity in microfluidic flow-focusing generators using variable temperature and flow rate. *Analytical chemistry*, 81**,** 2399-2402.

TADROS, T. 2004. Application of rheology for assessment and prediction of the long-term physical stability of emulsions. *Advances in colloid and interface science*, 108**,** 227-258.

TADROS, T. 2006a. Principles of emulsion stabilization with special reference to polymeric surfactants. *Journal of cosmetic science*, 57**,** 153-169.

TADROS, T., IZQUIERDO, P., ESQUENA, J. & SOLANS, C. 2004. Formation and stability of nano-emulsions. *Advances in colloid and interface science*, 108**,** 303-318.

TADROS, T. F. 2006b. *Applied surfactants: principles and applications*, John Wiley & Sons.

TADROS, T. F. 2008. Colloid aspects of cosmetic formulations with particular reference to polymeric surfactants. *Colloids in cosmetics and personal care*, 4**,** 1-34.

TADROS, T. F. 2013. *Emulsion formation and stability*, John Wiley & Sons.

THUMMAR, A., SASTRY, N., VERMA, G. & HASSAN, P. 2011. Aqueous block copolymer–surfactant mixtures—Surface tension, DLS and viscosity measurements and their utility in solubilization of hydrophobic drug and its controlled release. *Colloids and Surfaces A: Physicochemical and Engineering Aspects*, 386**,** 54-64.

TOPEL, Ö., ÇAKıR, B. A., BUDAMA, L. & HODA, N. 2013. Determination of critical micelle concentration of polybutadiene-block-poly (ethyleneoxide) diblock copolymer by fluorescence spectroscopy and dynamic light scattering. *Journal of Molecular Liquids*, 177**,** 40-43.

TORKKELI, A. 2003. *Droplet microfluidics on a planar surface*, VTT Technical Research Centre of Finland.

TREFALT, G. & BORKOVEC, M. 2014. Overview of DLVO theory. *Laboratory of Colloid and Surface Chemistry, University of Geneva,* 29.

TSONOPOULOS, C. & WILSON, G. 1983. High- temperature mutual solubilities of hydrocarbons and water. Part I: Benzene, cyclohexane and n- hexane. *AIChE Journal,* 29**,** 990-999.

TU, F. & LEE, D. 2014. Shape-changing and amphiphilicity-reversing Janus particles with pH-responsive surfactant properties. *Journal of the American Chemical Society,* 136**,** 9999-10006.

TUZAR, Z. 1996. Overview of polymer micelles. *Solvents and Self-organization of Polymers.* Springer.

WOODWARD, R. P. 2013. Surface tension measurements using the drop shape method. *First Ten Angstroms), http://www. first tenangstroms. com/pdfdocs/STPaper. pdf. Accessed,* 28.

XIULI, L., JIAN, X., WANGUO, H. & DEJUN, S. 2004. Effect of additives on the cloud points of two tri-block copolymers in aqueous solution. *Colloids and Surfaces A: Physicochemical and Engineering Aspects,* 237**,** 1-6.

YALKOWSKY, S. H. 1999. *Solubility and solubilization in aqueous media,* American Chemical Society Washington, DC.

YE, A., HEMAR, Y. & SINGH, H. 2004. Influence of polysaccharides on the rate of coalescence in oil-in-water emulsions formed with highly hydrolyzed whey proteins. *Journal of agricultural and food chemistry,* 52**,** 5491-5498.

YOUNG, R. J. & LOVELL, P. A. 2011. *Introduction to polymers,* CRC press.

ZANA, R. 1996. Critical micellization concentration of surfactants in aqueous solution and free energy of micellization. *Langmuir,* 12**,** 1208-1211.

ZANA, R. 2002. Dimeric (gemini) surfactants: effect of the spacer group on the association behavior in aqueous solution. *Journal of colloid and interface science,* 248**,** 203-220.

ZANA, R. & XIA, J. 2003. *Gemini surfactants: synthesis, interfacial and solution-phase behavior, and applications,* Crc Press.

ZHANG, K.-M., NI, O.-Q., HUANG, J.-D., DAI, Y.-M. & ZHAO, H.-R. 2018. Study on the flow of highly concentrated emulsions. *Journal of Dispersion Science and Technology,* 39**,** 1285-1290.

ZHANG, Y. & CREMER, P. S. 2010. Chemistry of Hofmeister anions and osmolytes. *Annual review of physical chemistry,* 61**,** 63-83.

ZHENG, Y. & DAVIS, H. 2000. Mixed micelles of nonionic surfactants and uncharged block copolymers in aqueous solutions: microstructure seen by cryo-TEM. *Langmuir,* 16**,** 6453-6459.

Appendices

Appendix 1 DSD for SDS-based emulsions

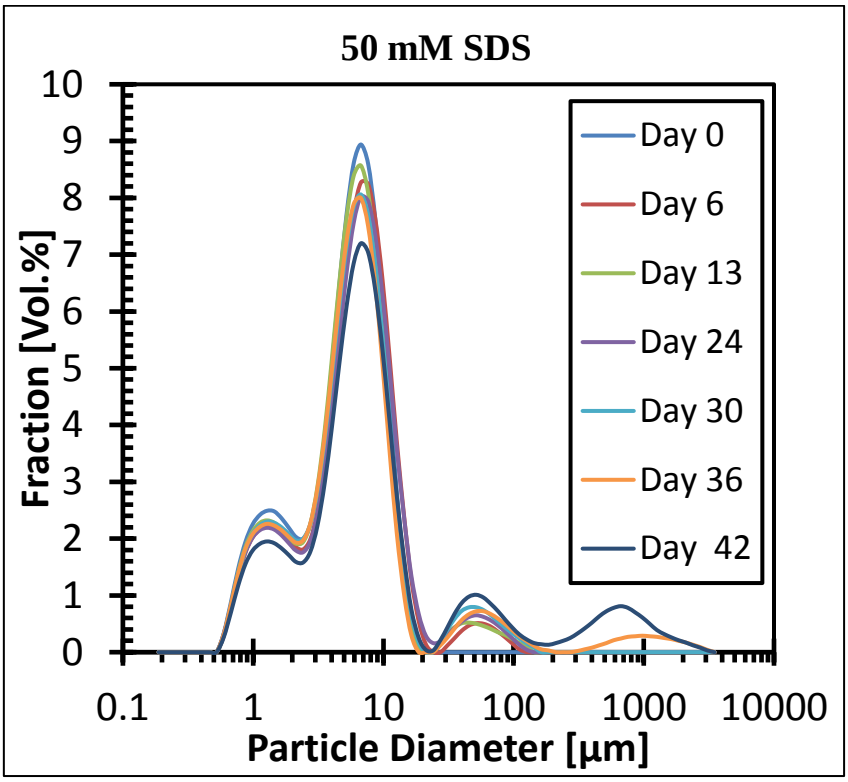

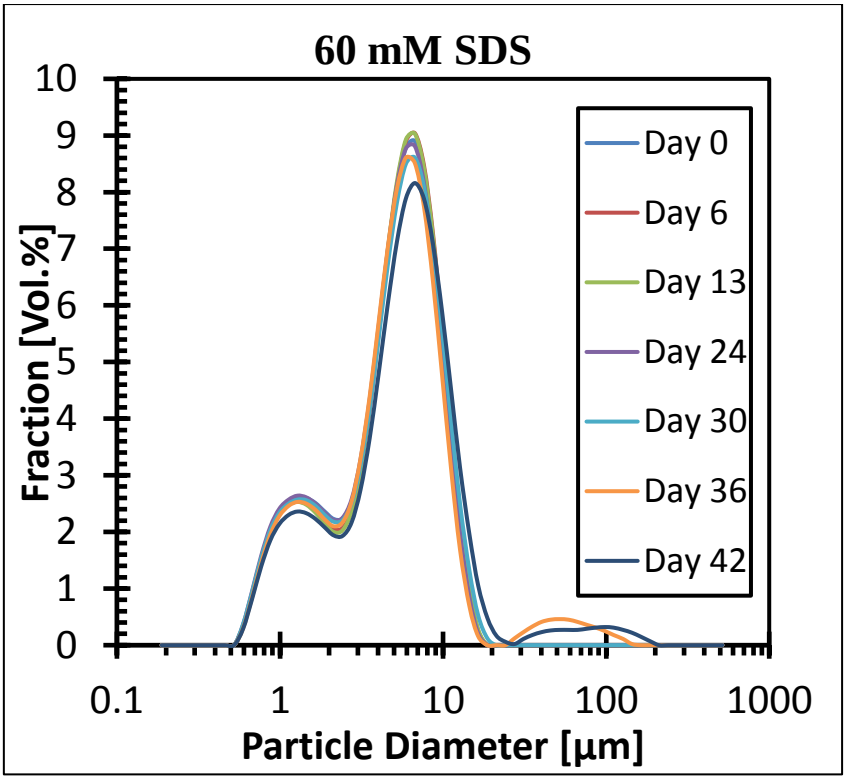

Appendix 2 DSD for CTAB-based emulsions

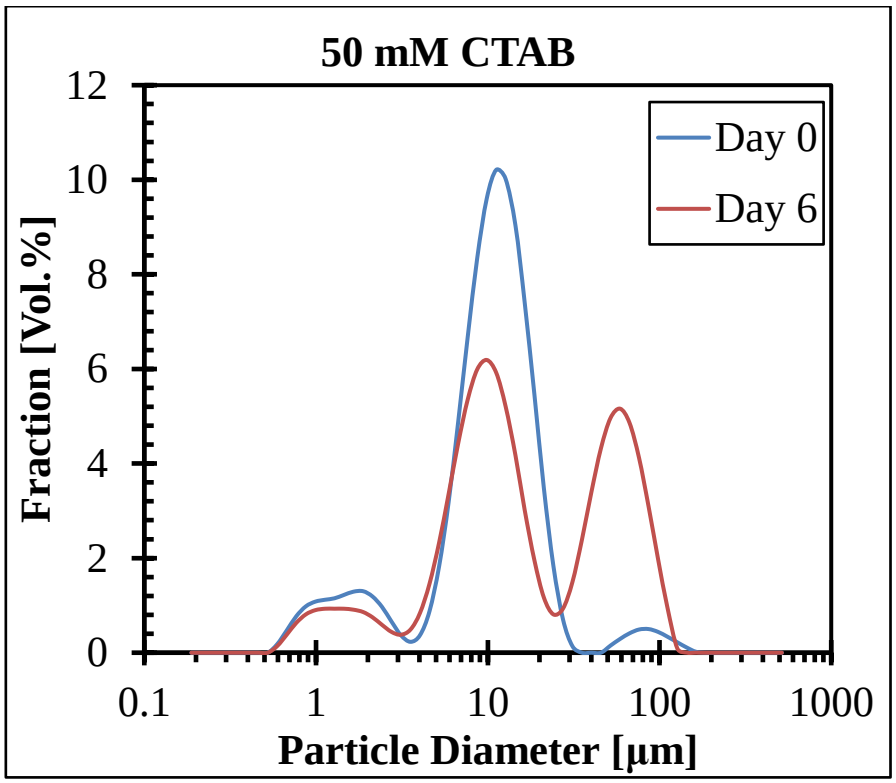

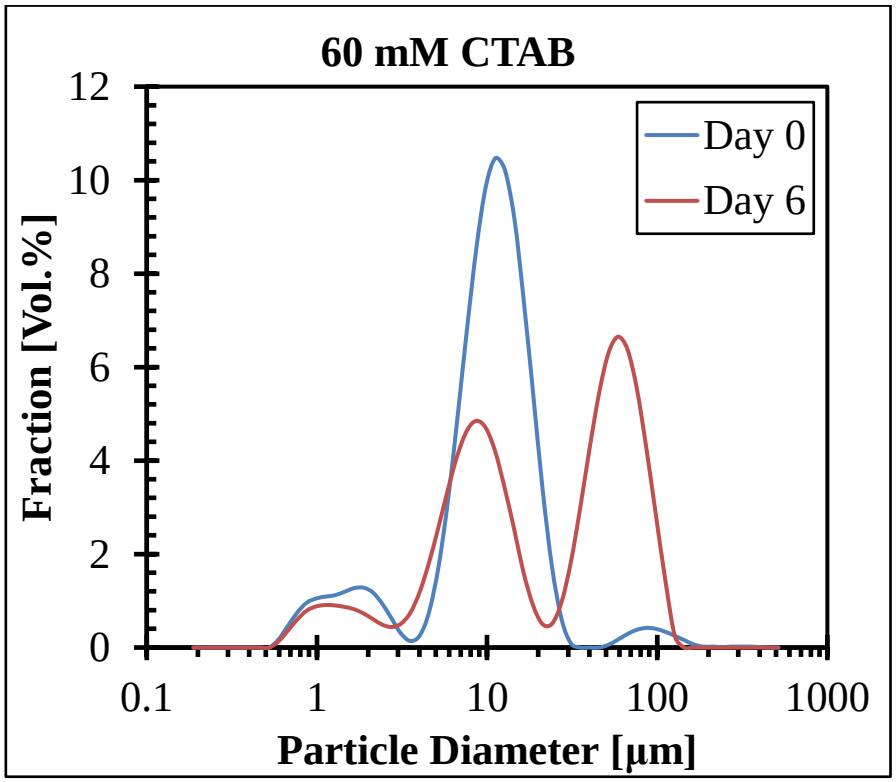

Appendix 3 DSD for $C_{12}E_4$-based emulsions

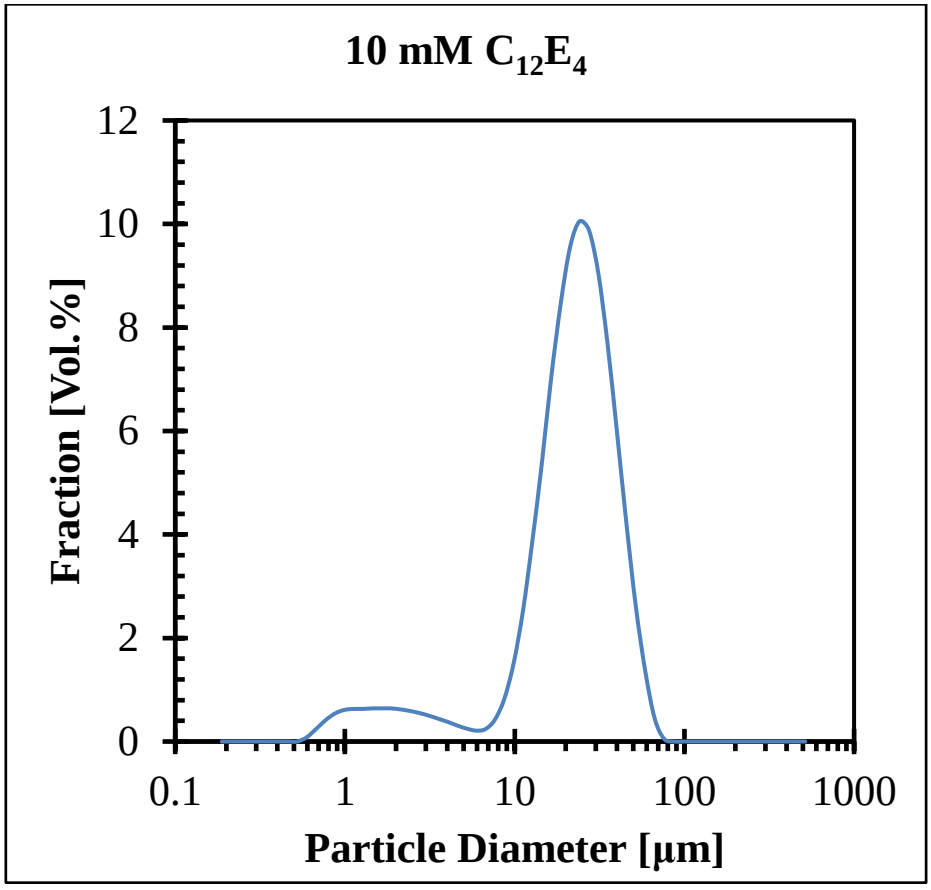

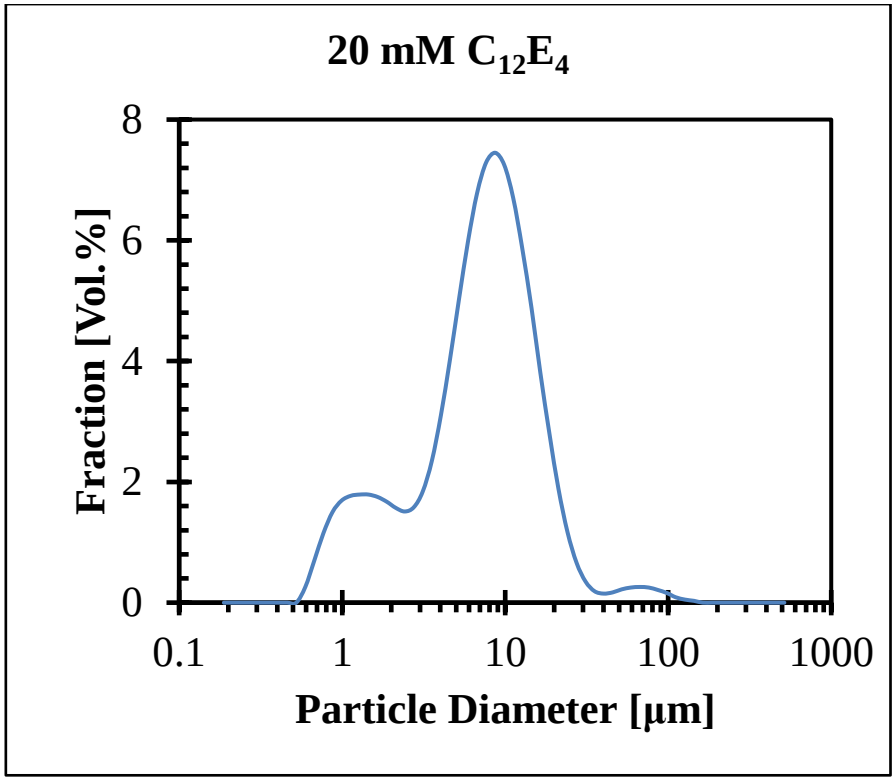

Appendix 4 DSD for $C_{12}E_4$/F127-based emulsions

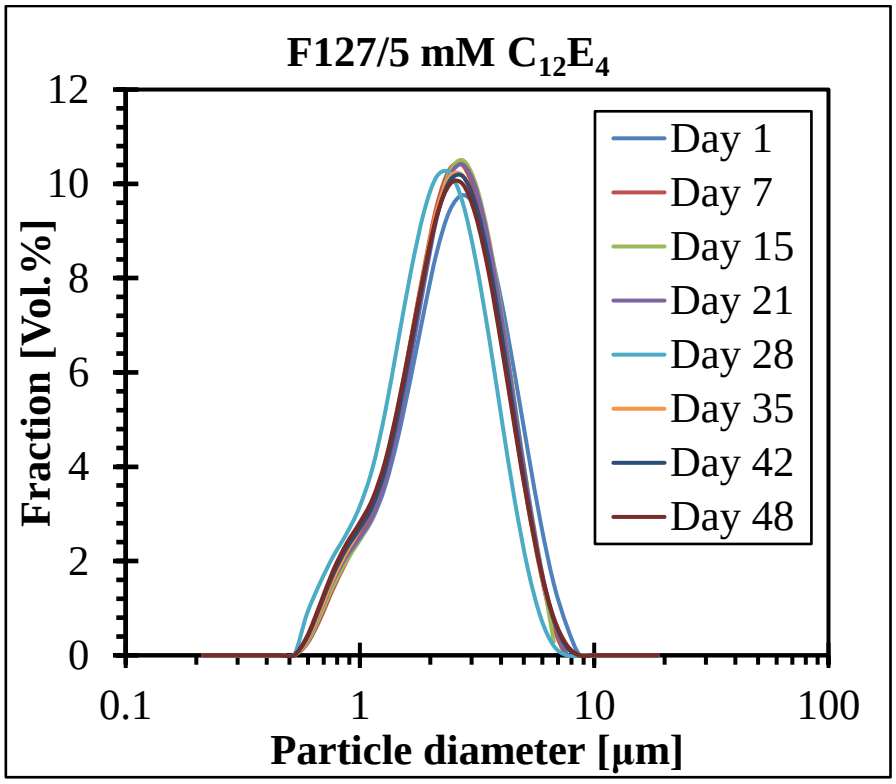

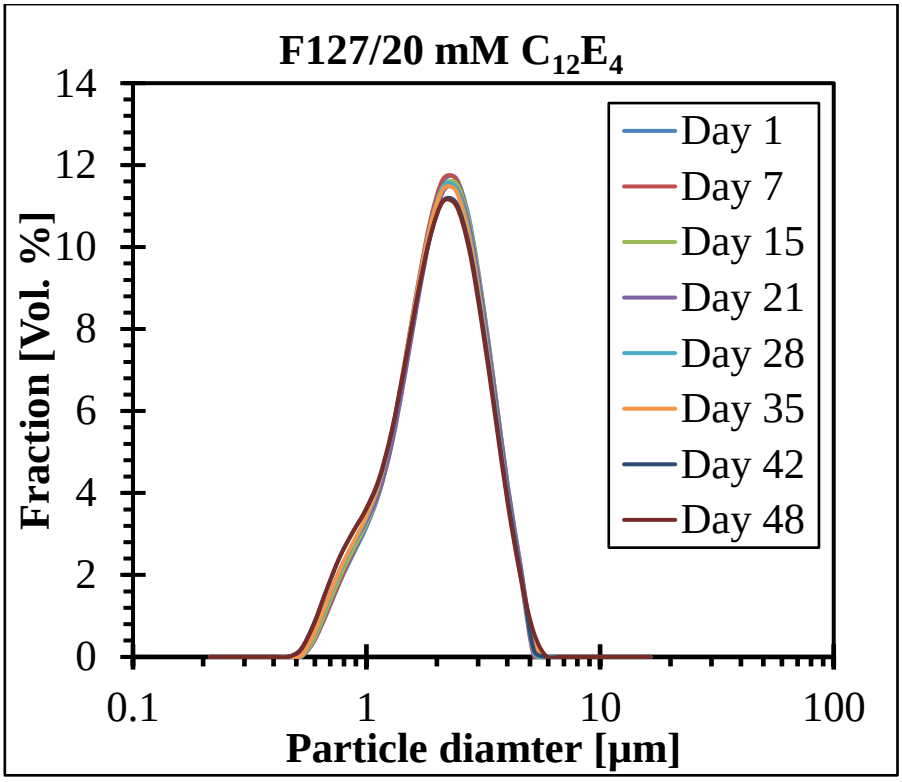

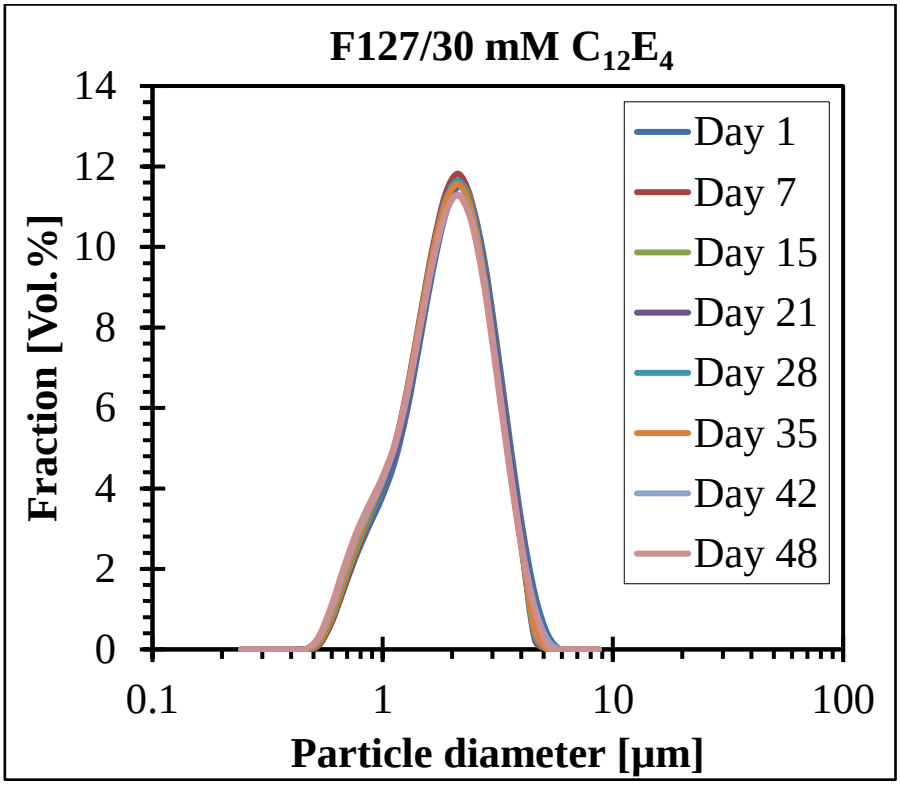

Appendix 5 DSD for SDS/F127-based emulsions

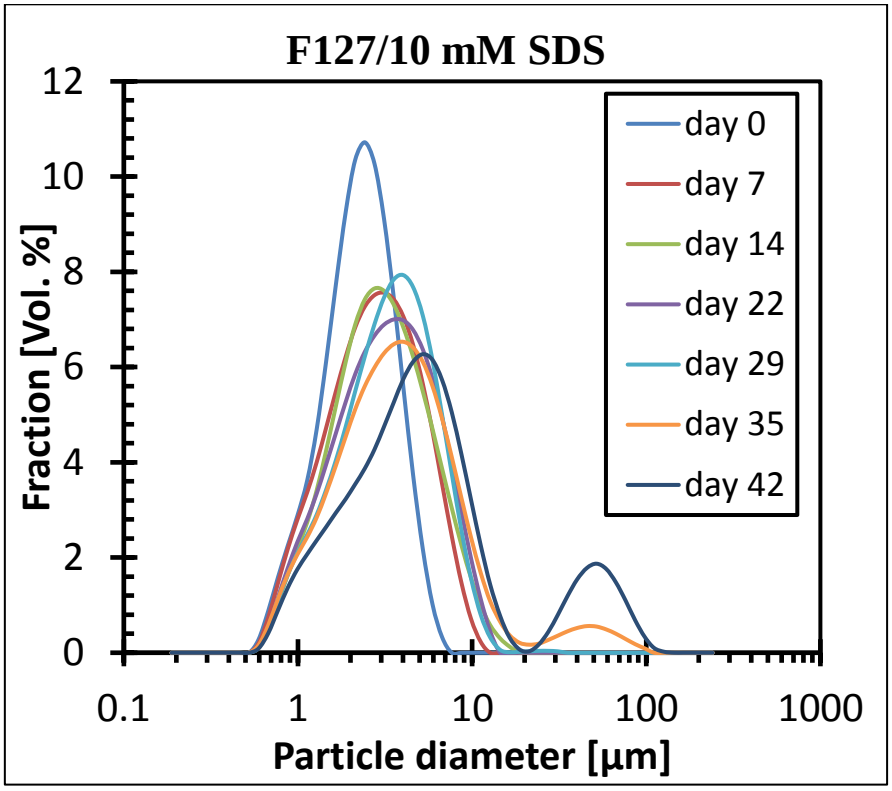

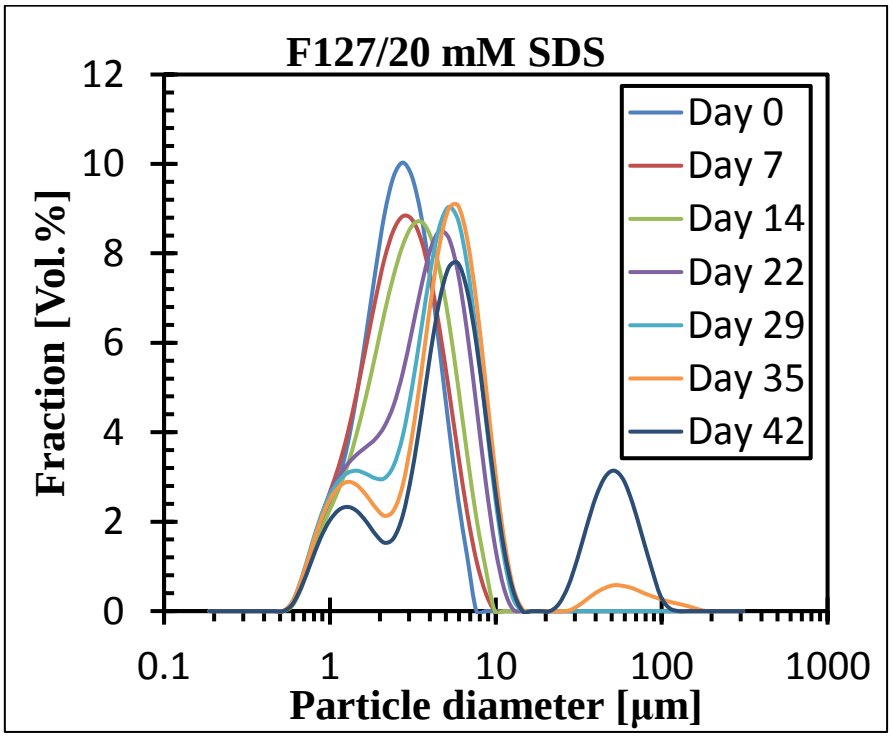

Appendix 6 Viscosity measurements for SDS/F127-based emulsions

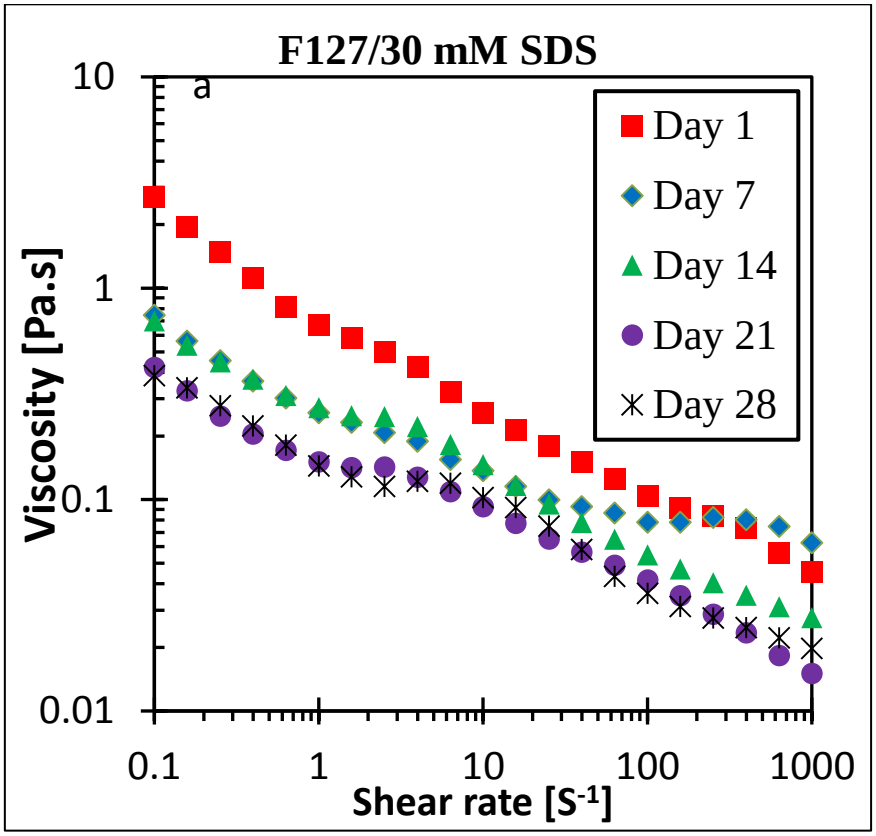

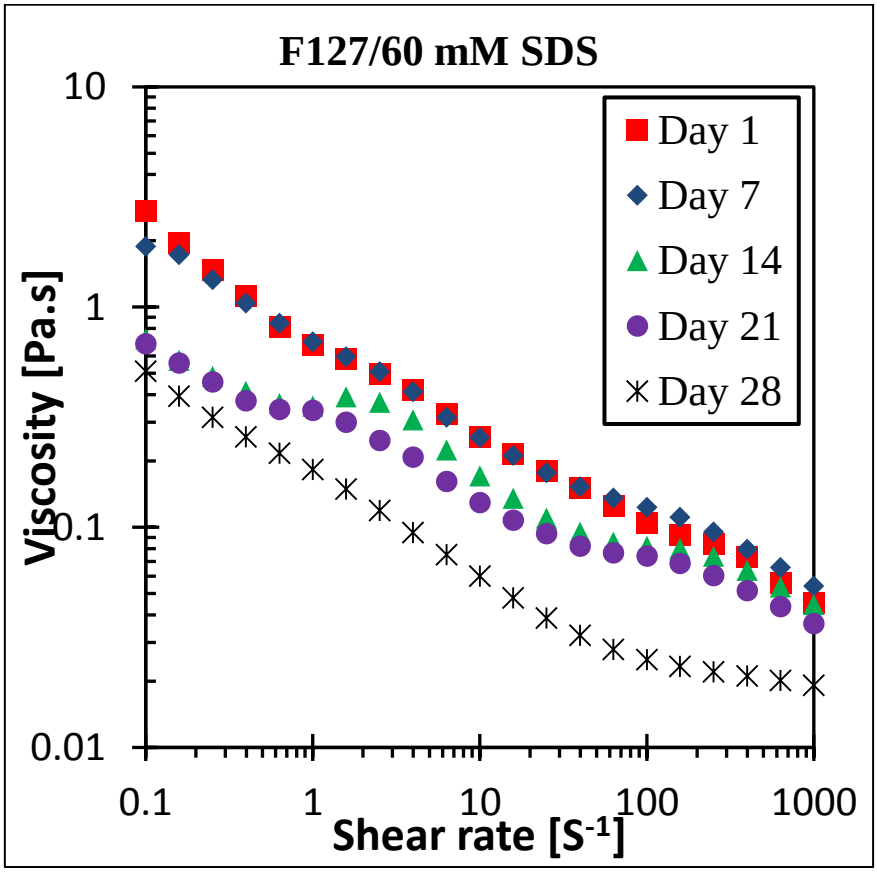

Appendix 7 Viscosity measurements for CTAB/F127-based emulsions

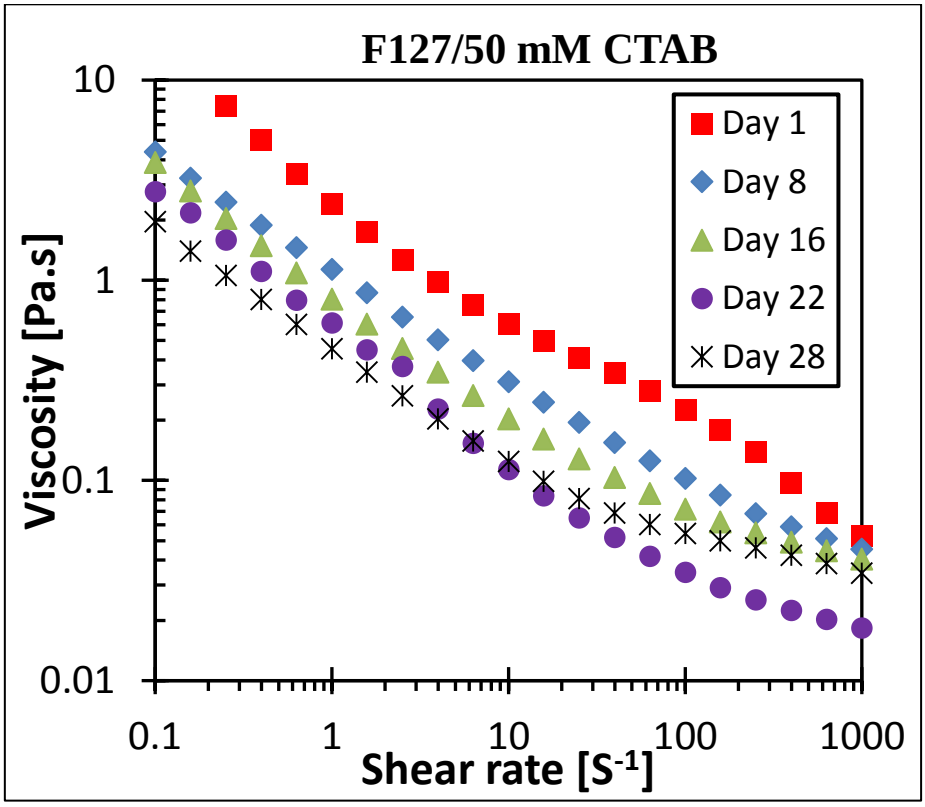

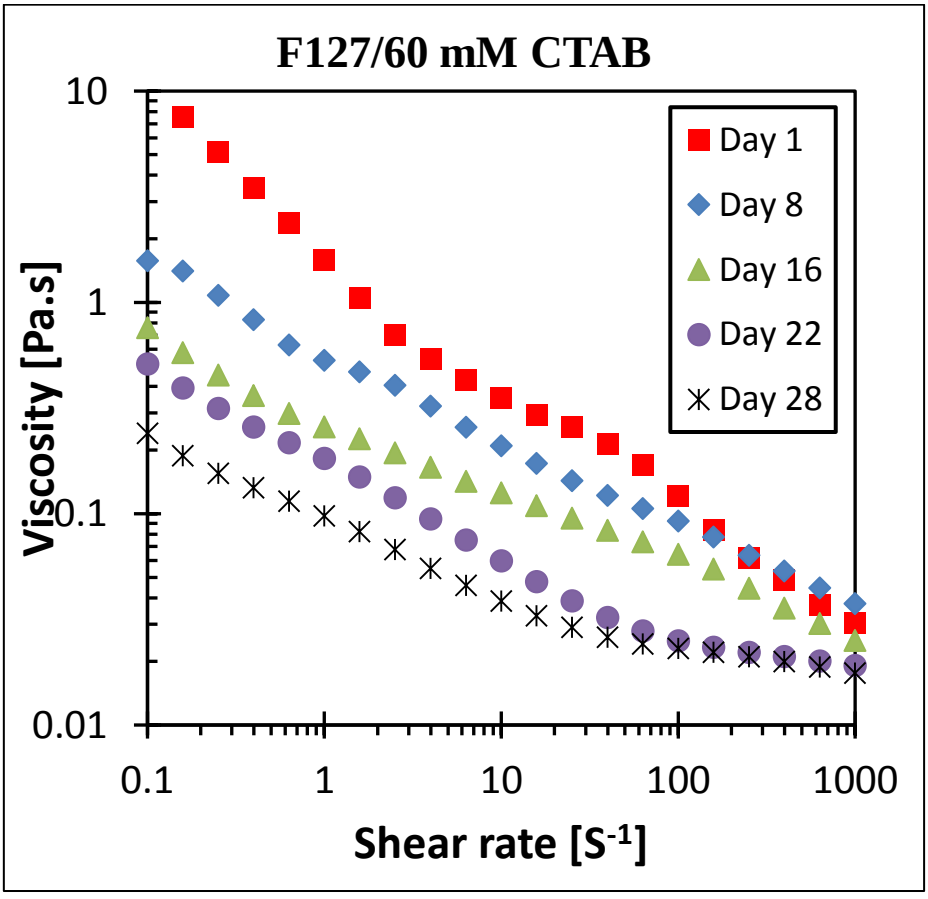

Appendix 8 Viscosity measurements for $C_{12}E_4$/F127-based emulsions

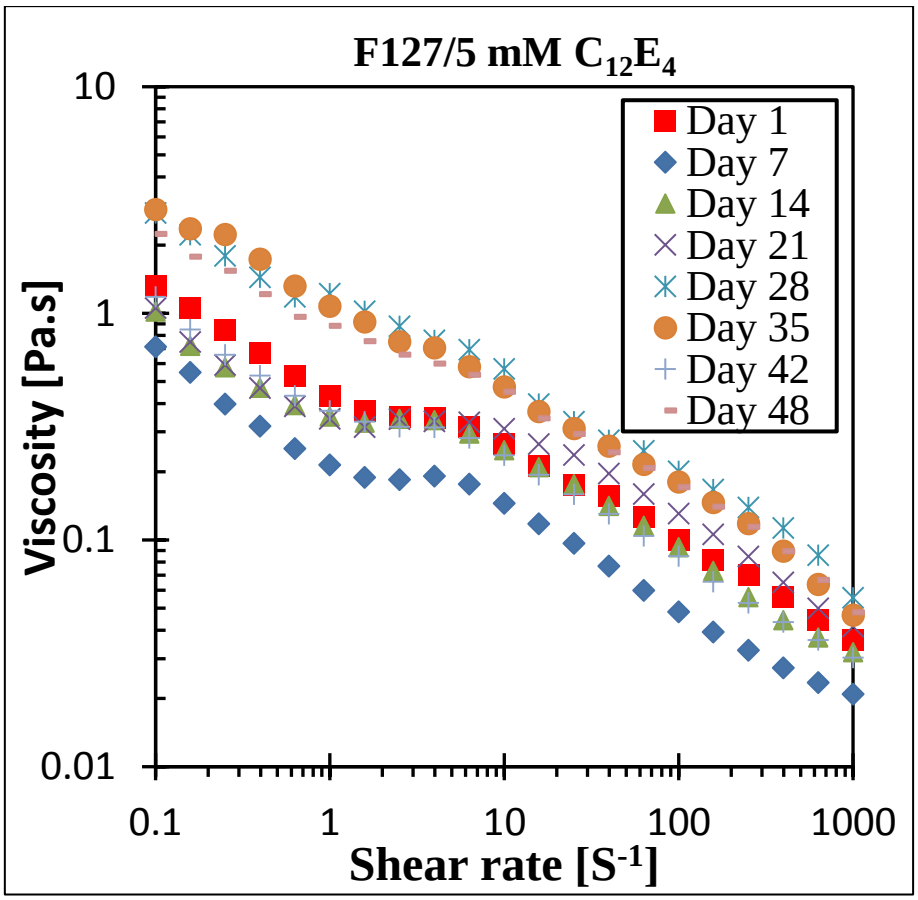

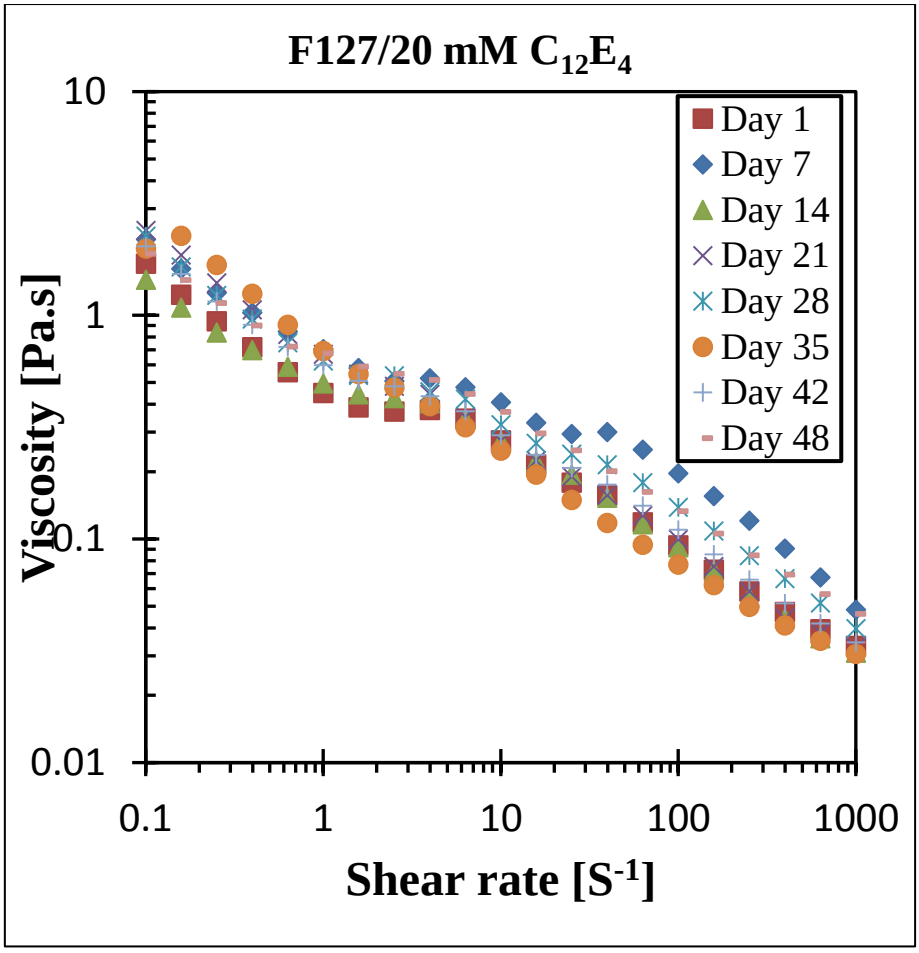

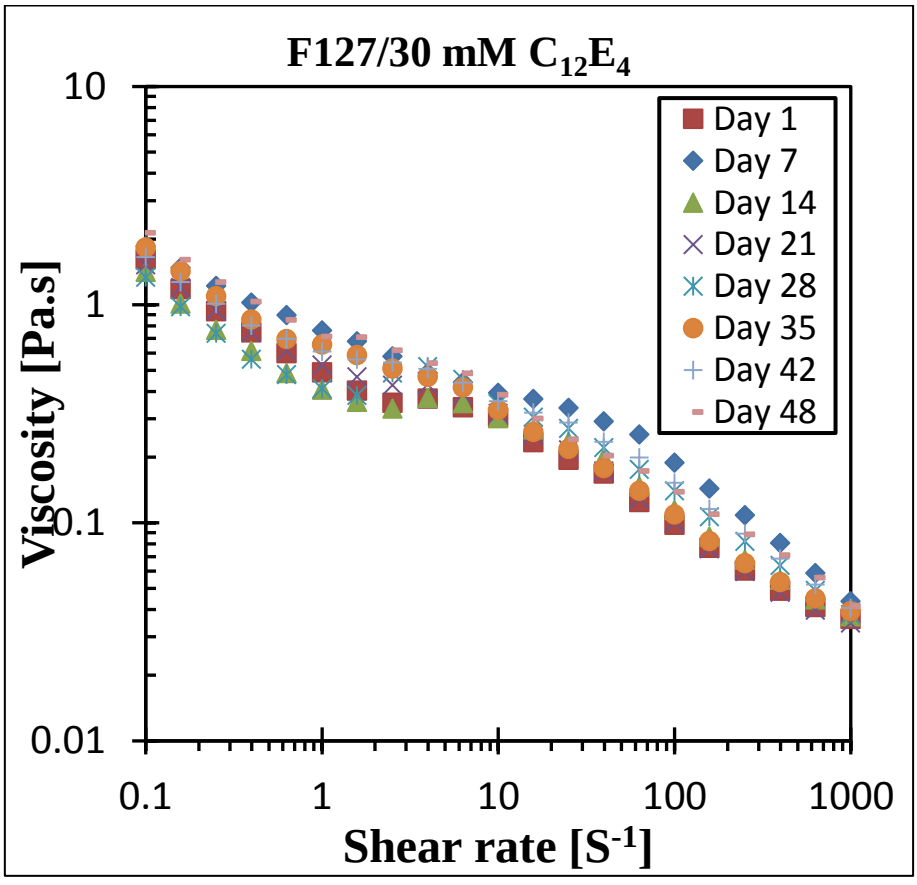

Appendix 9. Optical micrographs of 10 times diluted SDS/F127-based emulsions for first (a) and 37th day (b)

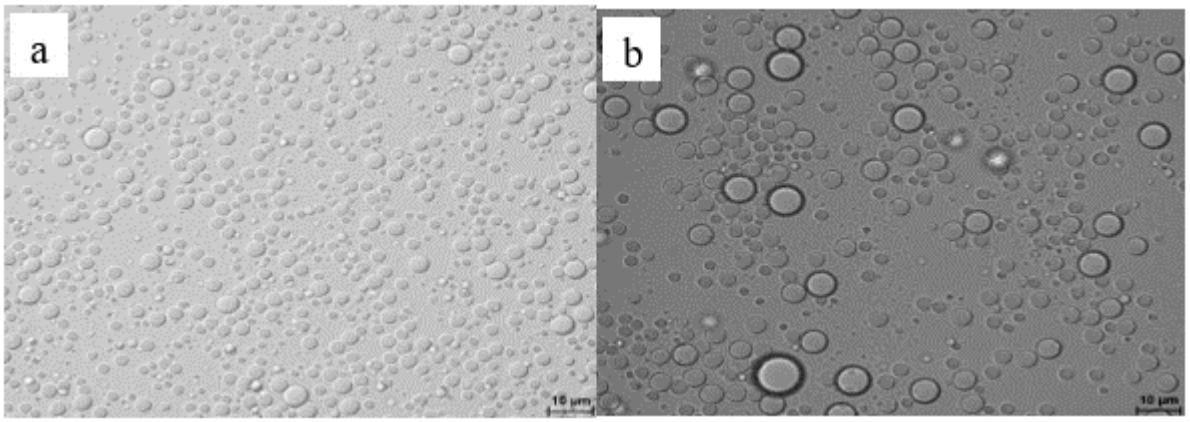

F127/30 mM SDS

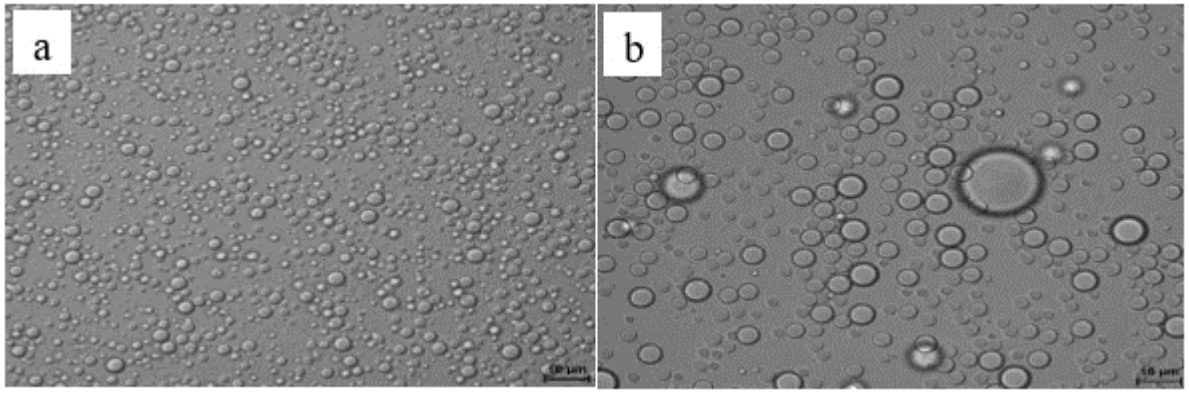

F127/60 mM SDS

Appendix 10 Optical micrographs of 10 times diluted CTAB/F127-based emulsions for first (a) and 35th day (b)

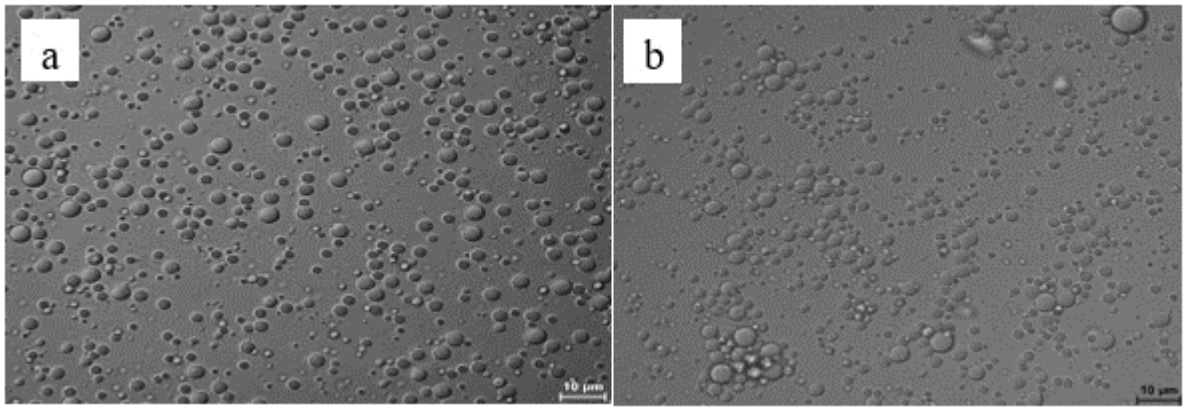

F127/50 mM CTAB

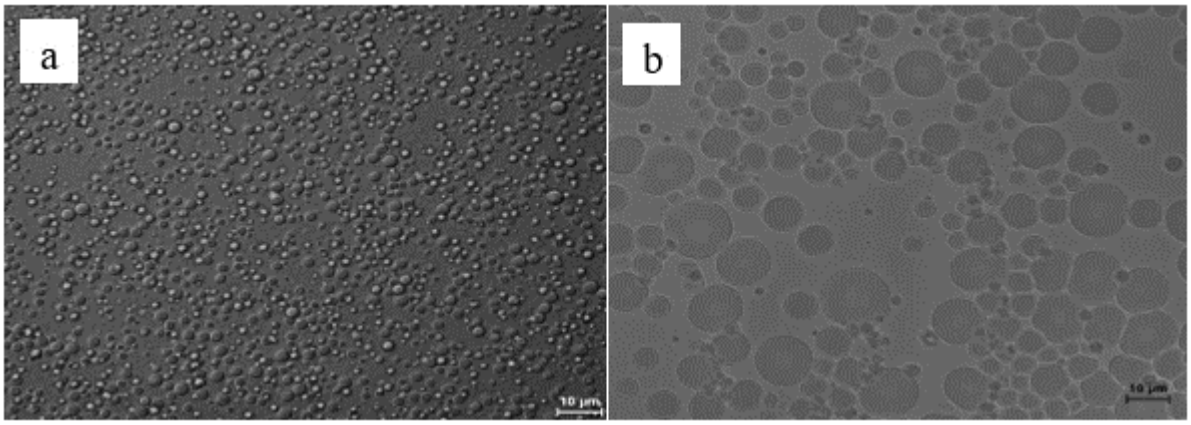

F127/60 mM CTAB

Appendix 11 Optical micrographs of 10 times diluted $C_{12}E_4$/F127-based emulsions for first (a) and 42th day (b)

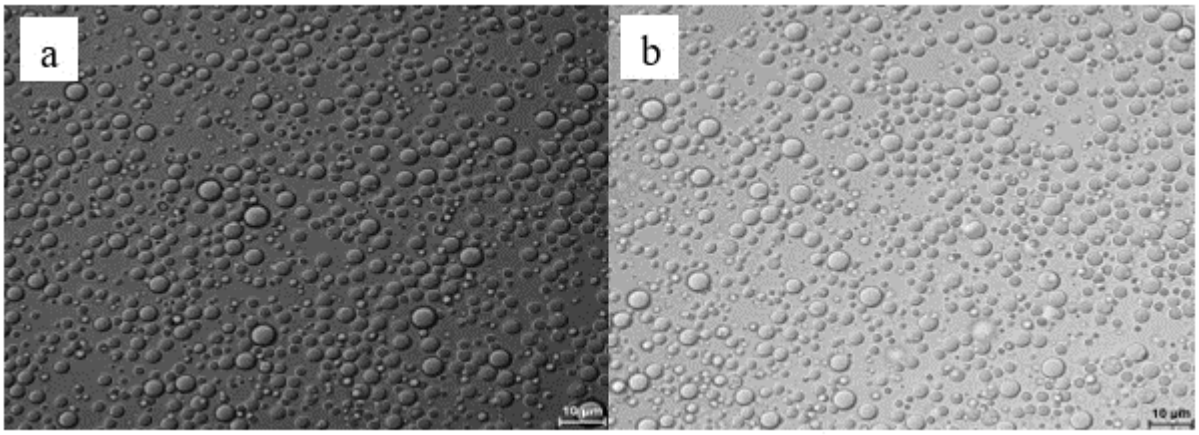

F127/5 mM $C_{12}E_4$

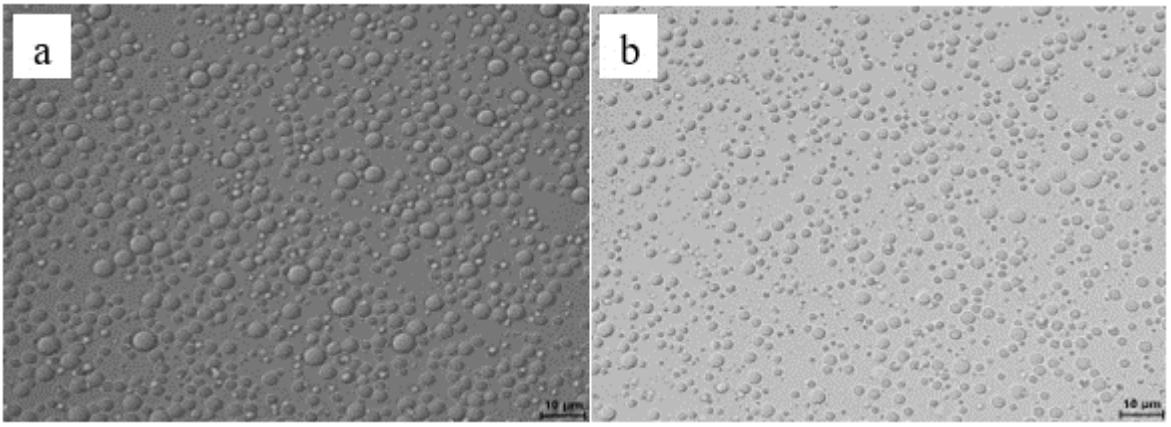

F127/20 mM $C_{12}E_4$

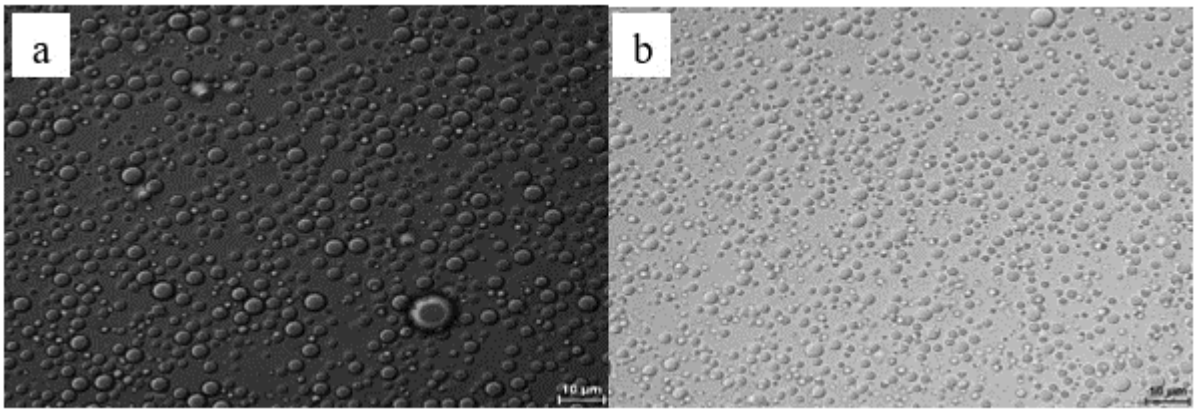

F127/30 mM $C_{12}E_4$